



LIBRARY
Michigan State
University

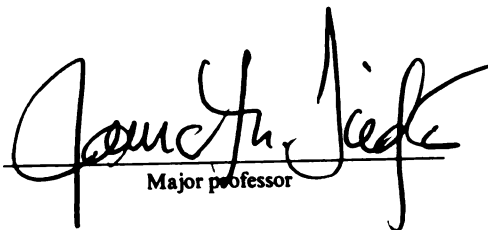
This is to certify that the
dissertation entitled
THE ECOLOGY OF SPIROCHETES IN METHANOGENIC
BIOREACTORS

presented by
Sherry Lynn Dollhopf

has been accepted towards fulfillment
of the requirements for

Ph.D. degree in Microbiology

Date July 3, 2001


Major professor

PLACE IN RETURN BOX to remove this checkout from your record.
TO AVOID FINES return on or before date due.
MAY BE RECALLED with earlier due date if requested.

DATE DUE	DATE DUE	DATE DUE

THE ECOLOGY OF SPIROCHETES IN METHANOGENIC BIOREACTORS

By

SHERRY LYNN DOLLHOPF

A DISSERTATION

**Submitted to
Michigan State University
in partial fulfillment of the requirements
for the degree of**

Doctor of Philosophy

Microbiology and Molecular Genetics

2001

ABSTRACT

THE ECOLOGY OF SPIROCHETES IN METHANOGENIC BIOREACTORS

By

SHERRY LYNN DOLLHOPF

Methane is a potent greenhouse gas, and the release of methane from ruminant animals, termites, waste treatment and anaerobic sediments plays a significant role in global warming models. Spirochetes occur in many methanogenic environments including termite hindguts, rumen contents, dental plaque, human gastrointestinal and reproductive tracts, and anoxic sediments. Many spirochete species of medical and environmental importance are difficult to cultivate and study *in vitro*. To investigate the ecology of spirochetes in methanogenic environments, the unusual enrichment of spirochete species in laboratory scale glucose-fed methanogenic bioreactors was studied using 16S rRNA and rDNA based molecular techniques, pure culture, and coculture experiments. The bacteria and archaea communities associated with the spirochetes were also described.

The enrichment of *Spirochaeta* and *Treponema* related species was observed in multiple bioreactors operated at low dilution rates (0.06 to 0.17 days⁻¹) inoculated with freshwater river sediment, sewage sludge, and rumen contents. *Spirochaeta* sp. str. R8 was isolated from bioreactor fluid and was shown to compose 25 to 45 % of the bioreactor community by fluorescent *in situ* hybridization. Strain R8 fermented glucose to acetate, ethanol, lactate, hydrogen, and carbon dioxide. These products were formed and utilized in bioreactor fluid, indicating that the spirochetes played an important role in

the c

\hat{y}_i

relat

and

sup

con

pre

rate

S_p

str

1/

con

the

the carbon flow within the bioreactors. At dilution rates of 0.25 days⁻¹ and above, the *Spirochaeta* sp. str. R8 population decreased, while a population of *Clostridium ramosum* related organisms increased. Competition experiments between *Spirochaeta* sp. str. R8 and *Clostridium ramosum* str. S9 in continuous culture demonstrated the strain R8 was a superior competitor for glucose at low dilution rates, provided that a sufficient supply of coenzyme A precursors were supplied in the medium. Without added coenzyme A precursors, strain S9 and R8 coexisted in approximately equal numbers at all dilution rates tested. Coculture of *Methanobacterium bryantii* or *Methanosarcina mazei* with *Spirochaeta* sp. str. R8 relieved the coenzyme A requirement and increased cells yields of strain R8 significantly. Competition of strains R8 and S9 in the presence of *Methanobacterium bryantii* allowed strain R8 to outcompete S9 in the absence of extra coenzyme A. This dissertation demonstrates the importance of cooperative interactions in the function and structure of microbial communities.

Dedication

**To Mike, for being there during each crisis
I have encountered and created in our life together.
Life would not be the same without you.**

ham.

more

been

also

extra

opp

visi

and

rese

had

ab

ACKNOWLEDGMENTS

My thanks to everyone, friends and family, that has helped me through each flaming hoop and unexpected result of my thesis. I am especially thankful to my lab-mates and classmates (Merry, Denise, Frank, Carol, Ben, Dan, Joe, and others) who have been there for serious discussions, good times, and everything in-between. Many thanks also to the members of my committee for being accessible and generous with their excellent guidance and advice. Lastly, I would like to thank Dr. Tiedje for giving me the opportunity to be a part of his lab and the Center for Microbial Ecology. Without his vision and support I would not have had the opportunity to attend numerous conferences and summer classes, to interact with multi-disciplinary groups, and to pursue my own research interests. Many graduate students do not have the same opportunities that I have had, and I am grateful for it. Above all else, I am grateful for his tremendous faith in my abilities, that in itself has meant the most.

LIST

LIST

CHA

I

7

Y

CE

TABLE OF CONTENTS

LIST OF TABLES	ix
LIST OF FIGURES	x
CHAPTER 1 – COMPETITION AND COOPERATION IN MICROBIAL COMMUNITIES	1
Introduction	1
Types of microbial species interactions	2
Negative interactions and community structure	4
Positive interactions and community structure	8
Investigating microbial species interactions	12
Enrichment culture	12
Coculture	13
Microscopy	15
Molecular methods	15
Implications	19
Thesis overview	20
Experimental design	23
References	24
CHAPTER 2 – PHYLOGENY OF BIOREACTOR ORGANISMS	30
Introduction	30
Materials & Methods	32
Reactor design and operation	32
Extraction and purification of community DNA	35
16S rDNA clone libraries	36
Bacterial isolates	37
Sequencing and sequence analysis	38
16S rRNA oligonucleotide probing	39
Results	42
Bacteria	42
Archaea	49
Clone libraries	49

16S rRNA oligonucleotide probes	49
Discussion	51
References	55
 CHAPTER 3 – THE IMPACT OF FERMENTATIVE ORGANISMS ON CARBON FLOW IN METHANOGENIC SYSTEMS UNDER CONSTANT LOW SUBSTRATE CONDITIONS	 58
Introduction	58
Materials & Methods	60
Bioreactor operation	60
Sample preparation and microscopy	60
DNA extraction and T-RFLP	61
16S rDNA analysis	62
Determination of intermediary metabolites	63
Spirochete isolate R8	63
Fermentation products	64
Maximum substrate utilization rates	64
Nucleotide sequence accession numbers	65
Results	65
Community structure	65
Intermediary metabolites	71
Maximum substrate utilization rates	72
Spirochete isolation and fermentation products	75
Discussion	75
References	80
 CHAPTER 4 – INTERPRETATION OF 16S RDNA T-RFLP DATA: APPLICATION OF SELF ORGANIZING MAP NEURAL NETWORKS AND PRINCIPLE COMPONENT ANALYSIS	 84
Introduction.....	84
Materials & Methods.....	86
Reactor operation and experimental design.....	86
Sampling	88
T-RFLP profiles	88
Clone libraries and sequencing	89
Community similarity	90
PCA.....	91
SOM.....	91

Results	92
Community similarity	92
PCA	94
SOMs	98
Terminal restriction fragment identification	102
Discussion	108
References	113
CHAPTER 5 – INTERSPECIES INTERACTIONS AFFECTING A <i>SPIROCHAETA</i> SPECIES IN A CARBON-LIMITED METHANOGENIC ENVIRONMENT	117
Introduction	117
Materials & Methods	118
Bioreactor operation	118
T-RFLP analysis	119
FISH	119
Isolation and culture techniques	122
16S rRNA gene sequencing	123
Continuous culture	123
Results	124
T-RFLP	124
FISH	127
Strain R8 and S9 characteristics	130
Competition in continuous culture	132
Methanogenic coculture	135
Discussion	138
References	143
CHAPTER 6 – CONCLUSIONS	146

Table

Table

Table
for the

Table
comm

Table
mea
mon

Table
by a

Table
in b

Table
com

Table

Table

Table
by

LIST OF TABLES

Table 1.1. Interactions among microbial species.....	3
Table 1.2. Basis of cooperative interactions.....	9
Table 1.3. The purpose and potential application of molecular microbial ecology methods for the study of interspecies interactions.....	18
Table 2.1. Phyla detected by 16S rRNA gene molecular methods in various reactor communities.....	43
Table 3.1. Similarity of bacterial <i>HaeIII</i> , <i>HhaI</i> , and <i>MspI</i> T-RFLP electropherograms as measured by Horn's community similarity index (Brower 1997) and Pearson product-moment correlation coefficient (Pearson 1926).....	68
Table 3.2. Production of intermediary metabolites in bioreactor HS and LS as determined by addition of [U- ¹⁴ C]glucose to the bioreactors.....	73
Table 3.3. Fermentation of glucose by isolate R8 and maximum substrate utilization rates in bioreactor R1.....	74
Table 4.1. Morisita community similarity indices for the R1, S2, and M3 bioreactor communities.....	93
Table 4.2. T-RFLP fragments with high factor loading.....	97
Table 5.1. Growth yields in glucose minimal medium.....	131
Table 5.2 Growth yields of <i>Spirochaeta</i> strain R8 in coculture with <i>Methanobacterium bryantii</i>	136

Figure
uptake

Figure
and
trans

Figure

Figure
bio

Figure
inc
ind
resp

Fig
bio
usi

Pa
24
47

=
Re

Fi
bio

31
of

LIST OF FIGURES

Figure 1.1. $\mu - s$ relationship of a copiotroph (A), an organism with high and low affinity uptake systems (B), and an oligotroph (C).....	6
Figure 1.2. Flow chart of molecular microbial ecology methods for community analysis and monitoring of specific phylogenetic groups of microorganisms. RT-PCR = Reverse transcription polymerase chain reaction.	16
Figure 1.3. Bioreactor design.....	21
Figure 1.4. Functional groups of microorganisms in glucose-fed methanogenic bioreactors.	22
Figure 2.1. Reactor operation and sampling. Dotted horizontal arrows indicate inoculation and solid horizontal arrows indicate reactor operation. Black and gray circles indicate sampling times for 16S rRNA gene clone libraries and bacterial isolation, respectively. Vertical arrows indicate an intentional organic shock load. (Facing)	33
Figure 2.2. Maximum likelihood tree of cloned bacterial 16S rRNA gene sequences from bioreactors and other methanogenic environments. The backbone of this tree was cast using 696 unambiguously aligned nucleotides between <i>E. coli</i> positions 95 and 1295. Partial sequences were then appended to the tree using the maximum likelihood algorithm with 261 unambiguously aligned nucleotides between <i>E. coli</i> positions 154 and 474. The origin of the cloned genes is as follows: RFS = Termite gut (Lilburn); WCHB1 = Aquifer (Dojka); EO = Reactor P1; HS = Reactors HS 5-8; LS = Reactors LS 1-4; S2 = Reactor S2; str. = Bacterial isolate from indicated reactor. (Facing).....	40
Figure 2.3. Maximum likelihood tree of cloned spirochete-related 16S rRNA genes from bioreactors and other methanogenic environments. This tree was calculated in ARB using 312 unambiguously aligned nucleotides between <i>E. coli</i> positions 154 and 478. The origin of the cloned genes is indicated as follows: RFS = Termite gut (Lilburn); WCHB1 =	

Aqui

Reac

Figur

Carta

align

rep

Figur

and

prob

met

Figur

isol

rest

face

Fig

Spe

SS

cal

we

pac

res

acc

me

Be

La

Sn

br

X

Aquifer (Dojka); EO = Reactor P1; HS = Reactors HS 5-8; LS= Reactors LS 1-4; S2 = Reactor S2; str. = Bacterial isolate from the indicated reactor..... 45

Figure 2.4. Neighbor-joining tree of *Archaea* 16S rDNA clones created from a Jukes-Cantor distance matrix. The matrix was calculated from analysis of 328 unambiguously aligned nucleotides of the 16S rRNA gene. Bootstrap values from 100 parsimony replicates are shown to the left of each node..... 48

Figure 2.5. Relative abundance of methanogen-related 16S rRNA in reactors LS 1 and 2 and HS 6 and 7 as determined by 16S rRNA membrane hybridization to oligonucleotide probes. The abundance of each group is expressed as a percentage of the total amount of methanogen-related 16S rRNA detected by all of the methanogen-specific probes used. 50

Figure 3.1. T-RFLP electropherograms of the *Hae*III digested SSU rDNA amplified from isolate R8 and bacterial communities LS, HS, and R1. Peaks corresponding to the restriction fragment length of the most frequently cloned SSU rRNA gene sequences are labeled. 66

Figure 3.2. Phylogenetic relationships of clones and isolates in the families *Spirochaetales* (A) or *Streptococcales* (B). Unambiguously aligned nucleotides of the SSU rRNA gene from *E. coli* position 111 to 465 (A) and 21 to 1477 (B) were used to calculate Kimura 2-parameter distance matrices (Kimura 1980). The phylogenetic trees were created with the neighbor-joining method (Saitou, Nei 1989). Neighbor-joining and parsimony bootstrap values (50 % or higher) are listed above and below each node, respectively. Scale bar = 10 % difference in nucleotide sequence positions. Genbank accession numbers are as follows: *Streptococcus bovis*, M58835; *Streptococcus macedonicus*, Z94012; *Streptococcus mutans*, S70358; *Streptococcus equi*, S70324; *Bacillus subtilis* str 168, D26185; *Lactobacillus acidophilus* subspp. *johnsonii*, M99704; *Lactococcus lactis* subspp. *Lactis*, M58837; *Streptococcus salivarius*, M58839; *Streptococcus parauberis*, X89967; *Brachyspira hyodysenteriae*, M57741; *Treponema bryantii*, M57737; *Spirochaeta zuelzeri*, M88725; *Spirochaeta* sp. str. *Mastotermes*, X79548; *Spirochaeta caldaria*, M71240; *Spirochaeta stenostrepta*, M88724; *Spirochaeta*

and

MS

and

AFI

and

Figure

char-

show

was

this

sex

resp

Figure

B) a

vari

next

Fig

graph

sim

sc

frag

ind

wh

Fig

M

bo

to

re

aurantia str. J-1, M57740; *Spirochaeta litoralis*, M88723; *Spirochaeta halophila*, M88722; *Spirochaeta* sp. str. PL12MY, RDP short ID str.PL12MY; *Spirochaeta* sp. str. *Antarctica*, M87055; *Leptospira inadai*, Z21634; EO-XIV, AF149879; EO-XI, AF149878; EO-V, 149881; EO-I, AF149883 (Fernandez et al. 1999); LSII, AF218216; and HSI, AF218221 (Fernandez et al. 2000). (Facing)..... 69

Figure 4.1. Timeline for reactors R1, S2, and M3. Time is measured in number of volume changes (x-axis not to scale). Sampling times are indicated by numbered circles, which show the number of volume changes that occurred since the target organic loading rate was achieved in reactors S2 and M3. Control reactor R1 operated for over 2 years prior to this study. Reactors S2 and M3 were inoculated from river sediment and municipal sewage sludge, respectively. Flow rate and HRT are shown above and below the timeline respectively. 87

Figure 4.2. PCA ordination of *Bacteria* T-RFLP peak height data for reactors M3 (A and B) and S2 (C and D) during phase A (A and C) and Phase B (B and D). The amount of variability accounted for by each factor is on the axes in each panel. Sampling times are next to each point. 95

Figure 4.3. SOM clustering of T-RFLP fragments in reactor M3 (A) and S2 (B). The line graphs shown for each fragment represent the change in normalized peak height over time. The graphs are arranged according to the position of their winning node within the square SOM output. SOM groups I, II, III and IV are indicated. The letter A before the fragment length indicates fragments from *Archaea*-specific T-RFLP. Fragment lengths indicated in color are in the same SOM group in both reactors. (C) A timeline shows when groups I through IV were present in each reactor. (Facing)..... 99

Figure 4.4. Maximum likelihood tree of cloned *Bacteria* 16S rRNA genes from reactors M3 and S2 and other methanogenic environments. Clones retrieved in this study are in bold. The SOM group and terminal restriction fragment length (Group x : y bp) is shown to the left of each clone. The backbone of this tree was cast in ARB using 969 unambiguously aligned nucleotides between *E. coli* positions 95 and 1295. Partial

sequ
with
origi
EO.
react
(9) (

Fig
tree
boot
indic
grou
HR

Fig
enzy
Exc
mis

Fig
diff

Fig
for
gen
bic
alo

Fig
oli
the
w

sequences were appended to the tree in ARB using the maximum likelihood algorithm with 261 unambiguously aligned nucleotides between *E. coli* positions 154 and 474. The origin of cloned genes from other methanogenic environments is indicated as follows: EO, LS, HS = glucose-fed methanogenic reactors (11,12); HA = anaerobic vinasses reactor (15); RFS = termite hindgut (21); WCHB1 = hydrocarbon contaminated aquifer (9). (Facing)..... 103

Figure 4.5. Succession of methanogenic phylotypes in reactor S2. (A) Neighbor-joining tree of cloned *Archaea* 16S rDNA genes. The number next to each node indicates bootstrap values from 100 parsimony bootstraps. Numbers to the right of each bracket indicate the length of the 16S rDNA terminal restriction fragment for each phylogenetic group. (B) *Archaea* community T-RFLP profiles of reactors S2 and M3 after different HRTs in phase A. 107

Figure 5.1. 16S rRNA gene terminal restriction fragments generated with restriction enzyme *Hae*III and specificity of oligonucleotide probes used for *in situ* hybridization. Except for the two organisms noted, all sequences in the database had more than two mismatches with the oligonucleotide probes designed in this study. 121

Figure 5.2a. 16S rDNA T-RFLP electropherograms of bioreactor community M3 at different dilution rates. 125

Figure 5.2b. Change in normalized peak height of terminal restriction fragments unique for *Spirochaeta* species (closed symbols) and *Clostridium ramosum* (open symbols) generated by restriction of amplified bacterial 16S rRNA genes with enzyme *Hae*III from bioreactor communities S2 (■,□) and M3 (◇,◆). The dilution rate applied is shown along the top axis. 126

Figure 5.3. Micrographs of bioreactor fluid after hybridization with fluorescently labeled oligonucleotide probes. DAPI (left) and FISH (right) micrographs are shown for identical fields. Bioreactor community M3 after ten volume changes at $D = 0.17 \text{ days}^{-1}$ hybridized with probe SpiroR8-177 (A and B). Bioreactor community S2 after eight volume changes

a: D

hydro

Figure

(class

comm

Figure

str

part

pop

Figure

str

sepa

app

Fig.

S9

of

the

the

at $D = 0.13 \text{ days}^{-1}$ (C and D) and after seven volume changes at $D = 0.50 \text{ days}^{-1}$ (E and F) hybridized with probe ClostS9-182. 128

Figure 5.4. Percent of DAPI stained cells that hybridized with probes SpiroR8-177 (closed symbols) and ClostS9-182 (open symbols) in the S2 (■) and M3 (◆) bioreactor communities. The dilution rate applied is shown along the top axis. 129

Figure 5.5a. Population size of *Spirochaeta* sp. str. R8 (◆,●) and *Clostridium ramosum* str. S9 (◇,○) during competition in continuous mixed culture with 500 µg/mL of pantothenate supplied. The dashed line indicates the washout rate of a non-growing population. The dilution rate applied is shown along the top axis..... 133

Figure 5.5b. Population size of *Spirochaeta* sp. str. R8 (◆,●) and *Clostridium ramosum* str. S9 (◇,○) during competition in continuous mixed culture. Data is shown from two separate competition experiments performed under identical conditions. The dilution rate applied is shown along the top axis..... 134

Figure 5.6. Population size of *Spirochaeta* sp. str. R8 (●) and *Clostridium ramosum* str. S9 (○) during competition in continuous mixed culture. The arrow indicates the addition of 1.8×10^8 *Methanobacterium bryantii* cells to the chemostat. The dashed line indicates the washout rate of a non-growing population. The dilution rate applied is shown along the top axis. 137

INT

Intro

Micro

auton

learn

conn

To c

mech

man

appl

an e

head

form

met

me

the

lect

con

CHAPTER 1

INTERSPECIES INTERACTIONS IN ANAEROBIC MICROBIAL COMMUNITIES

Introduction

Microbial communities affect many aspects of the world in which we live. Microbial community function impacts human health, agriculture, waste treatment, nutrient cycling, and global warming, to name a few. Aside from our innate desire to learn about the world in which we live, our goal in studying microbial communities is to control and direct microbial functions to preserve and improve the quality of human life. To control and direct microbial activities, an understanding of the fundamental biological mechanisms underlying their activities is necessary. The harnessing of the ability of microbes to produce a variety of commercial products is an example of the successful application of this reductionist approach.

The difficult task of elucidating the biological processes and interactions within an entire microbial community may be necessary to understand many ecological and health-related problems. Along with the typical environmental controls and biological limitations of a single species that must be understood, multiple species, diverse metabolisms, and interspecies interactions must be taken into account. In complex microbial communities with multiple trophic levels and species numbers in the thousands, this task becomes daunting. The advent of high-throughput molecular technologies vastly improves our ability to describe and compare complex microbial communities, which should aid us in gaining an understanding of microbial communities.

The
animals sho
niche partit
play a majo
ecology has
our unders
natural env

Types of n

A p
other micro
survival an
metabolism
completely
the environ
them. Inte
exert little
necessary

Ne
(Table 1.1
but are no
species pr
microbial

The same basic principles that govern the community structure of plants and animals should apply to microbes as well. Thus we can expect competition for resources, niche partitioning, trophic interactions, mutualism and other interspecies interactions to play a major role in the structuring of microbial communities. Much research in microbial ecology has shown that basic ecological principles apply to microbial communities, but our understanding of how these principles actually work in complex communities in natural environments is still in its infancy.

Types of microbial species interactions

A prokaryotic cell within a microbial community interacts with a large number of other microorganisms simultaneously. The importance of these interactions for the survival and activity of the cell depends upon the proximity of the other cells and their metabolism. The nature of the interactions may be positive, negative, or neutral. A completely neutral relationship between two species in the same environment is rare if the environment they share allows diffusion of soluble and gaseous molecules between them. Interspecies interactions range from relatively weak non-specific interactions that exert little influence on the growth of either species, to strong interactions that are necessary for the survival of one or both species in a particular environment.

Negative species interactions include competition, parasitism, and predation (Table 1.1). Parasitism and predation are common between prokaryotes and eukaryotes, but are not as common between prokaryotic species. Only a few known prokaryote species prey upon other prokaryotes. The importance of predatory cells in natural microbial communities is unclear, but they are ubiquitous in natural environments.

Table 1.1. Common terms used to describe microbial interspecies interactions
(modified from references 17 and 45).

Term	Definition
------	------------

Table 1.1. Common terms used to describe microbial interspecies interactions (modified from references 17 and 45).

Term	Definition
Exploitative competition (Resource competition)	Populations inhibit each other when resources are limiting
Interference competition (Amensalism)	Populations inhibit each other by inflicting direct harm (ie producing a inhibitory substance)
Predation	One population consumes another in a destructive manner
Parasitism	One population inhibits or consumes another in a non-destructive manner
Commensalism	One population benefits from interaction with another population that is not affected
Protocooperation (Synergism)	Two populations interact in a way that is favorable to both, but not obligatory under the given conditions
Mutualism	Two populations interact in a way that is favorable to both and obligatory for at least one of the species under the given conditions
Syntrophism	A special type of mutualism in which two populations degrade a substrate that neither one could degrade alone
Symbiosis	A special type of highly evolved mutualism in which two populations can not survive with out each other

Viruses that prey on heterotrophic and phototrophic bacterial populations are also common in aquatic environments and affect community structure and population dynamics (2,55).

Positive, or cooperative, interactions between prokaryotic species include commensal, syntrophic, and symbiotic relationships (Table 1.1). Both symbiotic and commensal interactions are common between prokaryotes and eukaryotes. Examples include the symbiotic fixation of nitrogen in legumes and the commensal microflora of mammalian gastrointestinal tracts. Among prokaryotes, cooperative relationships appear to be more important in anaerobic than in aerobic environments. The oxidation of compounds without highly oxidizing electron acceptors, such as oxygen or nitrate, requires a large enzymatic machinery and detailed metabolic conversions to gain energy. Consequently, complete anaerobic oxidation occurs in steps that are catalyzed by different organisms. The anaerobic food chain that results from the step-wise oxidation of organic compounds necessitates a greater level of interaction between microbial species (7,17,45). Highly structured environments, such as microbial mats and biofilms, are also characterized by a high level of interspecies interactions (positive and negative) due to the close proximity of cells and microscale chemical gradients that are important for the metabolism of the organisms within the community (38,53).

Negative interactions and community structure. Competition is an interaction that has a negative impact on the growth of the interacting species. Two types of competition between organisms are possible, exploitative competition and interference competition. Exploitative competition refers to the physical/biochemical race for uptake of substrate, while interference competition (a.k.a amensalism) refers to the direct infliction of harm

on a

repre

a spe

impa

ultim

comp

prod

gene

som

mae

thus

mic

upon

gro

mod

com

con

(4)

calc

inter

by

on competing species. The negative impact of competition can be mathematically represented by a coefficient that decreases the growth rate, or increases the death rate, of a species depending upon the concentration of other competitors. The species that is impacted the least by the presence of other competitors (i.e. has the smallest coefficient) ultimately wins the competition, excluding the other species (24). Interference competition is common in microbial communities, especially in soil environments. The production of a wide variety of antibiotics by fungi and bacteria, and the evolution of genes to combat these antibiotics, attests the importance of interference competition in some microbial communities.

Many microbes have similar nutritional and energetic demands that they must meet from a limited pool of organic and inorganic compounds in natural environments; thus, exploitative or substrate competition may be the most common type of negative microbial species interaction. The outcome of resource competition is solely dependent upon the concentration of the substrate in the environment and the shape of the Monod growth curve (s versus μ) of the competing organisms (32,41) (Figure 1.1). The Monod model of substrate dependent specific growth rate [$\mu = \mu_{max} s/(s + K_s)$] is the most common mathematical equation used for microbial growth under substrate limiting conditions because of its simplicity and accuracy in fitting most cases reasonably well (4). A large number of experimental studies of single substrate competition in chemostat cultures support this model (13,15,16,25,26,41).

According to the Monod model, bacteria can use two different strategies to increase their competitiveness for a single substrate (Figure 1.1). One strategy is typified by oligotrophs, organisms adapted to stable, low-nutrient environments that have high

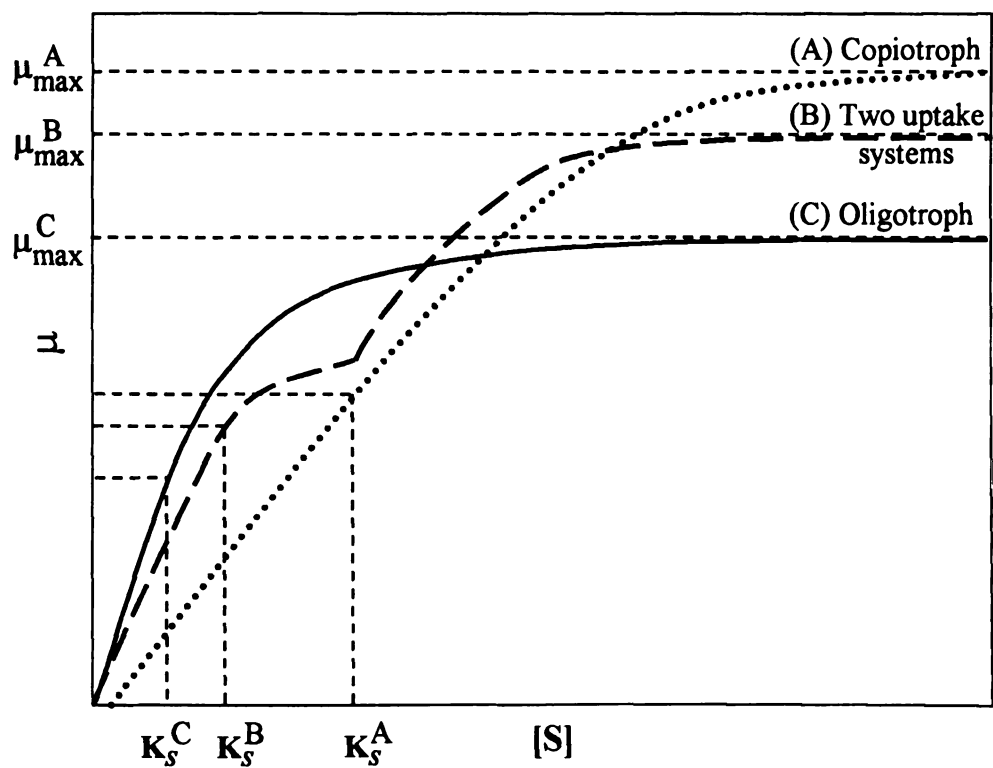


Figure 1.1 μ versus s relationship of a copiotroph (A), an organism with high and low affinity uptake systems (B), and an oligotroph (C).

substr

typical

that h

strate,

and lo

11),

for th

struct

area

a hyd

low le

where

affin

alter

hydro

the c

than

are o

more

possi

1910

substrate affinity and relatively low maximum specific growth rates. The other strategy is typified by copiotrophs, organisms adapted to fluctuating, high-nutrient environments that have lower substrate affinity and higher maximum specific growth rates. These strategies are not necessarily mutually exclusive. Many microorganisms have both high and low affinity uptake systems that are induced under the appropriate conditions (Figure 1.1); however, obligate oligotrophs and copiotrophs are also known that are specialized for these two different lifestyles (14).

In anaerobic environments single substrate competition is a major force in structuring the microbial community. For example, competition for hydrogen in anaerobic environments is fierce, and organisms that can't compete in environments with a hydrogen partial pressure below their thermodynamic limits are only present at very low levels. Hydrogen-consuming methanogens are generally not active in environments where nitrate-, sulfate-, or iron-reducers are active because these organisms have a higher affinity for hydrogen than methanogens. This is not only due to the thermodynamics of different electron-accepting processes, but also to the lower affinity of methanogens for hydrogen (29).

Despite intense resource competition, many conditions and adaptations allow for the co-existence of species. The presence of multiple substrates and the need for more than one nutrient (e.g. carbon, oxygen, nitrogen, phosphate, etc.) in natural environments are obvious mechanisms for co-existence of similar species. When growth is limited by more than one substrate, such as carbon and nitrogen simultaneously, co-existence is possible. Multiple substrate limitation is a large subject and is reviewed elsewhere (9,10,15,16,31). In addition, the sources of carbon and energy in natural environments are

diverse

such a

tempor

during

For in

amount

comple

carbon

applied

implic

load (1

newly

togethe

microb

well b

Quite

transfe

Transf

Sidirec

two d

betwee

the con

diverse, potentially creating different niches for microbes to occupy. Other conditions, such as predation, environmental perturbations, non-homogeneous micro-habitats, temporal variability, and interference competition, can disrupt competitive exclusion during competition for a single substrate, allowing many species to coexist (6,19,23,48). For instance, studies of glucose-fed methanogenic reactors have found a surprising amount of redundancy among organisms capable of fermenting glucose. In these completely mixed reactors competitive exclusion was presumably excluded by the use of carbon and energy sources other than glucose and the alternating feed-starve cycles applied to the some of the reactors (11,12,56). This redundancy had important implications for functional recovery of the reactors after application of an organic shock load (11,21).

Positive interactions and community structure. Odum (1983) (35) noted that newly introduced species tend to interact negatively, while species that have evolved together over long periods of time tend to develop positive interactions. Considering that microbes are the oldest forms of life on earth, positive interactions among microbes may well be the most common interspecies interaction occurring in microbial communities. Quite a few positive species interactions between microbes are understood, and the transfer of molecules between the cooperating species has been defined (Table 1.2). Transfer of molecules between cooperating species may be unidirectional or bidirectional. Cooperative interactions may depend upon transfer of molecules between two different metabolic types of organisms, or may require specific communication between co-evolved species. An example of a non-specific unidirectional cooperation is the consumption of the waste products of one bacterium by another. Even this type of

Table 1.2. Specificity of some cooperative interspecies interactions between prokaryotes.

Interaction		Organisms involved		Molecules transferred	
Nutritional cross-feeding (general)		Auxotroph → Prototroph		Growth factors (constitutive excretion)	
Low Specificity	Food chain	Trophic level A → Trophic level B		Waste products (organic acids, etc)	
	Hydrogen transfer	H ₂ producer → H ₂ consumer		Fatty acid, etc → Acetate + H ₂ H ₂ + Ac ^{ox} → H ₂ O + Ac ^{re}	
	Oxygen protection	Anaerobe ↔ Aerobe		Oxygen Waste Products (organic acids)	
	Sulfur recycling	H ₂ S producer ↔ H ₂ S oxidizer		S ⁰ + Organic C → CO ₂ + S ⁻² CO ₂ + S ⁻² + light → Organic C + S ⁰	
High Specificity ^a	Anaerobic methane oxidation	Methanogen → Sulfate-reducer		CH ₄ + 2H ₂ O → CO ₂ + 4H ₂ SO ₄ ⁻² + 5H ₂ → H ₂ S + 4H ₂ O	
	Nutritional cross-feeding (specific) ^a	Auxotroph ↔ Prototroph		Growth factors (inducible excretion) Inducer molecules	
	Interspecies signaling	Species A ↔ Species B		Homoserine lactones Siderophores	
	Obligate symbiosis	Green sulfur epibiont ↔ β-proteobacterium central rod		Unknown	

^a Hypothetical interaction.

simpl

where

anaer

in the

therm

depen

of a

organ

hydro

acids

(Tab

organ

prod

incre

exam

bact

cell

spec

that

Mic

com

simple interaction creates growth conditions that are different than those in pure culture, where most of our knowledge of metabolism is gained.

The most well studied cooperative interaction between prokaryotic species in anaerobic environments is the syntrophic interaction of two metabolically distinct species in the degradation of a substrate that neither species could degrade alone because of thermodynamic constraints. The term syntrophic specifically implies that both partners depend on each other for some metabolic activity that can not be replaced by the addition of a cofactor or nutrient (46). Syntrophic interactions between hydrogen-oxidizing organisms, such as methanogens, sulfate-reducers, or homoacetogens, and a variety of hydrogen-producing fermentative bacteria are necessary for the degradation of fatty acids, ethanol, glycolic acids, and aromatic compounds under anaerobic conditions (46) (Table 1.2). Synergistic interspecies hydrogen transfer also benefits sugar-fermenting organisms by allowing them to produce more hydrogen and oxidized fermentation products, increasing the energy yield per molecule. Other interspecies interactions that increase mineralization rates in anaerobic environments are poorly understood. For example, undefined interactions between saccharolytic spirochetes and cellulolytic bacteria, such as *Spirochaeta caldaria* and *Clostridium thermocellum*, enhance the rate of cellulose degradation as much as two-fold over the rate of degradation by the cellulolytic species alone (40,49).

Many anaerobes have nutritional requirements for certain vitamins or amino acids that may also be the basis of cooperative interactions among microbial species. Microorganisms found in food products and animal or plant associated environments commonly require multiple amino acids and vitamins that are found in adequate supply in

their

isolat

and

auxo

that

contr

Inde,

litbo

vitan

prod

inter

the s

main

hom

Legn

Plan

uni

imp

shir

com

char

the

their environment. However, a survey of microorganisms revealed that organisms isolated from environments that would not necessarily have an abundance of vitamins and amino acids, such as sediments and other aquatic environments, are often auxotrophic for one to several vitamins such as biotin, thiamine, or cobalamin, suggesting that these vitamins may be supplied by other community members (this study). In contrast to aquatic environments, prototrophs were more common in soil environments. Independent of the environment from which they were isolated, autotrophic and lithotrophic microorganisms were the most likely metabolic groups to synthesize all vitamins and amino acids *de novo*. The excretion of large amounts of various organic products by autotrophs, especially photoautotrophs, is the basis of many cooperative interactions. The benefit of these interactions for the autotroph is not obvious, but include the stimulation of N_2 fixation, an increase in local CO_2 concentrations, and the structural maintenance of mat communities (17). The only large phylogenetic groups to homogeneously express prototrophy were the γ -proteobacteria (except the genera *Legionella* and *Haemophilus*, and few other cases of single vitamin requirements) and the *Planctomycetes*.

Interactions between guilds within anaerobic communities, aside from the unidirectional transfer of products through the anaerobic food chain, may be very important for stable ecosystem function. In a previous study of methanogenic bioreactors, shifts in the composition of the methanogenic guild corresponded to dramatic compositional changes in the fermentative bacterial community. These compositional changes did not appear to affect ecosystem function (12). It is not clear why a change in the species composition of hydrogenotrophic and acetotrophic methanogens should affect

ferme

effect

betwe

finer

and s

envir

to be

envir

comm

orga

Inve

Bei

four

of i

simp

simp

meth

The

cult

amm

fermentative species, or vice versa, as long as both hydrogen and acetate are removed effectively. This concerted change in the two guilds suggests that direct interactions between the fermentative and methanogenic guilds may exist that are important for the function of both guilds.

Microbial interactions such as those defined above that change degradation rates and substrate uptake profoundly affect our models of anaerobic mineralization in natural environments. In addition, species and strain specific cooperative interactions are likely to be one reason for the difficulty in culturing many microorganisms from natural environments. Because of the importance of interspecies interactions in microbial communities, a concerted effort must be made to study the physiology of assemblages of organisms.

Investigating microbial species interactions

Enrichment culture. The traditional enrichment culture technique developed by Beijerinck and Winogradsky at the beginning of the twentieth century is one of the foundations of microbial ecology. Enrichment cultures are especially useful for the study of interspecies interactions if an enrichment culture is viewed as a way to study a simplified community that is carrying out a specific biochemical process, rather than as simply a means to obtain a pure culture. Either continuous or batch enrichment culture methods can be utilized to simulate the natural environmental conditions more closely. The enrichment of ammonia-oxidizing bacteria is a good example of how enrichment cultures may be used in the study of substrate competition. Enrichment cultures for ammonia-oxidizing bacteria yield different organisms depending upon the concentration

of an

amm

amm

inter

comm

be n

techn

cultu

mem

The

meth

(8)

lead

Wga

sing

wher

such

Th

purp

the

spec

of ammonia used in the enrichment, indicating that there are at least two types of ammonia-oxidizing bacteria in nature that are specialized for different concentrations of ammonia.

Enrichment cultures are even more appropriate for the study of cooperative interactions. After simplifying a natural microbial community to those microbes connected to the process of interest, the members of the enrichment and their roles may be more easily discerned than in the natural environment. The use of molecular techniques (see below) to identify the members of an enrichment culture and subculturing of individual members may allow the elucidation of the roles of the dominant members and further understanding of the process as it occurs in natural environments. The discovery that a type II methanotroph could oxidize atmospheric concentrations of methane when cultivated in the presence of *Variovorax* species was made in such a way (8).

Coculture. Deliberate coculture of two organisms already in pure culture has also lead to many important discoveries about interspecies interactions. The coculture of two organisms in continuous and batch systems is a common method to study competition for single or multiple substrates, as mentioned above. Cases of coexistence of two species when competitive exclusion was expected are perhaps the most interesting outcome of such competition experiments. The coculture of two sulfide-oxidizing bacteria, *Thiobacillus*, a colorless sulfide-oxidizing bacterium, and *Thiocapsa*, a photosynthetic purple sulfur bacterium, under oxygen-limiting conditions resulted in the coexistence of the two species rather than the predicted exclusion of *Thiocapsa*. The *Thiobacillus* species produced incompletely oxidized sulfur compounds under oxygen-limited

condi:

electr

for su

cultu

orga

fatty

result

lead

techn

micro

spec

Mark

did n

prese

orga

in in

enri

sym

imp

sam

pro

inter

conditions. The *Thiocapsa* species used the incompletely oxidized sulfur compounds as electron donors rather than sulfide. Thus, the two species were no longer in competition for sulfide, but actually cooperated under habitat-simulating conditions (52).

The discovery of syntrophic growth through interspecies hydrogen transfer in the culture "*Methanobacillus omelianskii*" has lead to the isolation of a number of syntrophic organisms. A greater understanding of anaerobic degradation of even and odd-chained fatty acids, branched chain fatty acids, amino acids, ethanol, and aromatic compounds has resulted (46). Coculture of sulfide-oxidizing and sulfide-producing microbes has also lead to a greater understanding of the sulfur cycle in natural systems. The use of coculture techniques may significantly increase the culturability of environmentally important microorganisms as well. In a study of rice paddy soils, it was reported that different species of lactate and ethanol utilizers were isolated depending upon whether or not *Methanospirillum hungatei* was used in the enrichment medium. The organisms isolated did not require the presence of a methanogen in order to oxidize lactate or ethanol, yet the presence of the methanogen allowed the isolation of the numerically dominant soil organisms, while without the methanogen, organisms that were not numerically dominant in the environment were isolated instead (43). The idea of using coculture techniques in enrichment cultures, even when the process being studied is not thought to require any syntrophic interactions, may prove very helpful in the isolation of environmentally important microbes. Studying cocultures of organisms that are known to cohabitate the same environments may lead to the discovery of new interactions, even if there is no *a priori* reason that a coculture would be required for the organisms or processes of interest.

envir

betwe

Orga

form

betw

imag

hybr

envir

arran

Beza

sequ

posit

enric

radi

pop

tech

unac

form

have

com

Microscopy. The spatial distribution of microorganisms within their natural environment can be very important for their activity. The efficiency of metabolite transfer between two cells is inversely proportional to the distance between the two (47). Organisms that are known to interact in the syntrophic degradation of compounds often form specific structural arrangements that allow for the efficient transfer of molecules between the two populations in the environment (20,33). The use of microscopy and image analysis may therefore be very helpful in the study of interspecies interactions.

The use of 16S rRNA-targeted oligonucleotides in fluorescent *in situ* hybridization (FISH) allows the visualization of specific microbial populations in environmental samples (1). In conjunction with confocal laser scanning microscopy, the arrangement of cells in thin sections of biofilms and aggregates can also be seen. Because oligonucleotides can be designed for organisms that are only represented by sequence information, valuable information about uncultured organisms' morphology, position, and associations with other cells in their natural environment or in an enrichment culture can be described (Figure 1.2). The simultaneous application of FISH, radiolabeled substrates, and autoradiography can give additional information about which populations are utilizing different substrates (18,28,36). Information from these techniques may aid in design of enrichment strategies, including cocultures, for uncultivated microorganisms. In addition, studying the positioning and associations formed by cultivated microorganisms could indicate an interspecies interaction that we have overlooked that may be important for the *in situ* activity of the microorganisms.

Molecular methods. Our ability to describe the members of a microbial community has drastically improved in the last three decades due to the development of

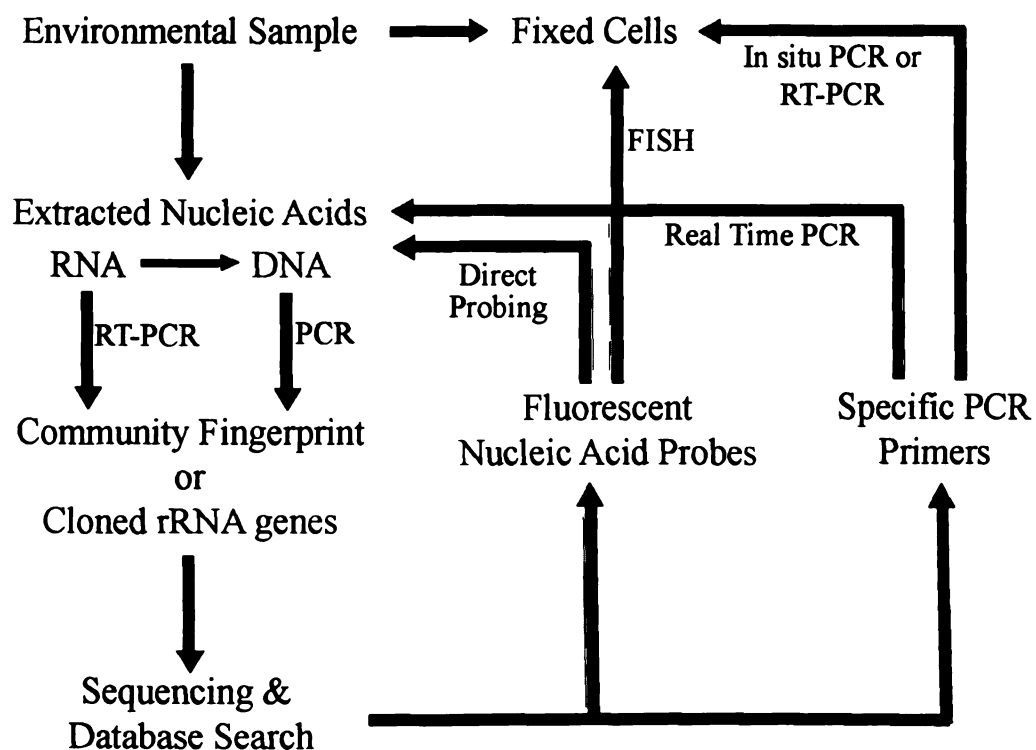


Figure 1.2 Flow chart of molecular microbial ecology methods for community analysis and monitoring of specific phylogenetic groups of microorganisms. RT-PCR = Reverse transcription polymerase chain reaction. FISH = Fluorescent *in situ* hybridization.

the pol

method

from er

in the

uncult

method

or bro

visuali

the stu

snapsht

enviro

microb

the se

enrich

organ

holisti

comp

finger

differ

well

micro

micro

the polymerase chain reaction (PCR) and 16S rRNA and DNA based phylogenetic methods (39,54) (Figure 1.2). Amplification and cloning of 16S rRNA genes directly from environmental samples has opened our eyes to the vast diversity of microorganisms in the natural environment, and has allowed the development of methods to learn about uncultivated microorganisms. Many different applications of 16S rDNA and rRNA methods allow the detection, and even quantification, of specific strains, species, genera, or broad phylogenetic groups (Table 1.3). Molecular methods that allow the *in situ* visualization of specific organisms, such as FISH, are among the most useful methods for the study of interspecies interactions. Other methods aim to provide a fingerprint, or snapshot, of microbial community composition, allowing the rapid comparison of many environmental samples. The use of molecular techniques to monitor the composition of microbial communities in enrichment cultures has greatly improved our understanding of the selective bias of the conditions applied (44). In addition, molecular analysis of enrichment cultures has resulted in the discovery of new interspecies interactions, organisms, and physiologies (8,22,30,50)

Another way to elucidate important interspecies interactions is to take a more holistic approach and study whole communities in their natural environment. Rapid comparison of microbial communities with DGGE, T-RFLP, and other community fingerprinting methods have allowed robust comparisons of microbial communities in different layers of microbial mats, soils, lake strata, freshwater and marine sediments, as well as changes in community structure over time (3,34,37,42,51,56). Quite a few microorganisms whose 16S rDNA gene sequences were retrieved from the same microenvironment repeatedly (i.e. the same depth layer of a microbial mat or stratified

Table 1.3 The purpose and potential application of molecular microbial ecology methods for the study of interspecies interactions

Method	Purpose	Application
--------	---------	-------------

Table 1.3. The purpose and potential application of molecular microbial ecology methods for the study of interspecies interactions.

Method	Purpose	Application
16S rRNA gene cloning and sequencing	Discovery of new 16S rRNA gene sequences and putative organisms	Basis for the design of oligonucleotide probes and PCR primers for other methods
Denaturing gradient gel electrophoresis (DGGE)	Rapid community fingerprint	Monitoring and comparison of communities or enrichment cultures
Terminal restriction fragment length polymorphism analysis (T-RFLP)	Rapid community fingerprint	Monitoring and comparison of communities or enrichment cultures
Fatty acid methyl ester analysis (FAME)	Rapid community fingerprint	Monitoring and comparison of communities or enrichment cultures
Real-time PCR	Quantification of specific target sequences	Monitoring and comparison of target sequence abundance in communities or enrichment cultures
16S rRNA gene microarrays	Quantification of a large number of target sequences simultaneously	Monitoring and comparison of communities or enrichment cultures
Fluorescent in situ hybridization (FISH)	Visualization and quantification of phylogenetic groups of organisms	Monitoring and comparison of specific populations in communities or enrichment cultures Description of physical associations of microorganisms
Single cell autoradiography and fluorescent in situ hybridization	Quantification and identification of microorganisms and function of interest	Description of physical associations of microorganisms and their activities

lake)

Comp

differe

Impl

impe

natu

pe'a

betw

hom

cont

prob

cult

but

of n

our

inte

the

new

env

lake) were eventually shown to have relatively strong interspecies interactions (37,38). Competition between species could also presumably be deduced if the size of two different microbial populations were inversely related over time.

Implications

Interspecies interactions have repeatedly been demonstrated to be extremely important for the *in situ* activity of microorganisms in many environments. In most natural habitats microbes are in close proximity to cells of other species. If bacteria in pelagic and benthic environments were homogeneously distributed, the average distance between cells would be between 122 and 12 μm . In reality, bacteria are not homogeneously distributed, but form aggregates, microcolonies, and biofilms that contain multiple species, thus the distance between cells in their natural habitat is probably much less than 12 μm on average (38). The study of microorganisms in pure culture has undoubtedly taught us much about general and environmental microbiology, but it has also caused many misconceptions of the true kinetic and metabolic capabilities of microorganisms in their natural habitats. These misconceptions significantly impact our models of biogeochemical transformations. The advances made in the study of interspecies interactions imply that the interactions that occur may be quite different from the paradigm of syntrophy formed from examples in anaerobic environments. Exploring new ideas about interspecies interaction may substantially increase the number of environmentally important microorganisms that can be cultivated.

Thesis over

The

anaerobic

understand

mammalian

communiti

settings an

concentrati

difficult. A

daily pro

communiti

microbial

syntrophic

bioreactor

different le

Pre

repeatedly

Many spe

cellulose-e

termite gi

dioxide, a

homoacet

repeated e

Thesis overview

The tight metabolic coupling and interspecies interactions necessary for the anaerobic degradation of organic matter are fascinating and important for our understanding of global carbon and nutrient cycling, wastewater treatment, and mammalian gastrointestinal tract communities. However, natural anaerobic microbial communities are very complex because of the variety of substrates available in natural settings and the fluctuation of physical parameters such as temperature, pH, and nutrient concentrations. Manipulating natural environments and communities is also very difficult. Anaerobic bioreactors fed continuously with glucose at a loading rate of $0.5 \text{ g} \cdot \text{l}^{-1} \cdot \text{day}^{-1}$ provided a manageable environment to examine methanogenic microbial communities (Figure 1.3). No electron acceptors were added to the chemostats, thus the microbial community should contain three main guilds of organisms: glucose fermenters, syntrophic fatty acid and ethanol fermenters, and methanogens (Figure 1.4). The bioreactors used in this study were inoculated from various sources and operated for different lengths of time (Figure 2.1).

Preliminary work on the microbial communities of these simple bioreactors repeatedly documented enrichment of spiral-shaped cells that resembled spirochetes. Many species of spirochetes are responsible for disease, while others flourish in cellulose-degrading environments such as salt marsh sediments, the rumen and the termite gut (5). Most spirochetes ferment sugars to acetate, ethanol, hydrogen, carbon dioxide, and lactate; however, recent termite-gut isolates were shown to be H_2/CO_2 homoacetogens (27). Spirochete species can be difficult to cultivate, therefore the repeated enrichment of the spirochetes in the bioreactors provided a unique opportunity

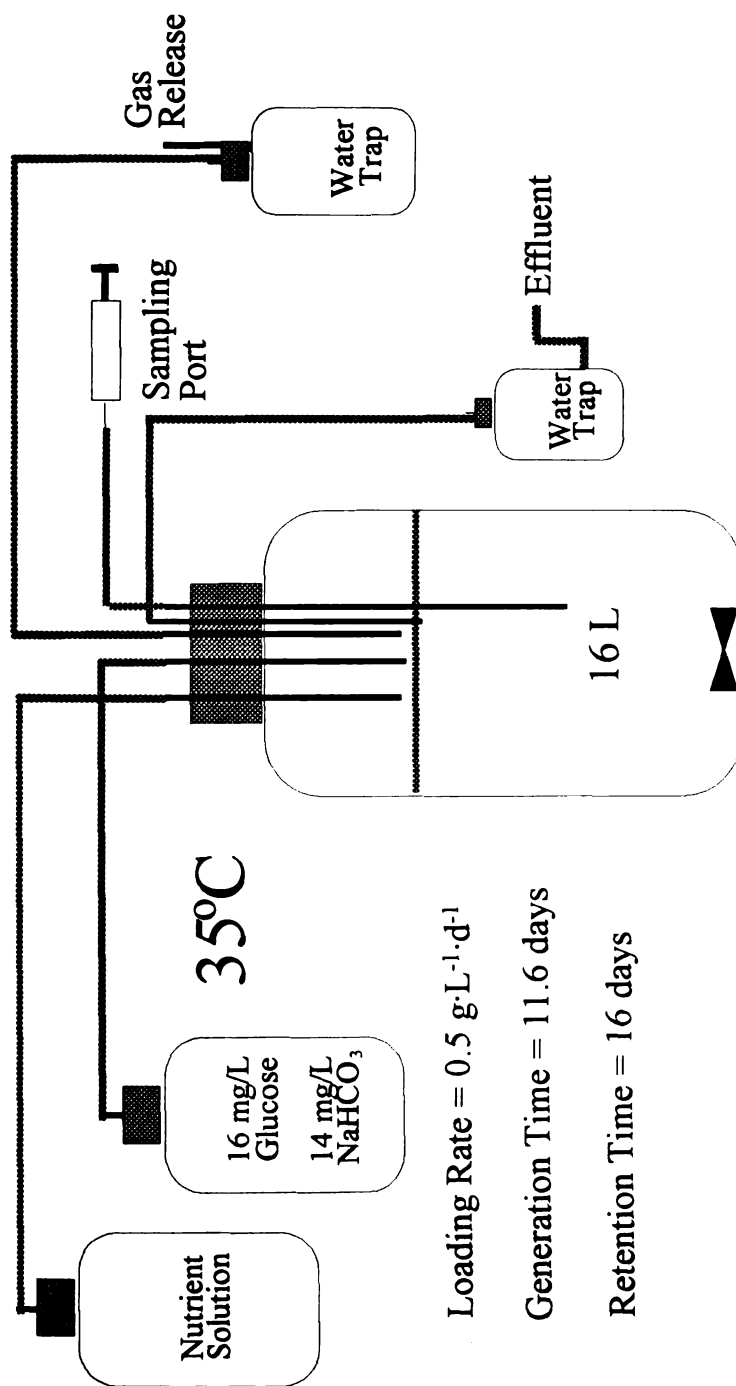


Figure 1.3. Bioreactor design.

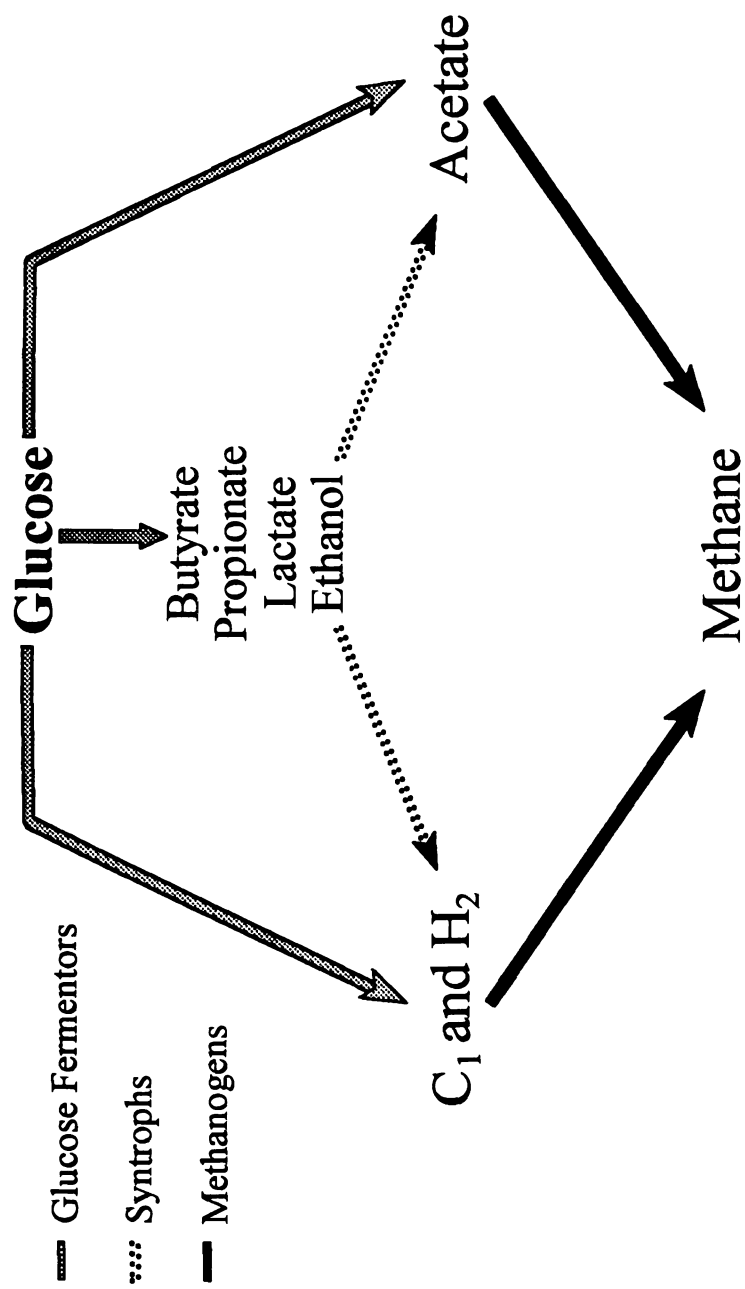


Figure 1.4 Functional groups of microorganisms in glucose-fed methanogenic bioreactors.

to stu

The f

these

Hyp

Hyp

Hyp

Hyp

Exp

the

biom

fluid

date

:DN

to study their biology and ecology in an environment that could be easily manipulated. The following hypotheses were evaluated concerning the ecophysiology of spirochetes in these methanogenic bioreactors:

Hypothesis 1: Spirochetes are members of the glucose fermenting guild in methanogenic bioreactors.

Hypothesis 2: Spirochetes dominate the glucose fermenting guild in methanogenic reactors when the *in situ* glucose concentration is low because they are adapted for growth at low substrate concentrations.

Hypothesis 3: Removal of H₂/formate by H₂-utilizing methanogen species increases the growth yield of spirochetes on glucose.

Hypothesis 4: Cooperative interactions other than interspecies hydrogen transfer exist between methanogens and spirochetes that are important to the ecology of both microorganisms.

Experimental design

Research presented in chapter 2 explores the microbial diversity and structure of the bioreactor communities. Chapter 3 addresses the ecological role of spirochetes in the bioreactor communities (Hypothesis 1) Spirochete strains were isolated from bioreactor fluid and characterized. ¹⁴C-labeled glucose was fed to bioreactor communities to determine the flow of carbon through the ecosystem. Molecular methods based on 16S rDNA were used to confirm that the spirochete strains isolated were the dominant

organ

glucose

the

study

include

described

of two

Clos

course

a sub

also

to d

cross

was

of th

Ref

1. A

2. B

3. B

organisms in the bioreactors. These studies revealed that spirochetes were fermenting glucose to hydrogen, acetate, and ethanol in the bioreactor community.

The question of why the spirochetes dominated the glucose-fermenting guild in the bioreactor communities required whole community, pure culture, and coculture studies. Chapter 4 presents the effects of dilution rate on the entire bioreactor community, including changes in spirochete and other glucose-fermenting populations. Chapter 5 describes the results of pure and mixed culture studies, including chemostat competition of two predominate strains isolated from bioreactor fluid, *Spirochaeta* sp. strain R8 and *Clostridium ramosum* strain S9. The results indicate that spirochetes are able to outcompete most other glucose-fermenting organisms provided that the spirochetes have a sufficient source of cofactors or vitamins required for growth.

The final questions about interactions between spirochetes and methanogens are also presented in chapter 5. Pure culture, coculture, and triculture experiments were used to demonstrate that the interaction between spirochetes and methanogens involved the cross-feeding of pantothenate or a similar molecule. The cross-feeding of pantothenate was also determined to be an important factor in determining the competitive advantage of the spirochete strain.

References

1. Amann RI, Ludwig W, Schleifer K (1995) Phylogenetic identification and in situ detection of individual microbial cells without cultivation. *Microbiol Rev* 59:143-169
2. Bergh O, Borsheim KY, Bratbak G, Heldal M (1989) High abundance of viruses found in aquatic environments. *Nature* 340:467-468
3. Buckley DH, Schmidt TM (2001) The structure of microbial communities in soil and the lasting impacts of cultivation. *Microb Ecol* DOI: 10.1007/s002480000108

4 B

5 C

6 D

7 D

8 D

9 D

10

11

12

13

14

15

16

17

4. Button DK (1985) Kinetics of nutrient limited transport and microbial growth. *Microbiol Rev* 49:270-297
5. Canale-Parola E (1977) Physiology and evolution of spirochetes. *Bacteriol Rev* 41:181-204
6. De Freitas MJ, Fredrickson AG (1978) Inhibition as a factor in the maintenance of the diversity of microbial ecosystems. *J Gen Microbiol* 106:307-320
7. Dolfing J (2001) The microbial logic behind the prevalence of incomplete oxidation of organic compounds by acetogenic bacteria in methanogenic environments. *Microb Ecol* DOI: 10.1007/s002480000076
8. Dunfield PF, Liesack W, Henckel T, Knowles R, Conrad R (1999) High-affinity methane oxidation by a soil enrichment culture containing a type II methanotroph. *Appl Environ Microbiol* 65:1009-1014
9. Dykhuizen DE, Davies M (1980) An experimental model: bacterial specialists and generalists competing in chemostats. *Ecology* 61:1213-1227
10. Egli T (1991) On multiple-nutrient-limited growth of microorganisms, with special reference to dual limitation by carbon and nitrogen substrates. *Antonie van Leeuwenhoek* 60:225-234
11. Fernandez A, Hashsham S, Dollhopf SL, Raskin L, Glagoleva O, Dazzo FB, Hickey RF, Criddle C, Tiedje JM (2000) Flexible community structure correlates with stable community function in methanogenic bioreactor communities perturbed by glucose. *Appl Environ Microbiol* 66:4058-4067
12. Fernandez A, Huang S, Seston S, Xing J, Hickey RF, Criddle C, Tiedje JM (1999) How stable is stable? Function vs community stability. *Appl Environ Microbiol* 65:3697-3704
13. Fredrickson AG (1977) Behaviour of mixed cultures of microorganisms. *Ann Rev Microbiol* 31:63-87
14. Fry JC (1990) Oligotrophs. In: Edwards CA (ed) *Microbiology of Extreme Environments*. Open University Press, Milton Keynes, pp 93-116
15. Gottschal JC (1985) Some reflections on microbial competitiveness among heterotrophic bacteria. *Antonie van Leeuwenhoek* 51:473-494
16. Gottschal JC (1993) Growth kinetics and competition - some contemporary comments. *Antonie van Leeuwenhoek* 63:299-313
17. Gottschal JC, Harder W, Prins RA (1992) Principles of enrichment, isolation, cultivation, and preservation of bacteria. In: Balows A, Truper HG, Dworkin M, Schleifer K (eds) *The Prokaryotes, A Handbook on the Biology of Bacteria*.

18 C

19 F

20 F

21 F

22

23

24

25

26

27

28

Ecophysiology, Isolation, Identification, Applications, vol 1. Springer-Verlag, New York, NY, pp 149-196

18. Gray ND, Howarth R, Pickup RW, Jones JG, Head IM (2000) Use of combined microautoradiography and fluorescence in situ hybridization to determine carbon metabolism in mixed natural communities of uncultured bacteria from the genus *Achromatium*. Appl Environ Microbiol 66:4518-4522
19. Hansen SR, Hubbel SP (1980) Single-nutrient microbial competition: Qualitative agreement between experimental and theoretical forecast outcomes. Science 207:1491-1493
20. Harmsen HJM, Kengen HMP, Akkermans ADL, Stams AJM, de Vos WM (1996) Detection and localization of syntrophic propionate-oxidizing bacteria in granular sludge by in situ hybridization using 16S rRNA-based oligonucleotide probes. Appl Environ Microbiol 62:1656-1663
21. Hashsham S, Fernandez A, Dollhopf SL, Dazzo FB, Hickey RF, Tiedje JM, Criddle C (2000) Parallel processing of substrate correlates with greater functional stability in methanogenic bioreactor communities perturbed by glucose. Appl Environ Microbiol 66:4050-4057
22. Holoman TRP, Elberson MA, Cutter LA, May HD, Sowers KR (1998) Characterization of a defined 2,3,5,6-tetrachlorobiphenyl-*ortho*-dechlorinating microbial community by comparative sequence analysis of genes coding for 16S rRNA. Appl Environ Microbiol 64:3359-3367
23. Huston MA (1994) Biological Diversity: The coexistence of species on changing landscapes. Cambridge University Press, New York, NY
24. Keddy PA (1989) Competition. Chapman and Hall, London; New York
25. Kuenen JG, Gottschal JC (1982) Competition among chemolithotrophs and methylotrophs and their interactions with heterotrophic bacteria. In: Bull AT, Slater JH (eds) Microbial Interactions and Communities, vol 1. Academic Press, London, pp 153-187
26. Kuenen JG, Harder W (1982) Microbial competition in continuous culture. In: Burns RG, Slater JH (eds) Experimental Microbial Ecology. Blackwell Scientific Publications, Oxford, pp 342-367
27. Leadbetter JR, Schmidt TM, Graber JR, Breznak JA (1999) Acetogenesis from H₂ plus CO₂ by spirochetes from termite guts. Science 283:686-689
28. Lee N, Nielsen PH, Andreasen KH, Juretschko S, Nielsen JL, Schleifer K-H, Wagner M (1999) Combination of fluorescent in situ hybridization and

29 L

30 M

31 M

32 M

33 M

34 M

35 C

36

37

38

39 P

- microautoradiography - a new tool for structure-function analyses in microbial ecology. *Appl Environ Microbiol* 65:1289-1297
29. Lovley DR, Dwyer DF, Klug MJ (1982) Kinetic analysis of competition between sulfate reducers and methanogens for hydrogen in sediments. *Appl Environ Microbiol* 43:1373-1379
 30. Maltseva O, Oriel P (1997) Monitoring of an alkaline 2,4,6-trichlorophenol-degrading enrichment culture by DNA fingerprinting methods and isolation of the responsible organism, haloalkaliphilic *Nocardioides* sp. strain M6. *Appl Environ Microbiol* 63:4145-4149
 31. Mateles RI, Chian SK, Silver R (1967) Continuous culture on mixed substrates. Mixed cultures - mixed substrates. In: Powell EO, Evans C, Strange RE, Tempest DW (eds) *Microbial physiology and continuous culture*. H.M.S.O., London, pp 233-239
 32. Monod J (1942) *Recherches sur la Croissance des Cultures Bacteriennes*. Hermann & Cie., Paris
 33. Nielsen AT, Tolker-Nielsen T, Barken KB, Molin S (2000) Role of commensal relationships on the spatial structure of a surface-attached microbial consortium. *Environ Microbiol* 2:59-68
 34. Nubel U, Garcia-Pichel F, Clavero E, Muyzer G (2000) Matching molecular diversity and ecophysiology of benthic cyanobacteria and diatoms in communities along a salinity gradient. *Environ Microbiol* 2:217-26
 35. Odum HT (1983) *Systems Ecology: An Introduction*. Wiley, New York
 36. Ouverney CC, Fuhrman JA (1999) Combined microautoradiography-16S rRNA probe technique for determination of radioisotope uptake by specific microbial cell types in situ. *Appl Environ Microbiol* 65:1746-1752
 37. Overmann J, Coolen MJL, Tuschak C (1999) Specific detection of different phylogenetic groups of chemocline bacteria based on PCR and denaturing gradient gel electrophoresis of 16S rRNA gene fragments. *Arch Microbiol* 172:83-94
 38. Overmann J, van Gernerden H (2000) Microbial interactions involving sulfur bacteria: implications for the ecology and evolution of bacterial communities. *FEMS Microbiol Rev* 24:591-599
 39. Pace NR (1997) A molecular view of microbial diversity and the biosphere. *Science* 276:734-740

40 P

41 P

42 F

43 R

44 S

45 S

46 S

47 S

48 S

49 S

50 T

51 U

40. Pohlschroeder M, Leschine SB, Canale-Parola E (1994) *Spirochaeta caldaria* sp. nov., a thermophilic bacterium that enhances cellulose degradation by *Clostridium thermocellum*. ArchMicrobiol 161:17-24
41. Powel EO (1958) Criteria for the growth of contaminants and mutants in continuous culture. J Gen Microbiol 18:259-268
42. Ramsing NB, Ferris MJ, Ward DM (2000) Highly ordered vertical structure of *Synechococcus* populations within the one-millimeter-thick photic zone of a hot spring cyanobacterial mat. Appl Environ Microbiol 66:1038-1049
43. Rosencrantz D, Rainey FA, Janssen PH (1999) Culturable populations of *Sporomusa* spp. and *Desulfovibrio* spp. in the anoxic bulk soil of flooded rice microcosms. Appl Environ Microbiol 65:3526-3533
44. Santegoeds CM, Nold SC, Ward DM (1996) Denaturing gradient gel electrophoresis used to monitor the enrichment culture of aerobic chemoorganotrophic bacteria from a hot spring cyanobacterial mat. Appl Environ Microbiol 62
45. Schink B (1992) Syntrophism among prokaryotes. In: Balows A, Truper HG, Dworkin M, Harder W, Schleifer K (eds) The Prokaryotes, A Handbook on the Biology of Bacteria: Ecophysiology, Isolation, Identification, Applications, vol 2. Springer-Verlag, New York, NY, pp 276-299
46. Schink B (1997) Energetics of syntrophic cooperation in methanogenic degradation. Microbiol Mol Biol Rev 61:262-280
47. Schink B, Thauer RK (1988) Energetics of syntrophic methane formation and the influence of aggregation. In: Lettinga G (ed) Granular anaerobic sludge: microbiology and technology. Pudoc, Wageningen, The Netherlands, pp 5-17
48. Smith KA, Arah JRM (1985) Anaerobic micro-environments in soil and the occurrence of anaerobic bacteria. In: Jensen V, Kjoller A, Sorensen LH (eds) Microbial Communities in Soil. Proceedings of 33rd FEMS-symposium. Copenhagen. Elsevier Science Publishing Co., London, pp 247-261
49. Stanton TB, Canale-Parola E (1980) *Treponema bryantii* sp. nov., a rumen spirochete that interacts with cellulolytic bacteria. Arch Microbiol 127:145-156
50. Teske A, Sigalevich P, Cohen Y, Muyzer G (1996) Molecular identification of bacteria from a coculture by denaturing gradient gel electrophoresis of 16S ribosomal DNA fragments as a tool for isolation in pure cultures. Appl Environ Microbiol 62:4210-4215
51. Urakawa H, Yoshida T, Nishimura M, Ohwada K (2000) Characterization of depth-related population variation in microbial communities of a coastal marine sediment using 16S rDNA-based approaches and quinone profiling. Environ Microbiol 2:542-54

52. van den Ende FP, Meier J, van Gernerden H (1996) Coexistence of aerobic chemotrophic and anaerobic phototrophic sulfur bacteria under oxygen limitation. *FEMS Microbiol Ecol* 19:141-151
53. Wimpenny J, Manz W, Szewzyk U (2000) Heterogeneity in biofilms. *FEMS Microbiol Rev* 24:661-671
54. Woese CR (1987) Bacterial evolution. *Microbiol Rev* 51:221-271
55. Wommack KE, Ravel J, Hill RT, Colwell RR (1999) Hybridization analysis of Chesapeake Bay virioplankton. *Appl Environ Microbiol* 65:241-250
56. Zumstein E, Moletta R, Godon J-J (2000) Examination of two years of community dynamics in an anerobic bioreactor using fluorescence polymerase chain reaction (PCR) single-strand conformation polymorphism analysis. *Environ Microbiol* 2:69-78

Port:

artic

Crid

com

S.L.

proc

reac

Ferr

Hick

with

gluc

Intr

met

con

phy

of

con

rep

em

n

CHAPTER 2

PHYLOGENY OF METHANOGENIC REACTOR ORGANISMS

Portions of the work presented in this chapter were published previously in the following articles: Fernandez, A., Huang, S., Hashsham, S., **Seston, S.**, Xing, J., Hickey, R., Criddle, C., and Tiedje, J. 1999. How stable is stable? Function versus community composition. *Appl. Environ. Microbiol.* 65:3697-3704; Hashsham, S.A., A. S. Fernandez, **S.L. Dollhopf**, F.B. Dazzo, R.F. Hickey, J.M. Tiedje, and C.S. Criddle. 2000. Parallel processing of substrate corresponds with greater functional stability in methanogenic reactor communities perturbed by glucose. *Appl. Environ. Microbiol.* 66:4050-4057; and Fernandez, A., S.A. Hashsham, **S.L. Dollhopf**, L. Raskin, O. Glagoleva, F.B. Dazzo, R.F. Hickey, C.S. Criddle, and J.M. Tiedje. 2000. Flexible community structure correlates with stable community function in methanogenic reactor communities perturbed by glucose. *Appl. Environ. Microbiol.* 66:4058-4067.

Introduction

There are many diverse environments, natural and man-made, that produce methane. In all cases our knowledge of the environmental factors and organisms controlling methanogenesis is incomplete. We perhaps know the most about the physiology and ecology of organisms involved in the mesophilic, freshwater degradation of sugars to methane. Methanogenic communities metabolizing simple sugars should contain three main functional microbial groups, or guilds. The sugar-utilizing organisms represent one guild. The majority of organisms utilizing sugars in a methanogenic environment should be fermentative due to the lack of suitable electron acceptors, such as O_2 , NO_3^- , and SO_4^{2-} . A vast array of bacteria from many different phylogenetic groups

can

prod

envi

acet

met

uti

H₂

only

hou

men

and

eth

me

con

car

ma

wh

str

thi

in

gr

can ferment simple sugars. The hydrogen, carbon dioxide, organic acids, and alcohols produced by this guild are then utilized by the other two guilds found in methanogenic environments (23).

Acetate, one of the most common fermentative products, is used directly by acetoclastic members of the second guild - the methanogens. Two genera of acetoclastic methanogens are known, *Methanosarcina* and *Methanosaeta*. *Methanosarcina* spp. utilize H_2 and CO_2 , acetate, and methylated amines with generation times of 9 hours on H_2 and CO_2 and 17 hours on acetate. In contrast, all described *Methanosaeta* spp. utilize only acetate, for which they have a high affinity, and have doubling times greater than 24 hours (13). Other methanogens typically found in methanogenic reactors, such as members of the families *Methanobacteriaceae* and *Methanomicrobiaceae*, utilize formate and/or H_2 and CO_2 that is produced during the oxidation of glucose, propionate, butyrate, ethanol, and other fatty acids (21,23).

The syntrophic guild, the third functional group, depends upon H_2 utilizing methanogens to remove H_2 and/or formate from the environment. If H_2 or formate reach concentrations above 1 Pa and 10 μM , respectively, the oxidation of volatile fatty acids carried out by syntrophic organisms is no longer thermodynamically favorable (23). Two main phylogenetic groups of syntrophic bacteria have been described. The first group, which includes the genera *Syntrophobacter*, *Pelobacter*, and various sulfate reducing strains, is found within the delta subclass of the proteobacteria (10,11). The bacteria in this phylogenetic group oxidize ethanol, propionate, and other odd numbered fatty acids in syntrophic associations with hydrogen scavenging bacteria. The other phylogenetic group of syntrophic organisms, which includes the genera *Syntrophomonas*,

Synt

gram

com

clan

met

reve

com

com

und

see

Mat

com

sep

glu

prev

was

cyc

zve

was

Wep

Syntrophospora, and *Syntrophus*, are found in the low percent G+C subdivision of the gram-positive bacteria (1,29). These bacteria oxidize butyrate and some aromatic compounds in syntrophy with hydrogen scavengers (19,20).

In this study our goal was to explore a simple methanogenic community by cloning and identifying the most common bacteria and archaea in 14 continuously stirred methanogenic reactors fed glucose as the sole carbon and energy source. This analysis revealed sequences related to both cultivated and uncultivated prokaryotic species and corresponded well to other studies of methanogenic environments. In addition, we compared the species composition of reactors seeded from different sources, operated under slightly different conditions, or perturbed in some way and found that some species seemed to be indicative of certain reactor conditions.

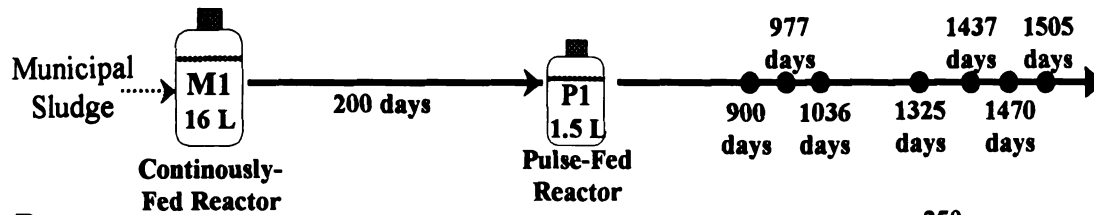
Materials & Methods

Reactor design and operation. Sequences were retrieved from similar continuously stirred, mesothermic (35°C), methanogenic reactors that were part of three separate studies (Figure 2.1). All reactors were fed via a buffered glucose solution ($8 \text{ g glucose} \cdot \text{liter}^{-1} + 6 \text{ NaHCO}_3 \text{ g} \cdot \text{liter}^{-1}$) and a 40X concentrated nutrient solution as previously described (28,12). In the first study a 1.5 liter reactor, designated reactor P1, was inoculated from a 16 L continuously fed reactor and supplied glucose in a 2-day cycle: $16 \text{ g} \cdot \text{liter}^{-1} \cdot \text{day}^{-1}$ for one day and $0 \text{ g} \cdot \text{liter}^{-1} \cdot \text{day}^{-1}$ the following day, resulting in an average loading rate of $8 \text{ g} \cdot \text{liter}^{-1} \cdot \text{day}^{-1}$ (Figure 2.1A). A constant dilution rate (0.1 day^{-1}) was maintained and a steady state was achieved after 400 days.

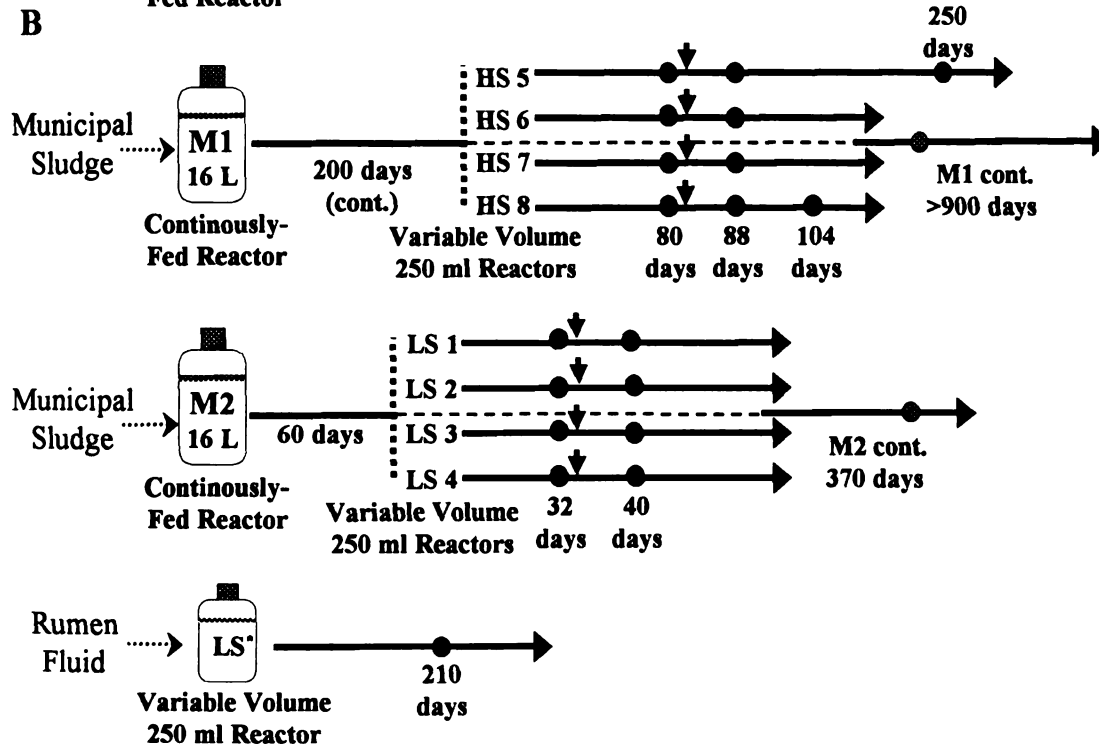
In the second experiment, four reactors [designated the high spirochete (HS) set] were inoculated with fluid from a 16 L methanogenic reactor that had operated for 200

Figure 2.1. Reactor operation and sampling. Dotted horizontal arrows indicate inoculation and solid horizontal arrows indicate reactor operation. Black and gray circles indicate sampling times for 16S rRNA gene clone libraries and bacterial isolation, respectively. Vertical arrows indicate an intentional organic shock load. HRT = hydraulic retention time.

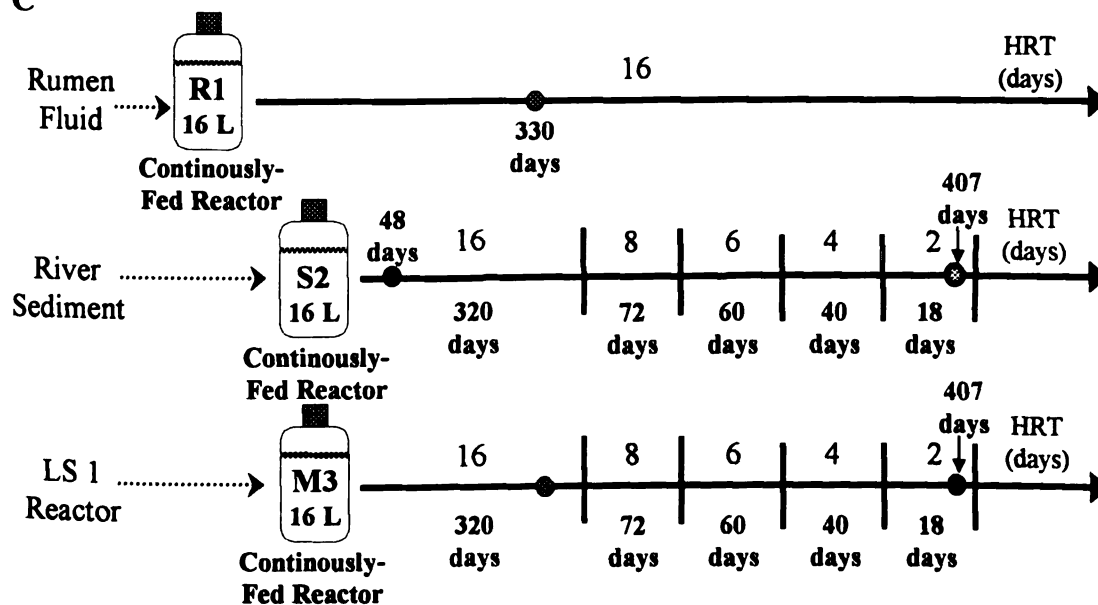
A



B



C



days

react

diffe

LS s

whic

μ M/

gluco

appr

50.5

orga

estat

nume

of th

Cad

prev

resp

pH

reac

115,

desc

ml s

days with glucose as the sole carbon and energy source (Figure 2.1B). The other four reactors [designated the low spirochete (LS) set] were inoculated with fluid from a different methanogenic reactor that had been supplied glucose for 60 days. The HS and LS sets were operated at steady-state conditions for 80 and 32 days, respectively, during which time the concentration of glucose in the reactors was below the detection limit (20 μM) of the HPLC methods used (12). Both sets were then perturbed with a shock load of glucose by instantaneously increasing the concentration of glucose in the reactor liquid to approximately 38 mM using a concentrated sterile stock solution that also contained a 50:50 mixture of NaHCO_3 and KHCO_3 in order to provide buffer for the additional organic acids expected from glucose.

In the third experiment, two reactors were inoculated and compared to a well-established control reactor (Figure 2.1C). Reactor R1 (Rumen 1) was inoculated from rumen fluid and operated under the above conditions for 400 days prior to the inoculation of the two new reactors. The two new reactors were inoculated from sediment of the Red Cedar River in Lansing, MI and a 250 ml variable volume reactor (LS 1) from the previous study and designated reactor S2 (Sediment 2) and reactor M3 (Municipal 3), respectively. Reactor chemical oxygen demand (COD), volatile fatty acids (VFAs), and pH were measured periodically in all reactors to monitor operating efficiency (12,28).

Extraction and purification of community DNA. Community DNA from reactors P1, HS 5-8, and LS 1-4 was extracted from 10 ml samples using a French press (15,000 lb/in²) for lysis and a phenol-chloroform DNA extraction method as previously described (5). Community DNA from reactors M1, R1, S2, and M3 was extracted from 2 ml samples with a bead-beater method (17).

HS 5

1999

prod

Esche

positi

ampl

positi

comp

clone

Bacte

prim

using

acco

whol

dema

zine

(72)

GCC

used

222

were

16S rDNA clone libraries. Bacteria and archaea clone libraries from reactors P1, HS 5-8, and LS 1-4 were constructed by Ana Fernandez as described in Fernandez *et. al.* 1999 (5). Briefly, the bacteria clone libraries were prepared from amplification products produced with a forward primer which corresponds to nucleotide positions 19 to 38 of the *Escherichia coli* rRNA and a reverse primer which corresponds to the complement of positions 1521 to 1541 (27). The archaea clone libraries were prepared from amplification products produced with a forward primer which corresponds to nucleotide positions 50 to 69 of the *E. coli* rRNA (14) and a reverse primer which corresponds to the complement of positions 958 (5'-[C/T]CCGGCGTTGA[A/C]TCCAATT-3') (2). All clone libraries from reactors LS*, R1, S2, and M3 were constructed by S. Dollhopf. Bacteria clone libraries from reactor S2 were constructed using the bacteria-specific primers 8F and 1392R. An archaea-specific clone library from reactor M2 was constructed using archaea-specific primers 21F and 958R (2).

All amplicons were cloned with the TA cloning kit (Invitrogen, Carlsbad, Calif.) according to the manufacturer's instructions. Direct amplification of plasmid DNA from whole cells of white colonies was accomplished with the following conditions: initial denaturation (92 °C for 2 min) followed by 35 cycles of denaturation (94°C for 30 s), annealing (67°C for 1 min), and extension (72°C for 3 min) and a single final extension (72°C for 7 min). Primers complementary to the TA cloning vector 5'-GCCGCCAGTGTGCTGGAATT-3' and 5'-TAGATGCATGCTCGAGCGGC-3' were used (30). The fragment size of these amplicons was checked by electrophoresis in 1 % agarose. PCR products of the right size (1,500 bp for bacteria and 900 bp for archaea) were digested simultaneously for 12 h with two restriction enzymes (*Hae*III and *Hha*I;

Gibco

resist

(wt %

buffe

resul

softw

abund

S2 w

chos

in m

agare

from

of N

in w

10 m

obtai

dilat

exce

nize

from

acce

Gibco BRL, Gaithersburg, MD) according to the manufacturer's specifications. The restriction fragments from each clone were separated by electrophoresis on a 3.5 % (wt/vol) MetaPhor agarose gel (FMC, Indianapolis, IN) in fresh 1X Tris-borate-EDTA buffer at 4 V/cm in a cold room and observed after staining with ethidium bromide. The resulting restriction banding patterns were normalized and compared with GelCompar software (version 3.1; Applied Maths, Kortrijk, Belgium). Clones representing the most abundant banding patterns for each sample were chosen for sequencing, except in reactor S2 where clones that potentially matched certain terminal restriction fragments were chosen for sequencing.

Bacterial isolates. *Spirochaeta* sp. str. M1-8, M2-8, R8 and M3-10 were isolated in mineral medium (24) plus 10 % (v/v) clarified rumen fluid, 5 mM glucose, 0.7 % agarose, and 50 $\mu\text{g ml}^{-1}$ rifampin adjusted to a pH of 7.2 (15). A dilution series of fluid from reactors M1, M2, R1, and M3 was done in 10 ml agar shake tubes with a headspace of $\text{N}_2:\text{CO}_2$ (80:20) and incubated at 37°C. Single colonies from the highest dilution tube in which growth occurred were picked with a sterile Pasteur pipette and serially diluted in 10 ml agar shake tubes. This was repeated three times to ensure that a pure culture was obtained. Liquid cultures were inoculated with a single colony picked from the highest dilution tube containing colonies. *Clostridium* sp. str. S9 was isolated in the same manner except tryptic soy broth plus 0.2 % (w/v) glucose, 1 mM dithiothreitol, and 50 $\mu\text{g ml}^{-1}$ rifampin was used instead of mineral medium. Isolate O94 was isolated by A. Fernandez from reactor P1 (6). *Spirochaeta* sp. str. R8 has been deposited in the DSMZ under accession number 13955. Genomic DNA from all isolates was extracted and purified

using

speci

ampli

insert

colum

the N

previ

gene

const

Data

(Sina

Math

limn

AF0

USO

Desu

Sym

M23

Strept

mel-

M71

Spor

using a Qiagen kit. The 16S rRNA gene of each isolate was amplified with bacteria-specific primers and cloned as described above.

Sequencing and sequence analysis. The 16S rDNA gene fragments were amplified for sequencing directly from whole cells containing the correct plasmid and insert as described above. The amplicons were then purified with Microcon-100 spin columns (Millipore Corp.). Sequences were obtained via the dye terminator method by the Michigan State University DNA sequencing facility with modified versions of previously described sequencing primers targeting conserved regions of the 16S rRNA gene (27). Alignment of sequences, mask construction, chimera check, and dendrogram construction were performed with ARB (26) and software provided by the Ribosomal Database Project (18). Dendrograms were constructed with PAUP^{*} 4.0s software (Sinauer Associates, Inc. Publishers, Sunderland MA). Genbank accession numbers are: *Methanobacterium formicicum*, Z29436; *Thermotoga maritima*, M21774; *Planctomyces limnophilus*, S39795; *Verrucomicrobium* sp., X99390; *Aminobacterium mobile*, AF073521; *Aminobacterium colombiens*, AF069287; *Anaerobaculum thermoterrenum*, U50711; Candidate division OP11, AF027030; *Escherichia coli*, D15061; *Desulfuromonas acetoxidans*, M26634; *Syntrophobacter fumaroxidans*, X82874; *Syntrophobacter* sp., X94911; *Clostridium ramosum*, X73440; *Eubacterium barkeri*, M23927; *Eubacterium hadrum*, ARB_7A6488B3; *Streptococcus bovis*, M58835; *Streptococcus macedonicus*, Z94012; *Propionibacterium acnes*, M61903; *Spirochaeta zuelzeriae*, M88725; *Spirochaeta* sp. str. *Mastotermes*, X79548; *Spirochaeta caldaria*, M71240; *Spirochaeta stenostrepta*, M88724; *Spirochaeta aurantia* str. J-1, M57740; *Spirochaeta halophila*, M88722; *Spirochaeta* sp. str. Antarctic, M87055; *Spirochaeta* sp.

str T

Legn

AF15

WCH

AF05

AF06

EO-3

AF14

EO-D

AF21

AO-D

react

centr

immu

chlor

The

spect

gel

desc

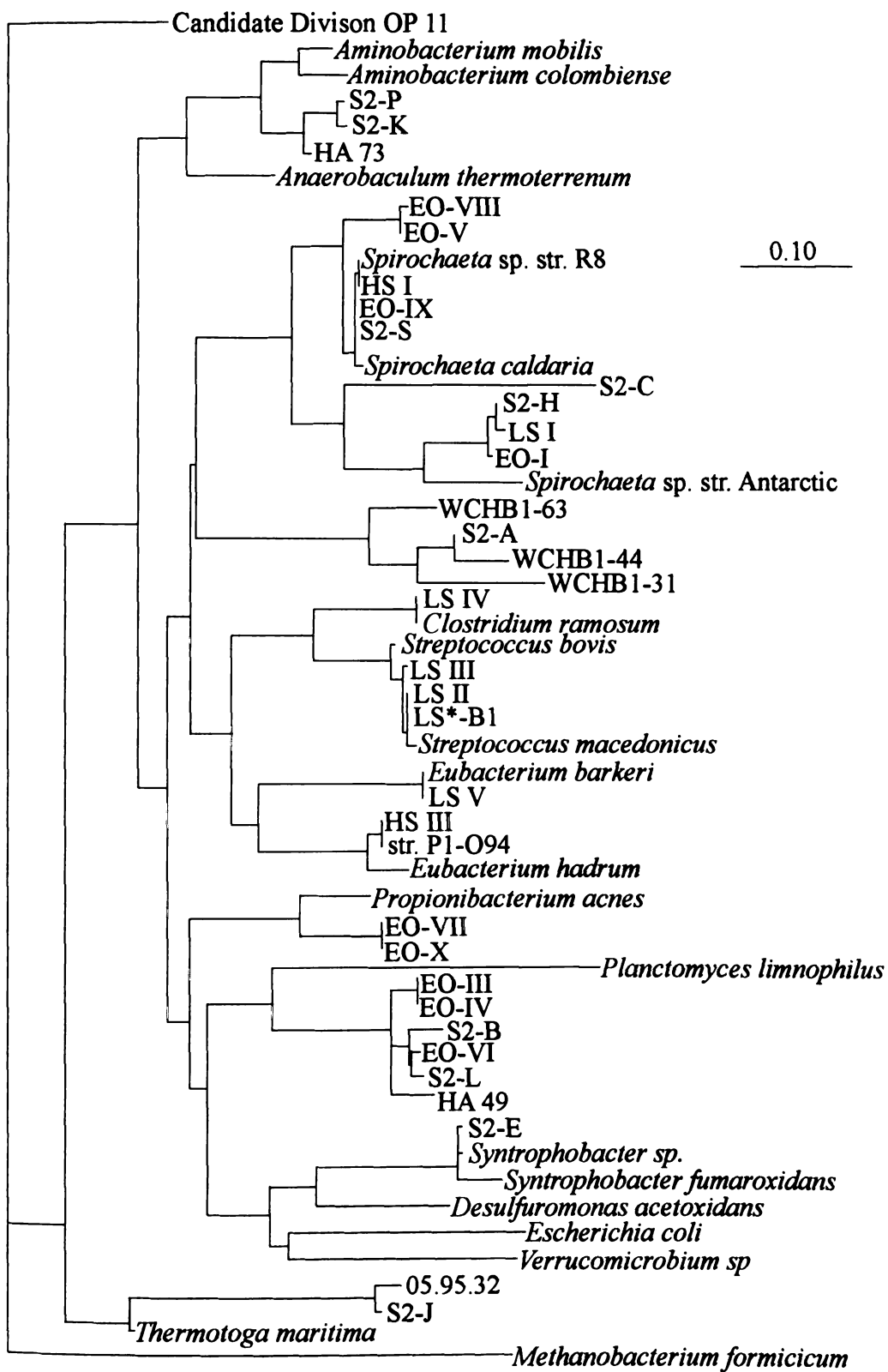
Meth

Mo

str. TM3, X97096; *Spirochaeta* sp. str. Masto., X79548; *Treponema* ZAS-1, AF093251; *Leptospira santarosai*, U12672; EO-IV, AF149889; LS*-B1, AF157108; HS-B26, AF157107; S2-A through S, AF338764-66 and AF339852-59; WCHB1-63, AF050568; WCHB1-44, AF050565; WCHB1-31, AF050569; WCHB1-40, AF050549; WCHB1-30, AF050551; WCHB1-91, AF050550; RFS 75, AF068421; RFS 60, AF068418; RFS 12, AF068335; RFS 84, AF068428; HA49, U81766; HA73, U81735; EO-XIV, AF149879; EO-XI, AF149878; EO-X, AF149886; EO-IX, AF149880; EO-VIII, AF149882; EO-VII, AF149885; EO-VI, AF149889; EO-V, AF149881; EO-III, AF149888; EO-II, AF149884; EO-I, AF149883; LSI, AF219215; LSII, AF218216; LSIII, AF218217; LSIV, AF218218; LSV, AF218219; HSI-III, AF218220-22; 05.95.32, ; AA-AD; AF339848-51; AO-I through IV, AF1498890-93.

16S rRNA oligonucleotide probing. Approximately 10 mL samples from reactors LS 1, LS 2, HS 6, and HS7 were taken immediately before the glucose pulse and centrifuged for 10 min at 8,000 X g. The supernatant was discarded and the pellets were immediately stored at -80°C until the nucleic acids could be extracted. Phenol-chloroform-isoamyl alcohol (100:24:1 [vol/vol/vol]) extraction was used to extract RNA. The concentration and quality of the extracted rRNA was measured spectrophotometrically at 260 nm and by electrophoresis through a 10% polyacrylamide gel. Quantitative rRNA membrane hybridizations were performed as previously described by Raskin et al. (21). The following reference organisms and probes were used: *Methanosarcina* sp. strain WH2 (S-G-Msar-0821-a-A-24), *Methanobacterium bryantii* M.o.H.G. (DSM 862) (S-F-Mbac-0310-a-A-22), *Methanosaeta concilli* FE (DSM 3013)

Figure 2.2. Maximum likelihood tree of cloned bacterial 16S rRNA gene sequences from bioreactors and other methanogenic environments. The backbone of this tree was cast using 696 unambiguously aligned nucleotides between *E. coli* positions 95 and 1295. Partial sequences were then appended to the tree using the maximum likelihood algorithm with 261 unambiguously aligned nucleotides between *E. coli* positions 154 and 474. Scale bar = 10 % difference nucleotide sequence. The origin of the cloned genes is as follows: HA = anaerobic vinasses reactor (7); EO = Reactor P1; HS = Reactors HS 5-8; LS = Reactors LS 1-4; S2 = Reactor S2.



(S-G-N)

1200-2

Result

reaction

were g

most f

16S r

phyla

within

83 %

Propic

Syntro

there

certain

differe

seque

Spiro

one *Sy*

ampli

conta

(S-G-Msae-0381-a-A-22), and *Methanogenium cariaci* JR1 (DSM 1497) (S-O-Mmic-1200-a-A-21) (22,25).

Results

Bacteria. Over 800 bacterial 16S rRNA genes were screened from 28 different reactor samples during the three separate experiments performed. These cloned genes were grouped according to their restriction enzyme banding patterns and the two to four most frequent gene types from each sample were chosen for sequencing. The bacterial 16S rRNA genes from the reactors were diverse, with sequences falling in six major phyla and ten different orders (Figure 2.2). The distribution of cloned 16S rRNA genes within bacterial phyla was 44.4 % *Spirochaetales* (16), 13.8 % of uncertain affiliation (5), 8.3 % *Eubacterium* (3), 8.3 % *Streptococcus* (3), 5.5 % *Mycoplasmatales* (2), 5.5 % *Propionibacterium* (2), 5.5 % *Thermotogales* (2), 5.5 % *Anaerobaculum* (2), 2.8 % *Syntrophobacter* (1) and 2.8 % in environmental clone group WCHB1-33 (1). Although there was significant diversity among the 16S rRNA genes cloned from the reactors, certain groups and sequences were found repeatedly in different reactors, despite differences in inoculum source, mode of operation, and amplification primers. Bacterial sequences retrieved from more than one reactor included sequences related to the genera *Spirochaeta*, *Clostridium*, *Eubacterium*, and *Streptococcus* (Table 2.1).

The largest number of sequences fell into the order *Spirochaetales* and at least one *Spirochaeta*-related sequence or isolate was obtained from 22 of 28 reactor samples amplified with bacteria-specific primers. The *Spirochaeta*-related group of sequences contained three subgroups, designated groups 1, 2, and 3 (Figure 2.3). Group 1 spirochete

Table 2 1 Microorganisms detected by 16S rRNA gene molecular methods in various bioreactor communities"

Reactor	PI 900 days	PI 977 days	PI 1036 days	PI 1325 days	PI 1437 days	PI 1470	PI 1505

Table 2.1. Microorganisms detected by 16S rRNA gene molecular methods in various bioreactor communities^a.

Reactor	P1 900 days	P1 977 days	P1 1036 days	P1 1325 days	P1 1437 days	P1 1470	P1 1505
Bacteria	Grp III Spiro. Grp II Spiro.	Grp II Spiro. Grp I Spiro. Thermotogales	Grp III Spiro. Unaffiliated Eubacterium	Grp I Spiro. Grp II Spiro. Propionibact.	Eubacterium	Unaffiliated	Propionibact. Unaffiliated
Archaea	Mbacterium	Mbacterium Msarcina	Mbacterium Msarcina	Mbacterium	Msarcina Mbacterium	Msarcina Mbacterium	Msarcina Mbacterium
Efficiency ^c (Cause)	> 95 %	> 95 %	> 95 %	> 95 %	< 95 % (unknown)	< 90 % (unknown)	< 90 % (unknown)
HS 5-8 80 days	HS 5-8 88 days	LS 1-4 32 days	LS 1-4 40 days	LS [*] 210 days	S2 48 days	S2 407 days	M3 407 days
Grp I Spiro.	Eubacterium Grp I Spiro.	Streptococcus Grp III Spiro.	Streptococcus Clostridium Eubacterium	Streptococcus	Thermotogales Anaerobaculum Grp III Spiro. Unaffiliated	Clostridium Grp I Spiro.	Clostridium Grp I Spiro.
Msarcina ^d Mbacteriales Mmicrobiales	Not determined	Msarcina ^d Mmicrobiales	Not determined	Not determined	Msarcina ^d Unknown	Msarcina Mbacterium	Msarcina Mbacterium
> 95 %	< 90 % (substrate shock)	> 95 %	< 90 % (substrate shock)	> 95 %	> 95 %	< 95 % (high flow rate)	< 95 % (high flow rate)

^aAll phyla detected by sequencing of 16S rRNA gene clone libraries unless otherwise noted.

^bSpiro. = Spirochaeta, Msarcina = Methanosarcina, Mbacteriales = Methanobacteriales, Mmicrobiales = Methanomicrobiales,

Msarcina = Methanosarcina, Mbacterium = Methanobacterium, Propionibact. = Propionibacterium

^cPercent reactor efficiency was determined by: [(Influent COD - Effluent COD)/Influent COD]*100.

^dDetermined by 16S rRNA membrane hybridization to oligonucleotide probes.

sequ

Spira

steno

Tryp

sequ

isolat

R1. n

Secu

Grou

obtai

repea

overe

(Figur

spiro

resen

spiro

from

with

and

diver

react

sequences were the most common sequences found and were most closely related to *Spirochaeta caldaria*, which belongs to a group of free-living spirochetes, including *S. stenostrepta* and *S. zuelzeriae*, that are phylogenetically more similar to host-associated *Treponema* species than they are to other free-living *Spirochaeta* species. Many cloned sequences from termite gut contents are also most closely related to *S. caldaria*. Three isolates, *Spirochaeta* sp. str. M1-8, M2-8, and R8, obtained from reactors M1, M2, and R1, respectively, had identical 16S rRNA genes and belonged to group 1 (Figure 2.3). Sequences identical to these reactor isolates were cloned directly from 11 of 14 reactors.

Spirochaeta group 2 sequences were 4 % divergent, on average, from group 1. Group 2 sequences were also quite closely related to cloned 16S rRNA sequences obtained from aquifer material (Figure 2.3). Sequences from group 2 were retrieved repeatedly from reactor P1, however, they were less common than group 1 sequences overall (Table 2.1). One isolate, strain M3-10, from reactor M3 also fell within group 2 (Figure 2.3). Group 3 spirochete sequences were 15 % divergent from the first two spirochete groups and clustered with cell wall-less organisms morphologically resembling *Mycoplasma* species, despite their phylogenetic affiliation with the spirochetes (7). Group 3 spirochete sequences were obtained from 5 separate samples from three different reactors (Table 2.1).

The second largest group of 16S rRNA sequences was 20 % divergent from any cultivated organism. Sequences belonging to this clade were retrieved from reactors P1 and S2 (Table 2.1). The four sequences were 5 % divergent from each other and 7 % divergent from HA 49, a cloned sequence from an anaerobic vinasses (winery waste) reactor (8). These sequences could not be affiliated with any bacterial phyla with

Fi

fre

Al

47

ge

R.

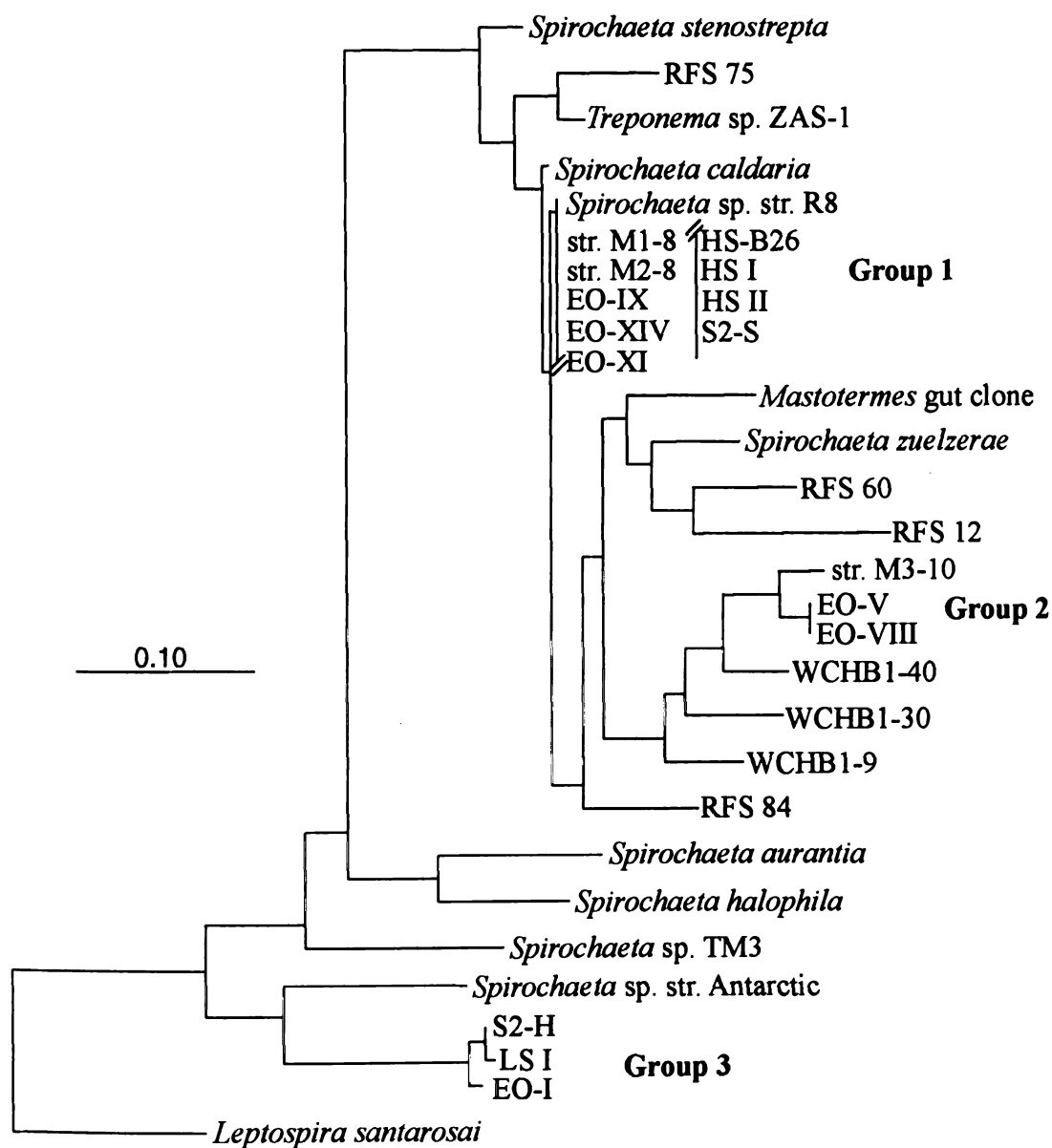


Figure 2.3 Maximum likelihood tree of cloned spirochete-related 16S rRNA genes from bioreactors and other methanogenic environments. This tree was calculated in ARB using 312 unambiguously aligned nucleotides between *E. coli* positions 154 and 478. Scale bar = 10 % difference in nucleotide sequence. The origin of the cloned genes is indicated as follows: RFS = Termite gut (15); WCHB1 = Aquifer (3); EO = Reactor P1; HS = Reactors HS 5-8; LS= Reactors LS 1-4; S2 = Reactor S2.

confi

seque

with

Ribo

with

from

prote

str F

rami

endo

Mye

these

sequ

react

4, ar

simi

were

same

acid,

Clos

confidence. Parsimony-based bootstrapping did not support the grouping of these sequences with the *Planctomyces* (data not shown). Godon *et al.* placed clone HA 49 with the *Planctomyces*, but they noted that this placement was questionable (8). In the Ribosomal Database Project (18), clone HA 49 is grouped with *Desulfuromonas* spp. within the delta-proteobacteria; however, clone HA 49 and the four related sequences from our reactors never clustered with *Desulfuromonas acetoxidans* or other proteobacteria in any analysis we performed.

Sequences from reactors LS 1-4 (Clone LS IV), S2 (Clone R), and *Clostridium* sp. str. R8 were 100 % identical to each other and to the 16S rRNA sequence of *Clostridium ramosum* (Figure 2.2). *C. ramosum*, *C. spiroforme*, and *C. cocleatum* form a group of endospore-forming organisms that are phylogenetically located within the *Mycoplasmatales* order, despite their genus name *Clostridium*. Unlike most clostridia, these organisms do not produce butyrate as an end product of glucose fermentation. The sequences were found in reactors LS 1-4 on day 40 after perturbation with glucose and in reactor S2 on day 407 when flow rates were high (Table 2.1).

Three sequences related to *Eubacterium* species were found in reactors P1, LS 1-4, and HS 5-8. Clone LS V, which was retrieved from the LS 1-4 reactors, was 96 % similar to *Eubacterium barkeri*, while the other sequences from reactors P1 and HS 5-8 were 92 % similar to *Eubacterium hadrum*. Although *E. barkeri* and *E. hadrum*, have the same genus name and share many phenotypic traits, such as the production of butyric acid, their 16S rRNA gene sequences are in two different families within the order *Clostridiales*, thus the distance between these two sequences is quite large (Figure 2.2).

found

volum

type of

to the

oxidizi

from a

fumar

sequen

these

(05-95

This

shown

sequen

as the

organ

the en

fairly

ident

know

for elc

Sequences closely related to *Streptococcus macedonicus* and *S. caprinus* were found in reactors LS* and LS 1-4. These sequences were confined to the 250 ml variable volume reactors. Two coexisting clones, EO-VII and EO-X, were also found in only one type of reactor (P1). EO-VII and -X had a sequence divergence of 0.5 % and were related to the *Propionibacterium* genus. Only one cloned sequence related to a known fatty-acid oxidizing, syntrophic bacterium was found. This sequence, S2-E, was 0.5 % divergent from an unnamed *Syntrophobacter* isolate and 4 % divergent from *Syntrophobacter fumaroxidans*.

The remaining sequences were quite divergent from their closest related sequence, and some of them can only be tentatively assigned to bacterial phyla. All of these sequences were found in reactors P1 and S2. Two sequences, one from reactor P1 (05.95.32) and one from reactor S2 (S2-J), cluster with *Thermotogales*-related sequences. This grouping is weakly supported by parsimony bootstrapping analysis (data not shown). Clones P and K from reactor S2 were 90.2 % similar to Clone HA 73, another sequence obtained by Godon et. al. (8), that clusters with a deep-branching clade known as the *Anaerobaculum thermoterrenum* group that contains many sequences and organisms from anaerobic environments. Clone S2-A from reactor S2 was placed within the environmental clone group WCHB1-33, which contains no cultivated organisms, with fairly high confidence. Lastly, clone S2-C from reactor S2 had less than 83 % sequence identity with any sequence in GenBank and could not be confidently affiliated with any known phyla. Chimera analysis did not indicate a high probability of a chimeric sequence for clone S2-C or any other sequence in this study.

Figur

Canto

unam

parisin

muele

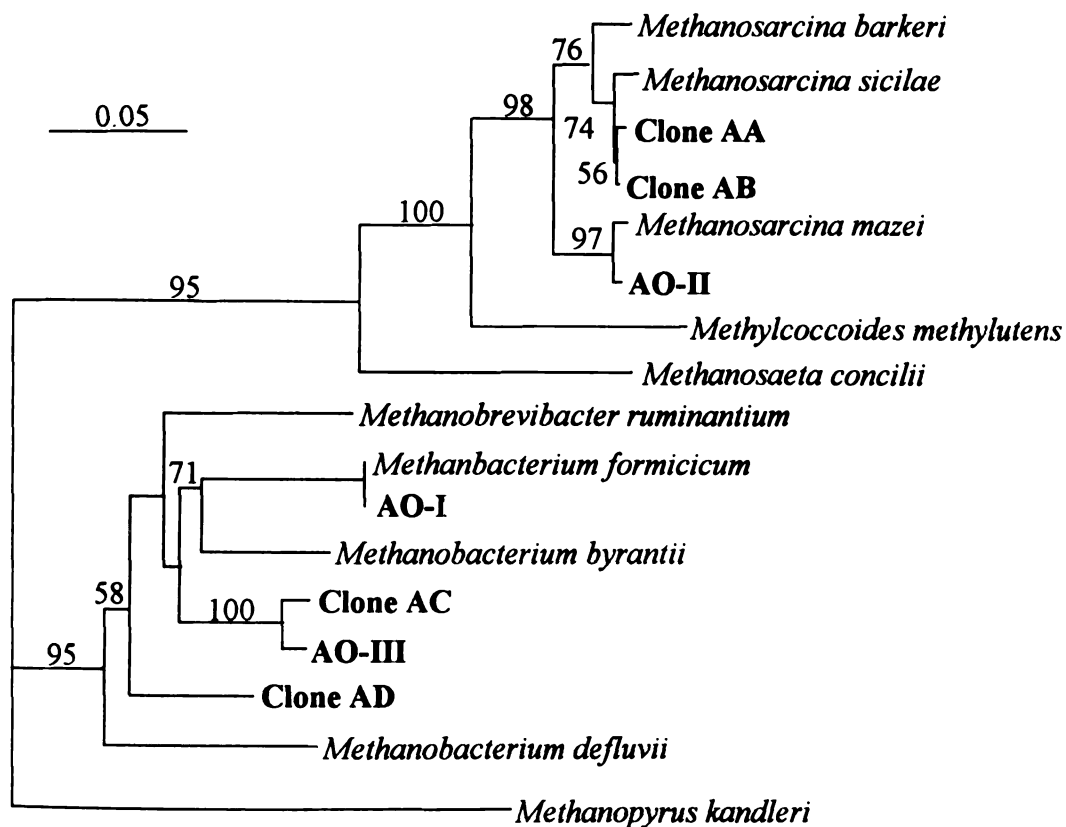


Figure 2.4 Neighbor-joining tree of *Archaea* 16S rDNA clones created from a Jukes-Cantor distance matrix. The matrix was calculated from analysis of 328 unambiguously aligned nucleotides of the 16S rRNA gene. Bootstrap values from 100 parsimony replicates are shown to the left of each node. Scale bar = 5 % difference in nucleotide sequence.

screen

were

that c

16S r

rRNA

1470.

and A

fairly

for A

seque

Metu

comp

specie

Metu

reacto

and 7

simila

25) I

for 63

metha

Archaea. (i) Clone libraries. Approximately 280 archaeal 16S rRNA genes were screened from 8 different reactor samples. Only the two to four most frequent gene types were sequenced from each sample, resulting in the sequencing of seven unique sequences that cluster within the kingdom *Euryarchaeota*. The sequence of AO-I, the most frequent 16S rRNA gene in reactor P1 from day 900 through 1325, was 100 % similar to the 16S rRNA gene sequence of *Methanobacterium formicicum* (Figure 2.4). On days 1437, 1470, and 1505 AO-II, which exhibited a 99.7 % similarity to *Methanosarcina mazei*, and AO-III, which was 92.0 % similar to *Methanobacterium bryantii*, were represented fairly equally in the clone library. A small number of clones matched the banding pattern for AO-I on day 1437, but this pattern was not detected on days 1470 or 1505.

The archaea clone library from reactor M3 yielded four different 16S rDNA sequences after screening 30 clones. Clones AA and AB were 98.5 % and 99 % similar to *Methanosarcina sicilae*, respectively (Figure 2.4). Two other clones, AC and AD, composed 17 % of the archaea clone library and grouped with *Methanobacterium* species. They were 92.2 % similar to each other and 90.4 % and 87 % similar to *Methanobacterium bryantii*. Clone AC and AO-III were only 1.7 % divergent.

(ii) 16S rRNA oligonucleotide probes. Two reactors from HS 5-8 and two reactors from LS 1-4 were chosen for rRNA membrane hybridization analysis: reactors 6 and 7 from the HS set and reactors 1 and 2 from the LS set. Replicate communities were similar within each set of reactors, but the HS and LS sets differed significantly (Figure 2.5). In the HS set, the *Methanosarcina* specific probe S-G-Msar-0821-a-A-24 accounted for $63\% \pm 1\%$ (Reactor 6) and $61\% \pm 1\%$ (Reactor 7) of the rRNA detected by all of the methanogen-specific probes used. The *Methanosaeta* specific probe S-G-Msae-0381-a-

Figure

2 and

olygon

the rot

specifi

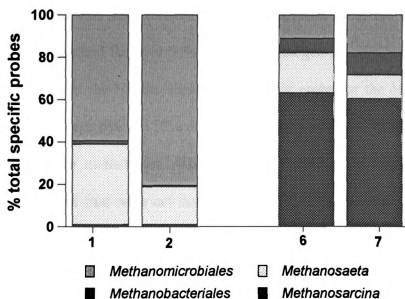


Figure 2.5 Relative abundance of methanogen-related 16S rRNA in reactors LS 1 and 2 and HS 6 and 7 as determined by 16S rRNA membrane hybridization to oligonucleotide probes. The abundance of each group is expressed as a percentage of the total amount of methanogen-related 16S rRNA detected by all of the methanogen-specific probes used.

LS 66

by all

up to

meth

Met

12000

and i

Order

% a

met

this s

meth

-

Discu

this s

e.g.

Sym

functi

form

exha

sim

A-22 accounted for $19\% \pm 4\%$ (Reactor 6) and $11\% \pm 5\%$ (Reactor 7). In contrast, in the LS set the *Methanosarcina* specific probe detected only $1\% \pm 0.3\%$ of the rRNA detected by all of the methanogen-specific probes, while the *Methanosaeta* specific probe detected up to 38% (Figure 2.5). Additional differences were found among CO₂-reducing methanogenic genera. Species belonging to the families *Methanomicrobiaceae*, *Methanocorpusculaceae*, and *Methanoplanaceae* detected using the probe S-O-Mmic-12000-a-A-21 accounted for over 60% of the methanogen-specific probes in the LS set and less than 20% in the HS set. Lastly, the specific probe for the *Methanobacteriales* Order detected between 6% and 12% of the methanogen rRNA in the HS set and between 0% and 1% of the methanogen rRNA in the LS set. There may have been other methanogens present that were not detected by the methanogen-specific probes used in this study; however, previous studies have found that these probes detect the majority of methanogens present in mesophilic sewage sludge digesters (9,22).

Discussion

Many of the sequences retrieved from the 14 methanogenic reactors sampled in this study were closely related to phyla that are expected in a methanogenic environment, e.g., *Spirochaeta*, *Eubacterium*, *Clostridium*, *Streptococcus*, *Propionibacterium*, *Syntrophobacter*, *Methanobacterium*, *Methanosarcina*, and *Methanomicrobiales*. The function of these organisms in methanogenic environments is well known, i.e. the fermentation of sugars, the oxidation of fatty-acids, and the formation of methane. An exhaustive 16S rDNA clone analysis of a fluidized-bed anaerobic vinasses reactor found similar genera (8). *Eubacterium*, *Clostridium*, *Propionibacterium*, *Methanobacterium*,

and

studi

and s

biofi

seque

The r

to the

the r

from

are c

or aq

unusu

RDP

EO-V

simi

(Fig

funct

near

2000

slide

this e

and *Methanosarcina* were found in similar proportions in both studies. In addition, both studies found more diversity within the bacteria than within the archaea.

In contrast to the Godon study, we found a much greater percentage of spirochete- and streptococci-related sequences, which may be related to the different substrate and biofilm-based ecosystem in the fluidized-bed vinasses reactor. The spirochete-related sequences found in the vinasses reactor were 8 % divergent from *Spirochaeta* sp. str. R8. The rest of the spirochete-related sequences from our reactors were not directly compared to those in the vinasses reactor because the portion of the 16S rRNA gene sequenced in the two studies for this group did not overlap (8). Many cloned spirochete sequences from other methanogenic environments, such as termite hind guts and aquifer material, are closely related to *S. caldaria* and *S. zuelzeri* (16). However, none of the termite gut or aquifer sequences were more than 95 % similar to any of the sequences we retrieved.

A significant number of sequences retrieved from the reactors were related to unusual phyla or were difficult to affiliate with any clade represented in GenBank or the RDP. Two of these unusual groups, the unaffiliated sequences (S2-L, EO-III, EO-IV, EO-VI) and the *Anaerobaculum*-related sequences (Clone K and Clone P), were most similar to 16S rRNA genes cloned from the anaerobic vinasses reactor mentioned above (Figure 2.2). Finding these two unusual groups in both types of reactors suggests that the function of the corresponding organisms is not related to the substrate or fluidized-bed nature of the vinasses reactor, but is a function also present in a completely mixed, glucose-fed, anaerobic reactor. The few cultivated organisms within the *Anaerobaculum* clade degrade amino-acids, suggesting this as a possible metabolism for the organisms in this group that were detected in both reactors, although the cultivated organisms are only

distan

corres

in the

larges

of the

more

sequen

sequen

85 % of

indica

introd

sequen

efficie

sequen

efficie

unaffi

reactio

reactio

were t

if seq

specie

distantly related to the sequences found here. The function of the organisms corresponding to the unaffiliated sequences can only be speculated. Their high frequency in the glucose-fed reactors would indicate that they ferment glucose, since this is the largest source of energy in the reactors. If they do utilize glucose, which is probably one of the most common sugars used in media, it is interesting that we have not cultivated more organisms with similar 16S rRNA sequences.

Some correlations between reactor efficiency and the dominant bacteria sequences present in each reactor were evident (Table 2.1). *Eubacterium* and *Clostridium* sequences were especially common when reactor efficiency was perturbed (i.e., less than 95 %). *Streptococcus* sequences appeared only in the variable volume 250 ml reactors, indicating that perhaps they were better adapted to stresses (such as occasional oxygen introduction) that may have been more pronounced in the smaller reactors. Spirochete sequences were generally the most common sequence type recovered when reactor efficiency was high. Other phyla, such as the *Thermotogales*-related and unaffiliated sequences, did not seem to be associated with a particular type of reactor or operation efficiency, and appeared only sporadically in the bioreactor communities. However, the unaffiliated sequences were associated with the unexplained decrease in efficiency of reactor P1, which eventually caused the fouling of this reactor (Table 2.1).

Methanobacterium was by far the most common archaea genus cloned from the reactors. The samples in which few to no *Methanobacterium* sequences were detected were taken within the first 50 days of reactor operation (Table 2.1). Based on the number of sequences retrieved, *Methanosarcina* species appeared to be the dominant acetoclastic species in the reactors. *Methanosaeta* sequences were only detected in samples taken

with

spec

with

ope

spe

LS

spe

com

cha

The

bo

bac

mes

incl

seq

com

ead

how

spe

S_{μ}

en

within the first 50 days of reactor operation. The observation that different methanogen species were present after the first 50 days of operation suggests that the environment within the reactors was highly selective for particular methanogenic species.

The composition of the methanogenic community also had an impact on the operating efficiency of the reactors, and reactors with relatively more *Methanosarcina* species were functionally more stable during the glucose perturbation applied to reactor LS 1-4 and HS 5-8 (4,12). In addition, a change in the particular *Methanobacterium* species and in the proportion of *Methanosarcina* species present in the archaea community of reactor P1 between days 1324 and 1437 corresponded with an abrupt change in the bacteria community and a steady decline in reactor operating efficiency. The cause of the change in both communities is unknown, but the simultaneous change in both communities suggests an interaction between fermentative and methanogenic bacteria that goes beyond typical interactions with obligately syntrophic organisms.

The results presented here show that even the highly selective environment of mesothermic glucose-fed methanogenic reactors can maintain a high level of diversity, including organisms that have no cultivated relatives, over long periods of time. The sequences detected in these simplified reactors corresponded closely with those found in comparable, but more complex, environments. The microbial community structure of each reactor varied to some extent without having a dramatic effect on reactor function, however the detection of certain organisms, such as *Eubacterium* and/or *Clostridium* species correlated with sub-standard reactor function. Other organisms, such as *Spirochaeta*, *Methanobacterium*, and *Methanosarcina* species dominated this environment when operating conditions were stable. This descriptive study provides

interc

insig

Refer

1 Au

2 De

3 De

4 Fe

5 Fe

6 Fe

7 Fr

8 Gc

9 Ha

10 H

interesting observations that could be the basis of further hypotheses, and should lead to insights into the interactions of microbial populations in methanogenic environments.

References

1. Auburger G, Winter J (1995) Isolation and physiological characterization of *Syntrophus buswellii* strain GA from a syntrophic benzoate-degrading, strictly anaerobic coculture. *Appl Microbiol Biotech* 44:241-248
2. DeLong EF (1992) Archaea in coastal marine environments. *Proc Natl Acad Sci USA* 89:5685-5689
3. Dojka MA, Hugenholtz P, Haack SK, Pace NR (1998) Microbial diversity in a hydrocarbon- and chlorinated-solvent-contaminated aquifer undergoing intrinsic bioremediation. *Appl Environ Microbiol* 64:3869-3877
4. Fernandez A, Hashsham S, Dollhopf SL, Raskin L, Glagoleva O, Dazzo FB, Hickey RF, Criddle C, Tiedje JM (2000) Flexible community structure correlates with stable community function in methanogenic bioreactor communities perturbed by glucose. *Appl Environ Microbiol* 66:4058-4067
5. Fernandez A, Huang S, Seston S, Xing J, Hickey RF, Criddle C, Tiedje JM (1999) How stable is stable? Function vs community stability. *Appl Environ Microbiol* 65:3697-3704
6. Fernandez A, Tiedje JM (2000) Characterization of a new microorganism able to overgrow dominant fermentative bacteria in methanogenic reactors. American Society of Microbiology General Meeting, Los Angeles
7. Franzman PD, Dobson SJ (1992) Cell wall-less, free-living spirochetes in Antarctica. *FEMS Microbiol Lett* 97:289-292
8. Godon J, Zumstein E, Dabert P, Habouzit F, Moletta R (1997) Molecular microbial diversity of an anaerobic digester as determined by small-subunit rDNA sequence analysis. *Appl Environ Microbiol* 63:2802-2813
9. Hansen SR, Hubbel SP (1980) Single-nutrient microbial competition: Qualitative agreement between experimental and theoretical forecast outcomes. *Science* 207:1491-1493
10. Harmsen HJM, Kengen HMP, Akkermans ADL, Stams AJM (1995) Phylogenetic analysis of two syntrophic propionate-oxidizing bacteria in enrichment cultures. *Syst Appl Microbiol* 18:67-73

11. Harmsen HJM, Wullings B, Akkermans ADL, Ludwig W, Stams AJM (1993) Phylogenetic analysis of *Syntrophobacter wolinii* reveals a relationship with sulfate-reducing bacteria. Arch Microbiol 160:238-240
12. Hashsham S, Fernandez A, Dollhopf SL, Dazzo FB, Hickey RF, Tiedje JM, Criddle C (2000) Parallel processing of substrate correlates with greater functional stability in methanogenic bioreactor communities perturbed by glucose. Appl Environ Microbiol 66:4050-4057
13. Koenig H, Stetter KO (1989) Archaeobacteria. In: Staley JT (ed) Bergey's Manual of Systematic Bacteriology, vol 2. Williams & Wilkins, Baltimore, MD, pp 2171-2216
14. Leadbetter JR, Breznak JA (1996) Physiological ecology of *Methanobrevibacter cuticularis* sp. nov. and *Methanobrevibacter curvatus* sp. nov., isolated from the hindgut of the termite *Reticulitermes flavipes*. Appl Environ Microbiol 62:3620-3631
15. Leschine SB, Canale-Parola E (1986) Rifampin-resistant RNA polymerase in spirochetes. FEMS Microbiol Lett 35:199-204
16. Lilburn T, Schmidt TM, Breznak JA (1999) Phylogenetic diversity of termite gut spirochaetes. Environ Microbiol 1:331-345
17. Loeffler FE, Ritalahti KM, Tiedje JM (1997) Dechlorination of chloroethenes is inhibited by 2-bromoethansulfonate in the absence of methanogens. Appl Environ Microbiol 63:4982-4985
18. Maidak BL, Cole JR, Lilburn TG, Parker CTJ, Saxman PR, Stredwick JM, Garrity GM, Li B, Olsen GJ, Pramanik S, Schmidt TM, Tiedje JM (2000) The RDP (Ribosomal Database Project) continues. Nucleic Acids Res 28:173-174
19. McInerney MJ (1992) The genus *Syntrophomonas* and other syntrophic anaerobes. In: Balows A, Truper HG, Dworkin M, Harder W, Schleifer K (eds) The Prokaryotes, A Handbook on the Biology of Bacteria: Ecophysiology, Isolation, Identification, Applications, vol 2. Springer-Verlag, New York, NY, pp 2048-2057
20. McInerney MJ, Bryant MP, Hespell RB, Costerton JW (1981) *Syntrophomonas wolfei* gen. nov. sp. nov., an anaerobic, syntrophic, fatty acid-oxidizing bacterium. Appl Environ Microbiol 41:1029-1039
21. Raskin L, Poulsen LK, Noguera DR, Rittmann BE, Stahl DA (1994) Quantification of methanogenic groups in anaerobic biological reactors by oligonucleotide probe hybridization. Appl Environ Microbiol 60:1241-1248

22. Raskin L, Stromley JM, Rittmann BE, Stahl DA (1994) Group-specific 16S rRNA hybridization probes to describe natural communities of methanogens. *Appl Environ Microbiol* 60:1232-1240
23. Schink B (1997) Energetics of syntrophic cooperation in methanogenic degradation. *Microbiol Mol Biol Rev* 61:262-280
24. Shelton DR, Tiedje JM (1984) Isolation and partial characterization of bacteria in an anaerobic consortium that mineralizes 3-chlorobenzoic acid. *Appl Environ Microbiol* 48:840-848
25. Stahl DA, Flesher B, Mansfield HR, Montgomery L (1988) Use of phylogenetically based hybridization probes for studies of ruminal microbial ecology. *Appl Environ Microbiol* 54:1079-1084
26. Strunk O, Ludwig W (1997) ARB: Software for phylogenetic analysis. Technical University of Munich, Munich, Germany
27. Weisburg WG, Barns SM, Pelletier DA, Lane DJ (1991) 16S ribosomal DNA amplification for phylogenetic analysis. *J Bacteriol* 173:697-703
28. Xing J, Criddle C, Hickey R (1997) Long-term adaptive shifts in anaerobic community structure in response to a sustained cyclic substrate perturbation. *Microb Ecol* 33:50-58
29. Zhao H, Yang D, Woese CR, Bryant MP (1990) Assignment of *Clostridium bryantii* to *Syntrophospora bryantii* gen.nov., comb. nov. on the basis of a 16S rRNA sequence analysis of its crotonate-grown pure culture. *Int J Syst Bacteriol* 40:40-44
30. Zhou J, Davey ME, Figueras JB, Rivkina D, Gilichinsky D, Tiedje JM (1997) Phylogenetic diversity of a bacterial community determined from Siberian tundra soil DNA. *Microbiology* 143:3913-3919

Da

ter

sub

In

the

of

re-

sig

im

or

in

as

at

of

CHAPTER 3

THE IMPACT OF FERMENTATIVE ORGANISMS ON CARBON FLOW IN METHANOGENIC SYSTEMS UNDER CONSTANT LOW SUBSTRATE CONDITIONS

These results will be published in the article: Dollhopf, S.L., Hashsham, S.A., Dazzo, F.B., Hickey, R.F., Criddle, C.S., and J.M. Tiedje. 2001. The impact of fermentative organisms on carbon flow in methanogenic systems under constant low substrate conditions. *Appl. Microbiol. Biotech. In Press.*

Introduction

The conversion of organic waste into methane, *i. e.* biomethanation, is a process that converts organic waste into useable energy, simultaneously reducing pollution and providing a source of renewable energy. Methane is also a potent greenhouse gas, and the release of methane from ruminant animals, termites, and anaerobic sediments plays a significant role in global warming (30). Although many of the bacteria and archaea that are involved in the anaerobic food chain are well known, the effect of different fermentative organisms on carbon flow through methanogenic environments has not been well studied. In sewage sludge and anaerobic sediments, 60 to 80 % of methane was produced from acetate, with the balance coming from H_2/CO_2 (5,17,35). Propionate, a precursor to acetate, accounted for 15 to 24 % of the methane formed during sewage sludge and glucose digestion, while butyrate contribution was negligible (8,18). In a study of

mesothermic cattle waste digestion, 13 and 8 % of the methane formed originated from propionate and butyrate, respectively (25). Alcohols have only been shown to be an important intermediate in the degradation of lactose (7). None of these previous studies examined the fermentative organisms present or attempted to correlate their physiology with the intermediary metabolites formed.

Molecular techniques now provide an opportunity to link the microbial community structure to the functional attributes of biomethanation (1). Other studies have concentrated on the connection between community structure and function during perturbations and changes in operating conditions (1,10,14,28,33). The effect of community structure on system function when substrate conditions are continually low has not been investigated in methanogenic systems. The purpose of this study was to address the fundamental question: Does community structure affect carbon flow in methanogenic systems when substrate concentrations are kept continually low? In particular we were interested in the influence of fermentative bacterial members on carbon flow, because their role seems to be overlooked in methanogenic systems. Microbial communities were characterized using SSU rDNA terminal restriction fragment length polymorphism (T-RFLP) analysis, SSU rDNA clone libraries, and phase contrast microscopy. Addition of [U-¹⁴C]glucose to bioreactors and maximum substrate utilization rates were used to identify important intermediates in glucose digestion. We found that acetate and ethanol were formed in bioreactors containing high number of spirochetes, while acetate and propionate were formed in bioreactors containing high numbers of streptococci. This suggests that microbial community structure can affect the path of carbon flow under constant low substrate conditions in methanogenic bioreactors.

Materials & Methods

Bioreactor operation. These studies were conducted in two variable volume methanogenic bioreactors and two continuously stirred tank reactors (CSTRs) that were operated at 34°C with an effective mean cell residence time (MCRT) of 16 days as described previously (14). Only the variable volume methanogenic bioreactors were used for ^{14}C -carbon flow studies. Separate substrate and nutrient solutions were fed continuously using syringe pumps at a rate of 12.5 and 5 ml/day (0.52 and 0.21 ml/hr), respectively (14). The volume of the variable volume bioreactors increased from 250 ml to 362 ml over 8 days. Every 8th day 112 ml of suspended culture was removed. This resulted in a glucose loading rate that varied between 0.4 to 0.28 g L⁻¹ d⁻¹. Reactor fluid from an 18 L CSTR that was inoculated with anaerobic digester sludge from the municipal wastewater treatment facility at Jackson, MI and had been maintained in the lab for over 3 years was used to inoculate the variable volume bioreactor HS (high-spirochete). Bioreactor HS was operated for 250 days before this study commenced. Variable volume bioreactor LS (low-spirochete) and CSTR R1 were inoculated with rumen contents at the same time and were operated for 210 and 330 days, respectively, before they were used in this study.

Sample preparation and microscopy. Samples (10 ml) were taken the day before addition of [U- ^{14}C]glucose for morphological analysis. Freshly collected samples were dispersed by multiple, rapid passages through a 25-gauge needle, and diluted to slight turbidity to achieve an ideal spatial density of separated cells (ca. 100 cells per micrograph) for morphotype recognition. Slides, photomicrographs, and digital images

were prepared as previously described (10). Classification of over 2,000 cells per sample into operational morphological units (OMU's) was performed using the CMEIAS© plug-ins (9,23) operating in UTHSCSA ImageTool Ver. 1.27 software (39). Averages and 95 % confidence intervals of OMU frequency were calculated by assuming that every photomicrograph represented an independent sample of the total community. Calculations of community similarity were performed using EcoStat Ecological Analysis software (Trinity Software, Plymouth, NH) based on relative abundance of each OMU.

DNA extraction and T-RFLP. Samples (1 ml) for community analysis were taken the day before addition of [U-¹⁴C]glucose and immediately stored at -80°C. DNA was extracted using a beadbeater™ method (24) modified by reducing the beadbeating intervals from 1 min to 30 s to minimize DNA shearing. Bacterial 16S rDNA was amplified using the primers 8F-Hex (AGAGTTTGATCCTGGCTCAG), which is specific for the domain bacteria, and 1392R (ACGGGCGGTGTGTRC), a universal reverse primer (1). The primer 8F-Hex was synthesized and labeled at the 5' end with the phosphoramidite dye 5-hexachlorofluorescein by Operon, Inc. (Alameda, CA). The amplification reaction consisted of 25 ng DNA, 0.5 µM of each primer, 0.2 mM of each deoxynucleoside triphosphate, 1.5 mM MgCl₂, 0.2 mg ml⁻¹ of BSA, 2.5 µl of 10X Taq buffer and 1 unit of Taq DNA polymerase (Boehringer Mannheim, Indianapolis, IN) in a 25 µl final volume. The amplification was performed using the following conditions: initial denaturation (95°C for 3 min) followed by 25 cycles of denaturation (94°C for 30 s), annealing (55°C for 30 s), and extension (72°C for 30 s) and a final extension of 72°C for 7 min. Three separate amplifications of each sample were performed, pooled, and purified using Microcon-100 spin columns (Millipore Corp., Bedford, MA) and digested overnight

with either *Hae*III, *Hha*I, or *Msp*I. Aliquots (2 μ l) containing approximately 30 ng of the digested DNA mixture and 2 fmol of GENESCAN-2500 TAMRA internal lane standard (Perkin Elmer Applied Biosystems, Foster City, CA) were then loaded onto a Perkin Elmer Applied Biosystems 373A automated sequencer by the MSU DNA Sequencing Facility. The resulting chromatograms were processed with GeneScan 2.1 (Perkin Elmer Applied Biosystems) to determine the size of each fragment. Community similarity was calculated using the GelCompar software package (version 4.2; Applied Maths, Kortrijk, Belgium). Following normalization (no background subtraction), Pearson product-moment correlation coefficients were used to calculate similarity matrices for each restriction enzyme digest (31). Alternatively, peaks were manually aligned and used to compute community similarity indices in EcoStat Ecological Analysis software (Trinity Software, Plymouth, NH). Individual peaks and peak height were substituted for species and species abundance, respectively. Identification of organisms corresponding to different terminal restriction fragments was accomplished by computer simulated restriction digests of the ribosomal database project (RDP) database, inspection of clone sequences, and actual amplification and digestion of DNA from 16S rDNA clones and isolates (27).

16S rDNA analysis. Amplification of bacterial SSU ribosomal DNA (rDNA), cloning, screening, and sequencing were performed as described previously (11). Thirty-six clones were analyzed for each sample and the most frequent clone type was selected for sequencing. Nearly full length sequences were obtained in both directions for all sequences. The 16S rDNA of spirochete isolate R8 was amplified as described above for community rDNA. Alignment of sequences, mask construction, and chimera check were performed using software provided by the Ribosomal Database Project (26) and ARB

(37). Dendrograms were constructed using ARB and PAUP* 4.0s (Sinauer Associates, Inc. Publishers, Sunderland, MA).

Determination of intermediary metabolites. Radiolabeled glucose was fed to the HS and LS bioreactors by replacing the normal substrate feed with an 8 g L⁻¹ solution of [U-¹⁴C]glucose with a specific activity of 0.015 mCi mmol⁻¹ and 7 g L⁻¹ NaHCO₃. The radiolabeled solution was fed continuously for 70 h to both bioreactors. Every 12 h, 1 ml samples were taken and immediately centrifuged at 10,000 x g for 10 min, acidified with 0.1 M H₂SO₄ (100 µl), and held at -20°C until analysis. The samples were analyzed for volatile fatty acids (VFA's) using a high pressure liquid chromatograph (Binary LC Pump 250, Perkin Elmer, Norwalk, Conn.) equipped with a 300-mm HPX-87H ion exclusion column (Bio-Rad Laboratories) connected to a Lambda-Max Model 480 LC spectrophotometer (Millipore, Milford, Mass.) set at 210 nm and a β detector (Insus Systems Inc., Tampa, Fla). The mobile phase was 0.013 N H₂SO₄ at 0.6 mL min⁻¹ with the column at 20°C. VFA's were identified by retention time using authentic radioactive and non-radioactive standards. A standard curve of area versus DPM was calculated using [U-¹⁴C]acetate of a known specific activity and also by collecting fractions of other radioactive compounds and counting them on a Tri-Carb 1500 liquid scintillation analyzer (Packard Instrument Company, Downers Grove, Illinois). A ratio of 1.55 DPM for every area unit was established. The detection limit for glucose and the individual VFA's with this system was approximately 20 µM. Soluble compound concentrations were converted to electron equivalents (e⁻) according to the oxidation state of each compound.

Spirochete isolate R8. The spirochete isolation medium consisted of a mineral medium (34) plus 10 % (v/v) clarified rumen fluid, 5 mM glucose, 0.7 % agarose, and 50

$\mu\text{g ml}^{-1}$ rifampin adjusted to a pH of 7.2 (21). A dilution series of R1 bioreactor fluid was done in 10 ml agar shakes with a headspace of $\text{N}_2:\text{CO}_2$ (80:20) and incubated at 37°C . Single colonies from the highest dilution tube in which growth occurred were picked with a sterile Pasteur pipette and serially diluted in 10 ml agar shakes. This was repeated three times to ensure that a pure culture was obtained. Liquid cultures were inoculated with a single colony picked from the highest dilution tube containing colonies. Rumen fluid was replaced by a cofactor solution (100X, pH 7.2) containing (per 100 ml): pyridoxal HCl, 10 mg; pyridoxal phosphate, 10 mg; calcium folinic acid, 2 mg; β -NAD, 2 mg; coenzyme A, 2 mg; FAD, 2 mg; nicotinamide, 1 mg; folic acid, 0.1 mg; riboflavin, 0.02 mg; thiamine pyrophosphate, 100 mg (19). Isolate R8 has been deposited in the DSMZ under accession number DSM 13955.

Fermentation products. Isolate R8 was grown in spirochete isolation medium for identification of fermentation products. Eight days after a 5 % (v/v) inoculation with an 8-day old culture fluid, visible turbidity developed. Samples were taken 6 and 8 days after inoculation and analyzed by HPLC for VFA's. Ethanol was measured using an enzyme assay (ethanol test kit 332-A, Sigma Chemicals, St. Louis, MO). Glucose was measured using hexokinase test kit 115 from Sigma Chemicals. Hydrogen was measured using a Hewlett Packard 6890 GC equipped with a mercury reduction gas detector.

Maximum substrate utilization rates. Substrate utilization rate assays were performed in 160 ml serum bottles containing 25 ml of R1 fluid, 10 mM acetate, propionate, butyrate, lactate, or ethanol and 10 mM phosphate buffer (pH 7.2). Reaction rates were determined by measuring the concentrations of acetate, propionate, butyrate, lactate, and ethanol over time by the methods indicated above. Methane was measured on

a Varian GC (model 3700) equipped with a Porapak Q column and a flame ionization detector.

Nucleotide sequence accession numbers. The SSU rRNA gene sequences determined in this study have been deposited in the GenBank database under accession numbers AF157107 and AF157108.

Results

Community structure. Bioreactors HS and LS were operated under identical conditions at an applied organic loading rate of 0.3 -- 0.4 g glucose·L⁻¹·day⁻¹ and were efficiently processing substrate with total VFA concentrations in the effluent less than 4 mM and chemical oxygen demand removal efficiencies of approximately 90 % (data not shown). Glucose concentrations were below the detection limit (20 µM) in both reactors throughout the duration of the experiment. Morphological analysis of bioreactors HS and LS revealed that they contained very different dominant microbial populations. Bioreactor HS contained two codominant morphotypes, single cocci and spiral-shaped cells, which comprised 33 ± 3 % and 37 ± 3 % of the community, respectively. LS was dominated only by cocci, which comprised 75 ± 2 % of the community and had only 0.5 % spiral-shaped cells. The cocci present in bioreactor LS were phase light and often found in clusters in contrast to the phase dark singly occurring cocci in bioreactor HS.

Visual inspection of the T-RFLP patterns from a *Hae*III restriction digest of amplified SSU rDNA from the two communities also showed that the HS and LS bacterial communities were quite different (Figure 3.1). We compared the T-RFLP patterns from all restriction digests by two methods. The Pearson product moment correlation coefficient

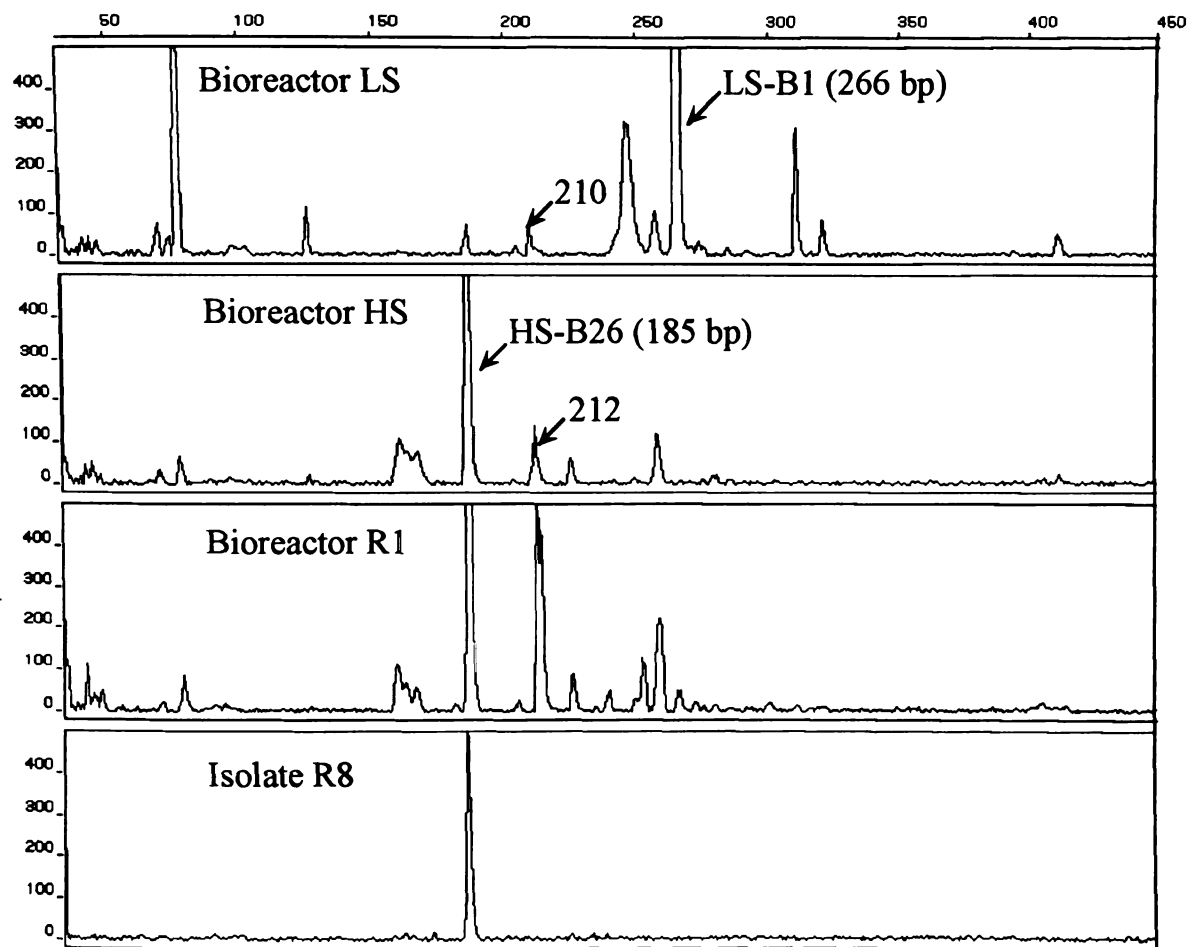


Figure 3.1. T-RFLP electropherograms of the HaeIII digested SSU rDNA amplified from isolate R8 and bacterial communities LS, HS, and R1. Peaks corresponding to the restriction fragment length of the most frequently cloned SSU rRNA gene sequences are labeled.

calculates similarity based on every point in the chromatogram produced by the laser dye reader, and does not require the identification and alignment of individual fragments (31). Correlation coefficients for HS and LS electropherograms from restriction enzymes *HaeIII*, *HhaI*, and *MspI* digests gave values below 0.50 for all digests (Table 3.1). Alignment of T-RFLP patterns and identification of each fragment allowed the computation of Horn's community similarity index (2) based on abundance of each terminal restriction fragment. Comparison of LS and HS electropherograms resulted in Horn similarity indices below 0.2 for all digests (Table 3.1). These results agree with the correlation coefficients and indicate that the HS and LS bacterial communities were indeed very different.

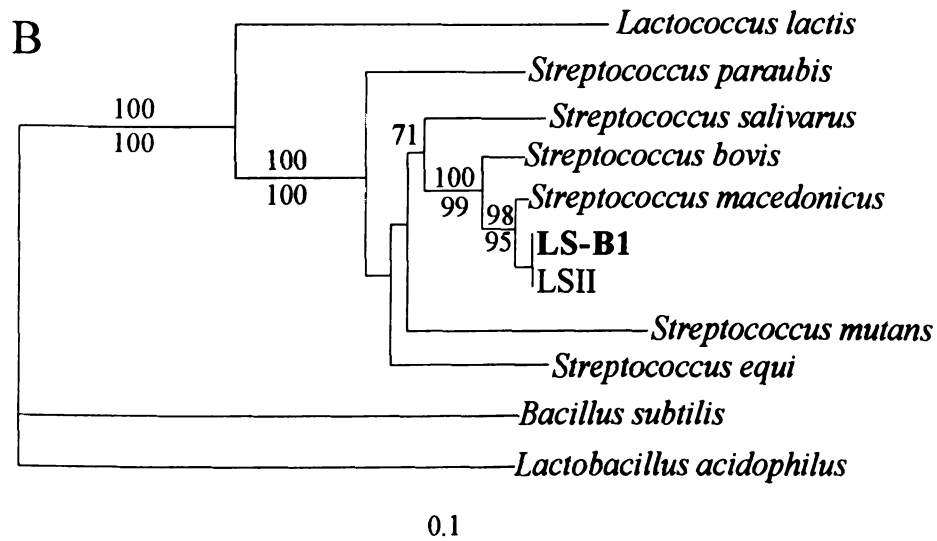
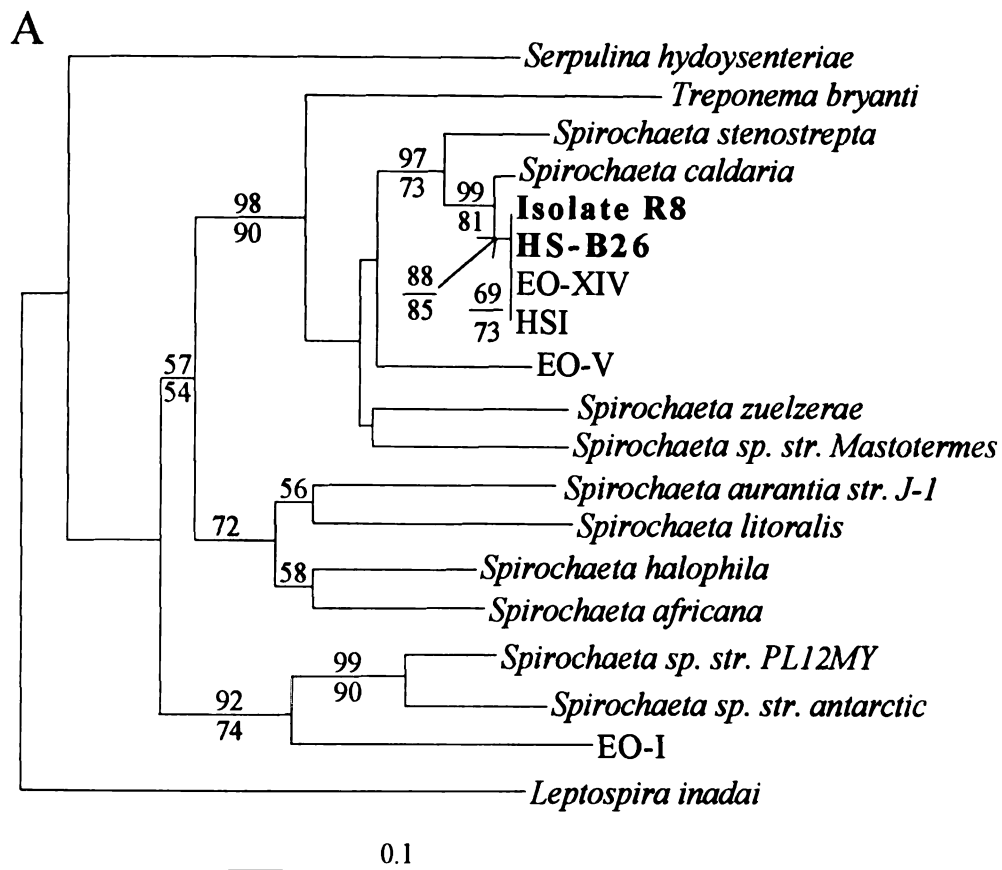
The most frequent SSU rDNA clone type from bioreactor HS, represented by clone HS-B26, accounted for 53 % of the total clones analyzed and was most closely related to *Spirochaeta caldaria*, with a sequence similarity of 99.5 % (Figure 3.2A). In bioreactor LS the most frequent clone type, represented by clone LS-B1, accounted for 50 % of the clones analyzed and was 98.3 % similar in sequence to *Streptococcus bovis* (Figure 3.2B). Digestion of clones obtained from HS and LS with *HaeIII* revealed a 185 base pair fragment that corresponded to clone HS-B26 and spirochete isolate R8, and a 266 base pair fragment that corresponded to clone LS-B1 (Figure 3.1). *HhaI* and *MspI* digestions confirmed that the dominant peaks in the HS and LS communities also corresponded to cloned sequences HS-B26 and LS-B1, respectively (data not shown).

The larger bioreactor R1 also contained a large proportion of spiral shaped cells. Because its larger volume provided us with reactor fluid to perform activity assays, the degree of community similarity between HS and R1 was ascertained using T-RFLP

Table 3.1. Similarity of bacterial *HaeIII*, *HhaI*, and *MspI* T-RFLP electropherograms as measured by Horn's community similarity index and Pearson product-moment correlation coefficient.

		LS	R1
		<i>HaeIII</i> / <i>HhaI</i> / <i>MspI</i>	<i>HaeIII</i> / <i>HhaI</i> / <i>MspI</i>
HS :	Horn	0.14 / 0.09 / 0.09	0.76 / 0.62 / 0.86
	Pearson	0.02 / 0.47 / 0.01	0.85 / 0.98 / 0.96
LS :	Horn		0.29 / 0.02 / 0.03
	Pearson		0.02 / 0.50 / 0.0

Figure 3.2. Phylogenetic relationships of clones and isolates in the families *Spirochaetales* (A) or *Streptococcales* (B). Unambiguously aligned nucleotides of the SSU rRNA gene from *E. coli* position 111 to 465 (A) and 21 to 1477 (B) were used to calculate Kimura 2-parameter distance matrices. The phylogenetic trees were created with the neighbor-joining method. Neighbor-joining and parsimony bootstrap values (50 % or higher) are listed above and below each node, respectively. Scale bar = 10 % difference in nucleotide sequence positions. Genbank accession numbers are as follows: *Streptococcus bovis*, M58835; *Streptococcus macedonicus*, Z94012; *Streptococcus mutans*, S70358; *Streptococcus equi*, S70324; *Bacillus subtilis* str 168, D26185; *Lactobacillus acidophilus* subspp. *johnsonii*, M99704; *Lactococcus lactis* subspp. *Lactis*, M58837; *Streptococcus salivarius*, M58839; *Streptococcus parauberis*, X89967; *Brachyspira hyodysenteriae*, M57741; *Treponema bryantii*, M57737; *Spirochaeta zuelzerae*, M88725; *Spirochaeta* sp. str. *Mastotermes*, X79548; *Spirochaeta caldaria*, M71240; *Spirochaeta stenostrepta*, M88724; *Spirochaeta aurantia* str. *J-1*, M57740; *Spirochaeta litoralis*, M88723; *Spirochaeta halophila*, M88722; *Spirochaeta* sp. str. *PL12MY*, RDP short ID str. *PL12MY*; *Spirochaeta* sp. str. *Antarctica*, M87055; *Leptospira inadai*, Z21634; EO-XIV, AF149879; EO-XI, AF149878; EO-V, 149881; EO-I, AF149883; LSII, AF218216; and HSI, AF218221.



analysis. The dominant terminal restriction fragment in bioreactors HS and R1 was a 185 bp fragment corresponding to the clone HS-B26 and isolate R8 (Figure 3.1). The two communities also shared other less abundant terminal restriction fragments, as reflected in the high community similarity values and correlation coefficients between HS and R1 (Table 3.1). Three separate samples taken from bioreactor R1 on the same day gave Horn similarity indices between 0.90 and 0.99 with a *Hae*III digest and two samples taken from bioreactor R1 two weeks apart yielded a Horn similarity index of 0.83 (data not shown).

Tentative identification of other community members was accomplished through *in silico* digestion of sequences in the RDP database. The 210 base pair fragment seen in the *Hae*III digest of the LS community corresponds to the predicted fragment size for *Selenomonas ruminantium*, an obligate anaerobe known to rapidly ferment lactate to propionate (3) (Figure 3.1). A 210 base pair fragment was not found in either the HS or R1 communities. A fragment of size 212 was found in communities HS and R1. This fragment was always distinguishable from the 210 base pair fragment in repeated PCR amplifications and T-RFLP gels of the three communities. Evidence for the presence of *Desulfovibrio* species in bioreactors HS and R1 was found in both the *Hha*I and *Msp*I digests with terminal fragment lengths of 97 and 509, respectively (data not shown). A terminal fragment of length 97 after digestion with *Hha*I is common to many species in the genus *Desulfovibrio*. A 509 base pair fragment resulting from digestion with *Msp*I also corresponds to the species *Desulfovibrio profundus*. Neither of these fragments was found in LS.

Intermediary metabolites. Approximately 13 % of the $0.34 \mu\text{mol e}^{-}\cdot\text{ml}^{-1}\cdot\text{hr}^{-1}$ entering the reactor accumulated in the pool of extracellular intermediary metabolites in

bioreactor HS (Table 3.2). Acetate and ethanol contributed fairly equally to these intermediary metabolites. Although ethanol contributed more electron equivalents than acetate, slightly more acetate was produced on a molar basis. Labeled propionate was not detected in the HS bioreactor over the course of this experiment.

In bioreactor LS approximately 10 % of the electron equivalents entering the system were found in soluble intermediates, similar to bioreactor HS (Table 3.2). The percentage of electron equivalents found in the soluble products indicates that both bioreactors were operating efficiently, and agrees with the operation efficiency of approximately 90 % calculated from chemical oxygen demand measurements of the bioreactor fluid (data not shown). In contrast to bioreactor HS, acetate was the more important fermentation intermediate, contributing twice as many electrons to the pool of intermediary metabolites than propionate. No ethanol was detected in bioreactor LS.

Maximum substrate utilization rates. Utilization rates for acetate, propionate, ethanol, lactate, and butyrate were determined for bioreactor R1 in order to confirm that the intermediates detected with [U-¹⁴C]glucose were utilized in a community that contained a high number of spirochetes (Table 3.3). Acetate and ethanol degradation began immediately, and acetate was formed concomitant with ethanol degradation (data not shown). The utilization rate for propionate was not significantly different than zero and butyrate utilization was very low. Lactate was not utilized until 10 h after inoculation with bioreactor fluid. The headspace of all bottles contained greater than 50 % methane after the substrate was utilized, indicating that the assay conditions were favorable for methanogenesis.

Table 3.2. Production of intermediary metabolites in bioreactor HS and LS as determined by addition of [U-¹⁴C]glucose to the bioreactors.

Intermediate	Production Rates ^a ($\mu\text{mol e}^- \cdot \text{ml}^{-1} \cdot \text{hr}^{-1}$)		Total electron equivalents ^b (%)	
	HS	LS	HS	LS
Acetate	0.19±0.02	0.23±0.02	5.7	6.8
Ethanol	0.25±0.04	None Detected	7.4	-
Propionate	None Detected	0.11±0.02	-	3.3

^a Production rates and 95 % confidence intervals calculated from linear regression analysis of dpm accumulation over time.

^b Percent total electron equivalents entering the reactor through glucose.

Table 3.3. Fermentation of glucose by isolate R8 and maximum substrate utilization rates in bioreactor R1.

	Isolate R8 Fermentation Products ($\mu\text{mol} \cdot 100 \mu\text{mol glucose}^{-1}$)	Bioreactor R1 Substrate Utilization Rates ^a ($\mu\text{mol} \cdot \text{ml}^{-1} \cdot \text{hr}^{-1}$)
Acetate	69	0.41 \pm 0.15
Ethanol	101	0.52 \pm 0.14
Propionate	0	0.02 \pm 0.02
Lactate	20.8	10 hour lag / 0.26 \pm 0.04
Butyrate	0	0.08 \pm 0.05
Hydrogen	144	Not Determined

^a Utilization rates and 95 % confidence intervals were calculated by linear regression analysis of substrate disappearance curves from duplicate assays.

Spirochete isolation and fermentation products. Serial dilution of R1 bioreactor fluid in agar shake tubes yielded more than 50 uniform colonies in the 10^8 dilution tube and no colonies in the 10^{10} dilution tube (there was no 10^9 dilution), suggesting that there were over 5×10^9 spirochetes ml^{-1} . All colonies were spherical, had a "cottonball-like" appearance, and were 2-3 mm in diameter, which is characteristic of spirochete colonies. Several colonies were picked and serially diluted. Microscopic inspection revealed that all of the isolates were long, thin spiral shaped cells typically between 20 and 50 μm long and 0.4 μm thick, with an average wavelength of 1.2 μm and average amplitude of 0.3 μm . This morphology was similar to that of the spirochetes seen in both the HS and R1 bioreactor communities. One isolate, R8, was chosen and serially diluted from isolated colonies two more times. Microscopic observation did not reveal any contaminating bacteria. The 16S rRNA gene of isolate R8 was 99.5 % similar to *S. caldaria* and 100 % similar to clone HS-B26 (Figure 3.2A). The most common T-RFLP fragment in the R1 and HS bacterial communities also corresponded to the fragment size of isolate R8 (Figure 3.1). Acetate, ethanol, and H_2 were the major fermentation products of isolate R8, with lactate being produced in smaller amounts under these culture conditions (Table 3.3).

Discussion

Both microscopy and T-RFLP indicated that *Spirochaeta* or *Treponema* species comprised a surprisingly high percent of the HS community. *Spirochaeta* species are found in many anaerobic environments, but they are generally not numerically dominant (13). Some *Treponema* species are pathogenic, but most known species are part of the normal oral, intestinal, and genital flora of mammals. *Treponema* species are rarely

numerically prevalent outside of their eukaryotic hosts (29). For example, a molecular study of a full-scale methanogenic vinasses (winery-waste) bioreactor reported that only 4 % of cloned 16S rRNA genes were spirochete-related. None of these sequences were over 92 % similar to the 16S rRNA sequences in our bioreactors (12). The termite hindgut is the only environment in which large proportions of *Treponema* species have been observed (22). The dominance of spirochetes in the absence of any eukaryotic host provides a unique opportunity to study their physiology and ecology, and may provide clues that will aid in the cultivation of the fastidious *Treponema* species implicated in oral and venereal diseases.

The agreement between the metabolism of spirochete isolate R8 and the intermediary metabolites in communities containing high numbers of spirochetes suggests that spirochetes controlled the carbon flow in these communities at low glucose concentrations (less than 20 μ M glucose). Spirochete isolate R8 fermented glucose to acetate, ethanol, and small amounts of lactate in pure culture. *Spirochaeta caldaria* and other *Spirochaeta* species typically ferment glucose to acetate, ethanol, H₂ and trace amounts of lactate through the Embden-Meyerhof pathway (4). Both acetate and ethanol appeared after the addition of [U-¹⁴C]glucose to bioreactor HS and were rapidly degraded during the maximum substrate utilization assay performed with R1 fluid, confirming that both substrates were produced and utilized in *Spirochaetaceae*-dominated methanogenic communities. In addition, T-RFLP results from two restriction digests suggested that *Desulfovibrio* species, which have been found to degrade ethanol to acetate in the presence of H₂-consuming methanogens (6), were present in both HS and R1 communities. Although isolate R8 also produced small amounts of lactate, the long lag

time before the utilization of lactate in the substrate utilization assays suggests that lactate was not an important intermediate in the HS community.

Free-living spirochete species are thought to be specialized competitors for glucose and other compounds typically produced during the breakdown of cellulose and similar compounds (13). Numerous mechanisms of enhanced survival and growth at low nutrient conditions have been documented in free-living spirochetes, including enhanced chemotaxis under nutrient limitation, dissimilation of amino acids and endogenous RNA under starvation conditions, and polyglucose storage (4,13). The repeated enrichment of spirochetes from different inoculum sources in glucose-fed reactors with stable, low organic loading rates suggests that spirochetes are indeed adapted to growth at low substrate concentrations. The convergence of the bacterial communities in bioreactors HS and R1 is an example of such an enrichment. Whether this is the result of enrichment of spirochetes from the inoculum or from invasion/cross-contamination is difficult to conclude without analyzing samples of the original inoculum.

Bioreactor LS contained a very different and perhaps more typical bioreactor community and carbon flow than bioreactors HS and R1. T-RFLP and microscopy data suggest that a *Streptococcus* species was the most common organism in the LS community (Figure 1 and 2B). Streptococci are commonly found in methanogenic digesters. Studies of bacterial populations in anaerobic piggery-waste and sewage sludge digesters found that approximately 30 - 70 % of the bacteria isolated on a habitat-simulating medium were *Streptococcus* species (15,38). The accumulation of radioactive acetate and smaller amounts of propionate from radiolabeled glucose agrees with previous studies in which acetate and propionate generally account for most of the methane

production in glucose digestion (8,18). The presence of streptococci, which typically produce lactate as well as acetate, suggests that lactate would be observed as a radiolabeled intermediate from [U-¹⁴C]glucose in LS; however, lactate is known to be rapidly fermented to propionate, while propionate oxidation is a much slower and energy-poor reaction. The fermentation of lactate to propionate may have been rapid enough to prevent the detection of lactate as an intermediate in this study. Members of genera such as *Selenomonas*, *Propionibacterium*, *Anaerovibrio*, *Pectinatus*, and *Desulfobulbus* are known to ferment lactate to propionate and acetate, with propionate being the major product (3,20,32,36). A terminal restriction fragment corresponding to a *Selenomonas* species was found in the LS community, suggesting that this type of organism may be responsible for the fermentation of lactate in the LS community.

In contrast to spirochetes, streptococci are usually thought to be adapted to high substrate concentrations and fast growth rates. In a shock loading experiment with similar glucose-fed bioreactors, excess glucose was added to four bioreactors communities containing large proportions of streptococci. The streptococci remained prevalent during the shock load, and were apparently able to grow rapidly enough to avoid being overcome by other species. In *Spirochaetaceae*-dominated bioreactors the spirochetes were overgrown by other species after the addition of excess glucose (10). Many organisms are known to have multiple enzyme systems that are employed under different substrate concentrations, and some streptococci have been reported to be facultative oligotrophs, *i. e.* able to grow under both high and low substrate conditions (16).

If streptococci are capable of growing well under low substrate conditions, why then did the LS community and *Spirochaetaceae*-dominated R1 community, which were

inoculated simultaneously from the same source, have two very different communities? The time between inoculation and analysis of the LS community was shorter (210 days) than for the R1 community (330 days), which could explain some of the difference in the two communities. The difference in the operation of bioreactors LS and R1 may also have inhibited a spirochete-rich community from developing in the smaller, variable volume LS bioreactor; however, both types of bioreactors have maintained spirochete-rich communities (10). A 185 bp fragment that corresponds to the dominant spirochete in the HS and R1 communities is present in the LS community T-RFLP pattern, although the height of the peak suggests that it is a minor component of the community. Given enough time under continuous low glucose conditions it is possible that this spirochete would have outcompeted the streptococci for glucose and taken over the LS community as it did in the R1 community.

This study illustrates that different fermentative organisms establish different routes of carbon flow in methanogenic communities when substrate concentrations are low. The importance of fermentative organisms in the overall pathway of anaerobic degradation has been somewhat overlooked in community analysis of methanogenic environments, while the organisms that catalyze the energetically more difficult steps of fatty acid oxidation and methane formation have been emphasized. Although the model system used here is much simpler than most bioconversion systems and natural environments, the general observation that different fermentative organisms can impact the pathway of organic carbon degradation is nonetheless applicable over a wide variety of environments. Including the physiologic properties of the fermentative organisms in methanogenic communities, such as varying substrate affinity, starvation survival and acid

tolerance, will improve our ability to model anaerobic degradation and methane production in natural environments.

References

1. Amann RI, Ludwig W, Schleifer K (1995) Phylogenetic identification and in situ detection of individual microbial cells without cultivation. *Microbiol Rev* 59:143-169
2. Brower JE, Zar JH, von Ende CN (1990) *Field and Laboratory Methods for General Ecology*. Wm.C.Brown, Dubuque, IA
3. Bryant MP (1984) Genus IX. *Selenomonas*. In: Krieg NR, Holt JG (eds) *Bergey's Manual of systematic bacteriology*, vol I. The Williams & Wilkins Co., Baltimore, pp 650-653
4. Canale-Parola E (1977) Physiology and evolution of spirochetes. *Bacteriol Rev* 41:181-204
5. Cappenberg TE, Prins RA (1974) Interrelations between sulfate-reducing and methane-producing bacteria in the bottom deposits of a fresh-water lake. III. Experiments with ^{14}C -labeled substrates. *Antonie van Leeuwenhoek* 40:457-469
6. Chartrain M, Zeikus JG (1986) Microbial ecophysiology of whey biomethanation: characterization of bacterial trophic populations and prevalent species in continuous culture. *Appl Environ Microbiol* 51:188-196
7. Chartrain M, Zeikus JG (1986) Microbial ecophysiology of whey biomethanation: intermediary metabolism of lactose degradation in continuous culture. *Appl Environ Microbiol* 51:180-187
8. Cohen A, Van Deursen A, Van Andel JG, Breure AM (1982) Degradation patterns and intermediates in the anaerobic digestion of glucose: Experiments with ^{14}C -labeled substrates. *Antonie van Leeuwenhoek* 48:337-352
9. Dazzo FB, Petersen M (1989) Applications of computer-assisted image analysis for microscopical studies of the *Rhizobium*-legume symbiosis. *Symbiosis* 7:193-210
10. Fernandez A, Hashsham S, Dollhopf SL, Raskin L, Glagoleva O, Dazzo FB, Hickey RF, Criddle C, Tiedje JM (2000) Flexible community structure correlates with stable community function in methanogenic bioreactor communities perturbed by glucose. *Appl Environ Microbiol* 66:4058-4067
11. Fernandez A, Huang S, Seston S, Xing J, Hickey RF, Criddle C, Tiedje JM (1999)

- How stable is stable? Function vs community stability. *Appl Environ Microbiol* 65:3697-3704
12. Godon J, Zumstein E, Dabert P, Habouzit F, Moletta R (1997) Molecular microbial diversity of an anaerobic digester as determined by small-subunit rDNA sequence analysis. *Appl Environ Microbiol* 63:2802-2813
 13. Harwood CS, Canale Parola E (1984) Ecology of spirochetes. *Annu Rev Microbiol* 38:161-192
 14. Hashsham S, Fernandez A, Dollhopf SL, Dazzo FB, Hickey RF, Tiedje JM, Criddle C (2000) Parallel processing of substrate correlates with greater functional stability in methanogenic bioreactor communities perturbed by glucose. *Appl Environ Microbiol* 66:4050-4057
 15. Hobson PN, Shaw BG (1974) The bacterial population of piggery-waste anaerobic digesters. *Wat Res* 8:507-516
 16. Ishida Y, Imai I, Miyagaki T, Kadota H (1982) Growth and uptake kinetics of a facultatively oligotrophic bacterium at low nutrient concentrations. *Microb Ecol* 8:23-32
 17. Jerris JS, McCarty PL (1965) The biochemistry of methane fermentation using ^{14}C -tracers. *J Wat Pollut Control Fed* 37:178-192
 18. Kaspar HF, Wuhrmann K (1978) Kinetic parameters and relative turnovers of some important catabolic reactions in digesting sludge. *Appl Environ Microbiol* 36:1-7
 19. Leadbetter JR, Schmidt TM, Graber JR, Breznak JA (1999) Acetogenesis from H_2 plus CO_2 by spirochetes from termite guts. *Science* 283:686-689
 20. Lee SY (1984) Genus XI. *Pectinatus*. In: Krieg NR, Holt JG (eds) *Bergey's manual of systematic bacteriology*, vol I. The Williams & Wilkins Co., Baltimore, pp 657-658
 21. Leschine SB, Canale-Parola E (1986) Rifampin-resistant RNA polymerase in spirochetes. *FEMS Microbiol Lett* 35:199-204
 22. Lilburn T, Schmidt TM, Breznak JA (1999) Phylogenetic diversity of termite gut spirochaetes. *Environ Microbiol* 1:331-345
 23. Liu J, Dazzo FB, Glagoleva O, Yu B, Jain A (2001) CMEIAS: A computer-aided system for the image analysis of bacterial morphotypes in microbial communities. *Microb Ecol* 41
 24. Löffler FE, Ritalahti KM, Tiedje JM (1997) Dechlorination of chloroethenes is inhibited by 2-bromoethansulfonate in the absence of methanogens. *Appl Environ Microbiol* 63:4982-4985

25. Mackie RI, Bryant MP (1981) Metabolic activity of fatty acid-oxidizing bacteria and the contribution of acetate, propionate, butyrate, and CO₂ to methanogenesis in cattle waste at 40 and 60°C. *Appl Environ Microbiol* 41:1363-1373
26. Maidak BL, Cole JR, Parker CT, Garrity GM, Larsen N, Li B, Lilburn TG, McCaughey MJ, Olsen GJ, Overbeek R, Pramanik S, Schmidt TM, Tiedje JM, Woese CR (1999) A new version of the RDP [Ribosomal Database Project]. *Nucleic Acid Res* 27:171-173
27. Marsh TL, Saxman P, Cole J, Tiedje JM (2000) Terminal restriction fragment length polymorphism analysis program, a web-based research tool for microbial community analysis. *Appl Environ Microbiol* 66:3616-3620
28. McCartney DM, Oleszkiewicz JA (1993) Competition between methanogens and sulfate reducers: Effect of COD:sulfate ratio and acclimation. *Wat Environ Res* 65:655-664
29. Miller JN, Smibert RM, Norris SJ (1992) The genus *Treponema*. In: Balows A, Truper HG, Dworkin M, Schleifer K (eds) *The Prokaryotes, A Handbook on the Biology of Bacteria: Ecophysiology, Isolation, Identification, Applications*, vol 2. Springer-Verlag, New York, NY, pp 3537-3555
30. Oremland RS (1988) Methanogenic bacteria. In: Zehnder A (ed) *Biology of Anaerobic Microorganisms*. Wiley, New York, NY
31. Pearson K (1926) On the coefficient of racial likeness. *Biometrika* 18:105-117
32. Prins RA (1984) Genus X. *Anaerovibrio*. In: Krieg NR, Holt JG (eds) *Bergey's manual of systematic bacteriology*. The Williams and Wilkins Co., Baltimore, pp 653-655
33. Raskin L, Rittmann BE, Stahl DA (1996) Competition and coexistence of sulfate reducing and methanogenic populations in anaerobic biofilms. *Appl Environ Microbiol* 62:3847-3857
34. Shelton DR, Tiedje JM (1984) Isolation and partial characterization of bacteria in an anaerobic consortium that mineralizes 3-chlorobenzoic acid. *Appl Environ Microbiol* 48:840-848
35. Smith PH, Mah RA (1966) Kinetics of acetate metabolism during sludge digestion. *Appl Microbiol* 14:368-371
36. Stams A-JM, Kremer DR, Nicolay K, Weenk GH, Hansen TA (1984) Pathway of propionate formation in *Desulfobulbus propionicus*. *Arch Microbiol* 139:167-173
37. Strunk O, Ludwig W (1997) ARB: Software for phylogenetic analysis. Technical University of Munich, Munich, Germany

38. Ueki A, Miyagawa E, Minato H, Azuma R, Suto T (1978) Enumeration and isolation of anaerobic bacteria in sewage digester fluids. *J Gen Appl Microbiol* 24:317-332
39. Wilcox CD, Dive SB, McDavid WD, Greer DB (1997) UTHSCSA ImageTool, University of Texas Health Science Center at San Antonio

CHAPTER 4

INTERPRETING 16S rDNA T-RFLP DATA: APPLICATION OF SELF-ORGANIZING MAPS AND PRINCIPAL COMPONENT ANALYSIS TO DESCRIBE COMMUNITY DYNAMICS AND CONVERGENCE

These results will be published in the article: Dollhopf, S.L., Hashsham, S.A., and J.M. Tiedje. 2001. Interpreting 16S rDNA T-RFLP data: Application of self-organizing maps and principal component analysis to describe community dynamics and convergence. *Microb. Ecol. In Press*.

Introduction

The use of molecular methods in microbial ecology has greatly expanded our ability to describe and monitor microbial communities; however, the collection of large amounts of data about a particular community does not necessarily lead to an understanding of the community, especially when noise and bias cloud data analysis. The problem of interpreting these data hinders our ability to learn what general principles control microbial diversity, community composition, interspecies interactions, and microbial processes. The management of microbial communities for practical applications, such as bioremediation and waste treatment, is also greatly impeded by our inability to predict community dynamics and function under variable environmental conditions. To better understand microbial communities, methods need to be developed that can integrate large amounts of environmental and molecular data as well as recognize patterns in data that may be relatively noisy.

Typically, microbial ecologists have relied on conventional statistical methods, such as correlation analysis and principal component analysis (PCA), for comparison of complex communities. These methods do not detect non-linear relationships, are confounded by experimental variability, and require normal or log-normal distributed data. Artificial neural networks (ANNs) may provide an alternative to conventional statistical methods because they detect non-linear relationships, allow the visualization of complex data, and remain robust despite experimental variation. In particular, Kohonen self-organizing maps (SOMs) have been used extensively in biological research for pattern recognition. Phylogenetic reconstruction, classification of proteins, and genomic analysis are a few applications of SOMs in molecular biology (18,31,33). Ecological applications for SOMs are also being explored for classification and modeling of populations and ecosystems (13,20). Only one study in microbial community analysis has previously used an ANN for community analysis and classification (25).

This study compares the ability of principal components analysis and self-organizing map neural networks to analyze 16S T-RFLP profiles of microbial communities in continuously-stirred, glucose-fed methanogenic bioreactors. The goal was not only to identify which samples were similar, but also to decipher community dynamics and describe specific phylotypes, i.e. phylogenetically similar organisms, that behaved similarly in different reactors. We observed that the composition of both reactor communities converged over the course of the experiment. In addition, we were able to identify phylotypes that occurred in both reactors in different phases of reactor operation. SOM analysis proved most useful in identifying all phylotypes that behaved similarly in

both communities, while PCA ordination clearly demonstrated community stability and dynamics during different periods of reaction operation.

Materials & Methods

Reactor operation and experimental design. Three 16-liter glucose-fed continuously stirred tank reactors were operated anaerobically at 34°C with a loading rate of 0.5 g glucose·l⁻¹·day⁻¹ and a hydraulic retention time (HRT) of 16 days by addition of 1.0 l·day⁻¹ of buffered glucose solution (8.0 g glucose·l⁻¹ + 7.0 g NaHCO₃·l⁻¹) plus 10 ml·day⁻¹ of concentrated nutrient solution (34). Reactor R1 (Rumen 1) was inoculated from rumen fluid and operated under the above conditions for over 330 days prior to this study (Figure 4.1). The other two reactors were inoculated from sediment of the Red Cedar River in Lansing, MI and from a 250 ml variable volume reactor seeded with sewage sludge from a previous study (17). These reactors were designated reactor S2 (Sediment 2) and reactor M3 (Municipal 3), respectively. Reactor chemical oxygen demand (COD), volatile fatty acids (VFAs), and pH were monitored biweekly.

The operation of the reactors was divided into two experimental phases, phase A and phase B (Figure 4.1). Phase A began when all reactors had achieved stable operation (COD removal above 90 %) at the target organic loading rate of 0.5 g glucose·liter⁻¹·day⁻¹ and lasted for 14 volume changes (224 days). All operating conditions were constant and percent COD removal remained above 90 % during phase A in all three reactors. During phase B, the effect of HRT on the microbial community was investigated by decreasing the HRT incrementally. The HRT of reactors S2 and M3 was manipulated by increasing the flow rate of the buffered glucose and nutrient solutions, thus increasing the organic

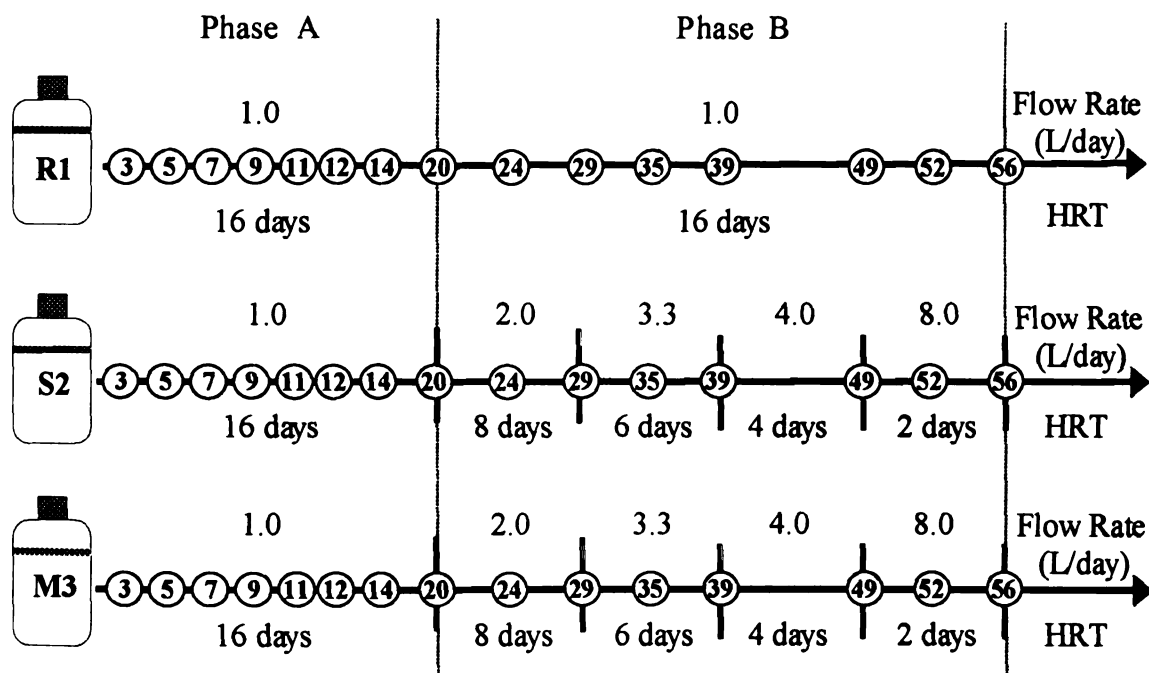


Figure 4.1. Timeline for reactors R1, S2, and M3. Time is measured in number of volume changes (x-axis not to scale). Sampling times are indicated by numbered circles which show the number of volume changes that occurred since the target organic loading rate was achieved in reactors S2 and M3. Control reactor R1 operated for over 2 years prior to this study. Reactors S2 and M3 were inoculated from river sediment and municipal sewage sludge, respectively. Flow rate and HRT are shown above and below the timeline respectively.

loading rate as well. Each new flow rate was maintained for at least nine volume changes before a subsequent increase. The HRT of the control reactor was constant throughout phase B. Percent COD removal remained above 85 % during phase B in all three reactors with the exception of one sample taken a few days after a short-term pump failure after 37 volume changes (data not shown).

Sampling. After reactors S2 and M3 had achieved a stable operating efficiency at the target organic loading rate, samples (2 mL) from each reactor were taken after 3, 5, 7, 9, 11, 12, and 14 volume changes (Figure 4.1). During phase B, samples (2 mL) from each reactor were taken immediately before each change of the HRT. Occasionally samples were taken at other times during phase B to check community stability (Figure 4.1). Samples were stored at -80°C until DNA extraction and T-RFLP analysis.

T-RFLP profiles. DNA was extracted from 2 mL of reactor fluid using a bead-beater/phenol-chloroform method (22). Bacteria or archaea community 16S rDNA was amplified using the primer pair 8F-Hex and 1392R (2) or 21F-FAM and 951R (8), respectively, digested with restriction enzyme *Hae*III, loaded on an automated sequencer (model 373A, Perkin Elmer Applied Biosystems), and processed with GeneScan (v2.1; Perkin Elmer Applied Biosystems) as previously described (10). Key samples were also digested with *Msp*I and *Hha*I to aid in the identification of matching 16S rRNA genes from clone libraries.

Variability of the relative intensity of each fragment was examined by analyzing three replicate samples from one reactor in parallel. The same 13 fragments were found in each replicate and the relative intensity, as ascertained by peak height measured in the electropherogram, had a standard deviation of 6 %. When the same replicates were

amplified and run on three separate T-RFLP gels, the standard deviation increased to 16 %. Only one sample and T-RFLP profile was analyzed for all other time points.

Clone libraries and sequencing. Bacterial clone libraries were created from reactor S2 samples taken after 3 and 56 volume changes. An archaeal clone library was created from a reactor M3 sample taken after 3 volume changes. Community DNA extraction and amplification were performed as described above, except that non-labeled PCR primers were used for amplification of community 16S rDNA. After amplification of the community DNA with the proper primer set, the amplicons were cloned into *E. coli* with the TA cloning kit (Invitrogen, Carlsbad, CA). Screening and sequencing were performed as previously described (12). Briefly, the cloned 16S rDNA gene fragments were amplified from whole cells using plasmid specific primers, checked for the proper size, and digested with *HaeIII* to screen for 16S genes that had terminal restriction fragments matching those found in community T-RFLP analyses. T-RFLP analysis was also performed on each clone to confirm the size of their terminal restriction fragment for the enzymes *HaeIII*, *MspI*, and *HhaI*.

Only clones matching predominant terminal restriction fragments found in both reactors were sequenced and analyzed. The amplified gene fragments were then purified with Microcon-100 spin columns (Millipore Corp.), and sequenced via the dye terminator method by the Michigan State University DNA sequencing facility with a universal primers targeting conserved regions of the 16S rRNA molecule. Approximately 1400 nucleotides were sequenced for clones L and J because they were divergent from cultivated phyla. Only partial sequences were obtained for the rest of the clones. Sequences were evaluated with the Check Chimera program of the Ribosomal Database

Project (RDP) and judged not to be chimeric (<http://www.cme.msu.edu/RDP/html/analyses.html>). Alignment of sequences, mask construction, and dendrogram construction were performed with ARB (27). The sequences determined in this study have been deposited in the GenBank database under accession no. AF338765 to AF338766 and AF339848 to AF339859.

Community similarity. The Morisita index of community similarity (I_M), which is based on Simpson's dominance index, was calculated in Ecostat software (Trinity Software, Plymouth, NH) using the formula:

$$I_M = \frac{2 \sum n_{i1} n_{i2}}{(l_1 + l_2) N_1 N_2}$$

where n_i is the number of individuals of species i , N is the total number of individuals sampled, and l is Simpson's dominance index for each community. Simpson's dominance index (l) was calculated using the formula:

$$l = \frac{\sum_{i=1}^s (n_i (n_i - 1))}{N(N - 1)}$$

where s is the total number of species in the community (5,32). This index ranges from 0-1, with 0 indicating that no species are shared between the two communities and 1 indicating complete identity. Because the index takes species abundance into account, communities that contain the same species but have different species abundance will have an index value less than 1. These equations were adapted to T-RFLP data by considering each terminal restriction fragment a separate species and peak height a measure of species abundance.

PCA. The data sets were tested for normality with MINITAB (v. 13.31; Minitab Inc., State College, PA) using the Anderson-Darling, Ryan-Joiner and Kolmogorov-Smirnov methods. PCA ordinations were calculated in StatView (v. 5.0.1; SAS Inc., Cary, NC) using correlation matrices produced from T-RFLP profiles that were normalized such that the sum of the peak heights of identified fragments equaled 10,000 fluorescent units. The complete data set consisted of 15 T-RFLP profiles (one for each sampling date) with the peak height of 66 unique fragments indicated for each profile. The data set was separated into individual analyses for each experimental phase and primer set to reduce the number of factors required to account for 85 % of the variation observed. All terminal restriction fragments with a peak height greater than 100 units were included in the analyses.

SOM. Self organizing maps organize large multidimensional data sets by mapping the input data onto a lower-dimensional array (19). A SOM has two layers: an input layer, which has the same number of nodes as there are input variables (e. g. species) and an output layer, which is a 2-D array of nodes with associated weights. Each input node is connected to every output node. During training, the output nodes, which initially have randomized weights, compete for the best match to the input. The output node that best matches the input becomes the winner. The winning node and its neighboring nodes are then updated so that it is more sensitive to the input with which it was presented. This competition occurs repeatedly over a set number of iterations, resulting in clusters of winning nodes that correspond to clusters within the input data (19). To verify the clustering pattern observed in the output, the training is redone a number of times, randomizing the initial weights each time. Because the initial weights

are randomized, the area of the output in which specific inputs cluster changes from one round of training to the next, but the grouping of the inputs should remain essentially the same if the SOM is accurately mapping the input on to the output space (7,25).

All neural computing was performed in NeuroSolutions software (v3.022, Consultants Level; NeuroDimensions, Gainesville, FL). The complete input data set included 15 T-RFLP profiles from each reactor containing 46 terminal restriction fragments from both the bacteria and archaea 16S rDNA primer sets. Terminal restriction fragments that were only observed once were not included. The T-RFLP profiles from each reactor were analyzed independently. Data were normalized so the sum of the peak heights of identified fragments equaled 10,000 fluorescent units, and then transformed within NeuroSolutions so that all values were between 1 and -1. The network parameters were selected based on trial runs and suggested values from NeuroDimensions. The input layer consisted of 46 nodes and the output layer consisted of a square Kohonen map of 15 X 15 nodes (225 output nodes total). The distance between the input and output nodes was calculated using the Euclidian distance measure. The Kohonen neighborhood size was initially set to 10 and then decreased linearly by 0.05 over 200 iterations. The initial learning rate of 0.01 also decreased linearly by 5×10^{-5} over 180 iterations. Five separate training runs of 500 iterations each were performed for the M3 and S2 data sets to confirm the clustering patterns within the SOM output layer.

Results

Community similarity. The S2 and M3 communities were very different at the beginning of phase A as measured by the Morisita community similarity (Table 4.1).

Table 4.1. Morisita community similarity indices for the R1, S2, and M3 bioreactor communities.

Sample ^a	Communities compared		
	S2 to M3	S2 to R1	M3 to R1
3	0.05	0.02	0.30
7	0.05	0.14	0.32
11	0.11	0.01	0.15
14	0.16	0.49	0.62
20	0.72	0.79	0.78
29	0.72	0.61	0.63
39	0.39	0.66	0.43
49	0.84	0.72	0.63
56	0.71	0.33	0.51

^a Sample numbers described in Figure 4.1.

During phase A, similarity indices between S2 and M3 varied, but by the end of phase A, comparison of the two communities yielded a similarity value of 0.72. Community similarity values between S2 and M3 remained above 0.70 for the rest of the experiment, except for sample 39 which was taken after a short-term pump failure in reactor M3. Both S2 and M3 communities were also similar to the R1 control community by the end of phase A. Only the application of a two day HRT caused the S2 and M3 communities to depart from the control (Table 4.1).

PCA. Distribution analysis of the data with the Anderson-Darling, Ryan-Joiner and Kolmogorov-Smirnov methods all indicated that the data varied significantly from a normal distribution. The data was skewed to the right, with more species having a relatively low abundance and few having a very high abundance. However, it has been shown that PCA can provide meaningful ordination of non-normal data (28,29). PCA ordination of the entire set of T-RFLP profiles for each reactor was very difficult to interpret because more than three factors were required to account for 85 % of the variability within the data. To allow a more detailed analysis of the bacteria and archaea communities, the T-RFLP profiles were separated into data sets for each reactor, experimental phase, and primer set, resulting in four different PCA ordination plots for each reactor.

The microbial community in control reactor R1 changed very little over the course of both experiments, and PCA of both the bacteria and archaea data sets from phase A and phase B periods extracted only one principal component factor (data not shown).

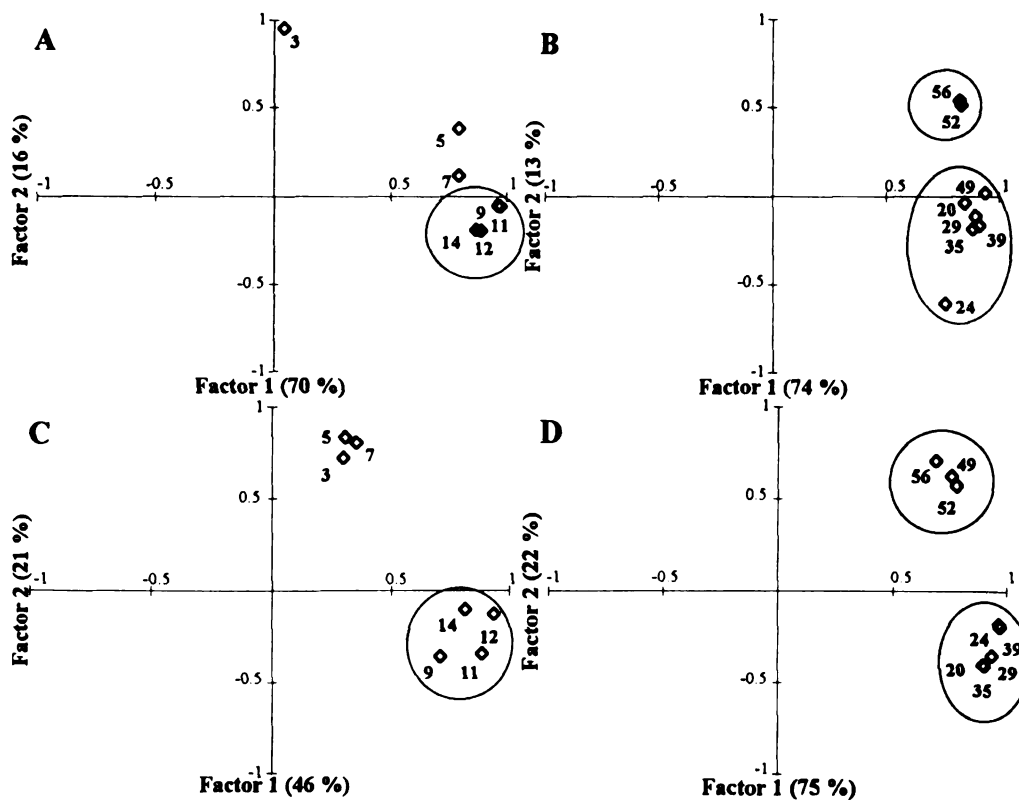


Figure 4.2. PCA ordination of bacteria T-RFLP peak height data for reactors M3 (A and B) and S2 (C and D) during phase A (A and C) and Phase B (B and D). The amount of variability accounted for by each factor is indicated on each axis. Sampling times are next to each point.

(i) Phase A. The M3 bacteria community changed during the first 7 volume changes of phase A, but was more stable after nine volume changes, as indicated by the tight clustering of samples 9, 11, 12, and 14 in a graph of Factor 1 versus Factor 2 (Fig 4.2A). The amount of explained variability in the data represented by the first factor increased with time. Restriction fragment 225 accounted for most of the variability in factor 1 (Figure 4.2A and Table 4.2). This fragment appeared five volume changes after start-up and increased steadily for six volume changes, after which its abundance stabilized. The variability represented by factor 2 decreased over time. Four fragments that were abundant during the beginning of phase A had high loading values for factor 2 (Table 4.2).

The S2 bacteria community also changed between 7 and 9 volume changes, and remained relatively stable thereafter (Figure 4.2C). The variability represented by factor 1 increased over time while that represented by factor 2 decreased. Four fragments explained most of the variability with factor 1, with fragment 185 having the highest loading (Table 4.2). Six terminal restriction fragments that were abundant early and then decreased were associated with factor 2 in the S2 community. Of these six fragments, two were also associated with factor 2 in the M3 community. A third factor was retained that accounted for 13.6 % of the variability in the S2 community during phase A. Five terminal restriction fragments that were abundant only in the sample taken seven volume changes after start-up had high loadings for this third factor (Table 2).

(ii) Phase B. During phase B, the M3 bacteria community was quite stable until the HRT was decreased to two days, as shown by the tight clustering of samples before the two day HRT (Figure 4.2B). The one outlying sample before the two day HRT was

Table 4.2. T-RFLP fragments with high factor loading.

Reactor	Phase A			Phase B	
	Factor 1	Factor 2	Factor 3	Factor 1	Factor 2
M3	225	78, 161, 203, 248,	NA ^a	115, 135, 185, 225	75, 125, 253, 258
S2	185, 250, 253, 286	69, 78, 203, 234, 267, 280	61, 67, 75, 125, 318	61, 67, 75, 125, 185	78, 253, 258, 309,

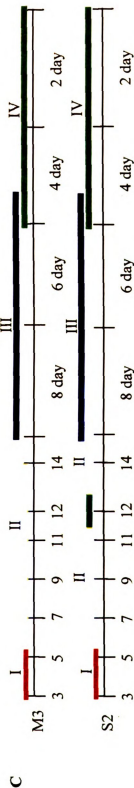
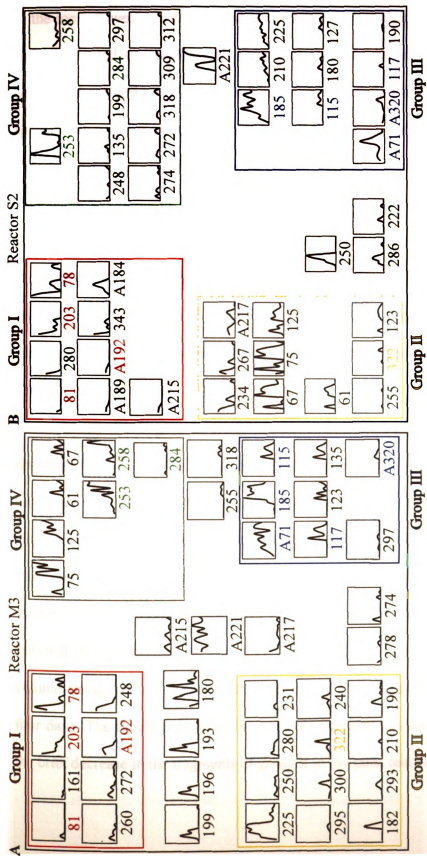
^aNot applicable

likely the result of a temporary pump failure directly before the sampling date. The S2 bacteria community was also stable for the majority of phase B, with only four and two day HRTs affecting the bacteria community (Figure 4.2D). In both communities the value of factor 1 changed very little during phase B. Four fragments in M3 and five fragments in S2 had high loadings for factor 1. The only fragment with a high loading for factor 1 in common between both communities was 185 base pairs in length. The amount of variability explained by factor 2 increased at higher flow rates. Four fragments in each community had high loadings for factor 2 with fragments 253 and 258 in common between the two communities (Table 4.2).

(iii) Archaea. The M3 archaea community changed very little during phase A and phase B. PCA extracted only one factor for each data set. Only during phase A in reactor S2 did significant changes occur in the archaea community. Two factors were extracted and the amount of variability explained by both changed over the 14 volume changes of phase A (data not shown). Values for factor 1 (61 %) decreased over time and the terminal restriction fragments A184, A189, and A215 had high loadings for this factor. Values for factor 2 (24 %) increased over time. Only fragment A217 had a high loading for this factor. Changes in HRT had little effect on the S2 archaea community, and only one factor was extracted from the S2 HRT archaea data set.

SOMs. Separate analyses of the M3 and S2 T-RFLP data resulted in four discernible groups of terminal restriction fragments in both outputs (Figure 4.3). The SOM grouped the fragments according to when they were most abundant in each reactor. As one moves counter-clockwise from the top left around the square SOM output layer, the time in which the fragments are abundant in the reactor progresses. Thus, fragments

Figure 4.3. SOM clustering of T-RFLP fragments in reactor M3 (A) and S2 (B). The line graphs shown for each fragment represent the change in normalized peak height over time. The graphs are arranged according to the position of their winning node within the square SOM output. SOM groups I, II, III and IV are indicated. The letter A before the fragment length indicates fragments from *Archaea*-specific T-RFLP. Fragment lengths indicated in color are in the same SOM group in both reactors. (C) A timeline shows when groups I through IV were present in each reactor. This figure is presented in color.



in the top left were most abundant at the beginning of phase A, while those in the top right dominated late in phase B. Fragments located between groups were intermediate between those groups. Fragments located in the center of the SOM either appeared sporadically or were present at constant levels throughout both experiments.

The four groups found in each reactor were very similar; however, they were not completely synonymous (Figure 4.3C). Group I was the same in both reactors and contained terminal restriction fragments that were abundant very early in phase A and then reduced drastically or disappeared afterwards. Group II fragments were abundant during the end of phase A in both reactors; however, group II fragments in reactor S2 persisted longer than those in reactor M3, and had a bimodal abundance pattern (Figure 4.3B).

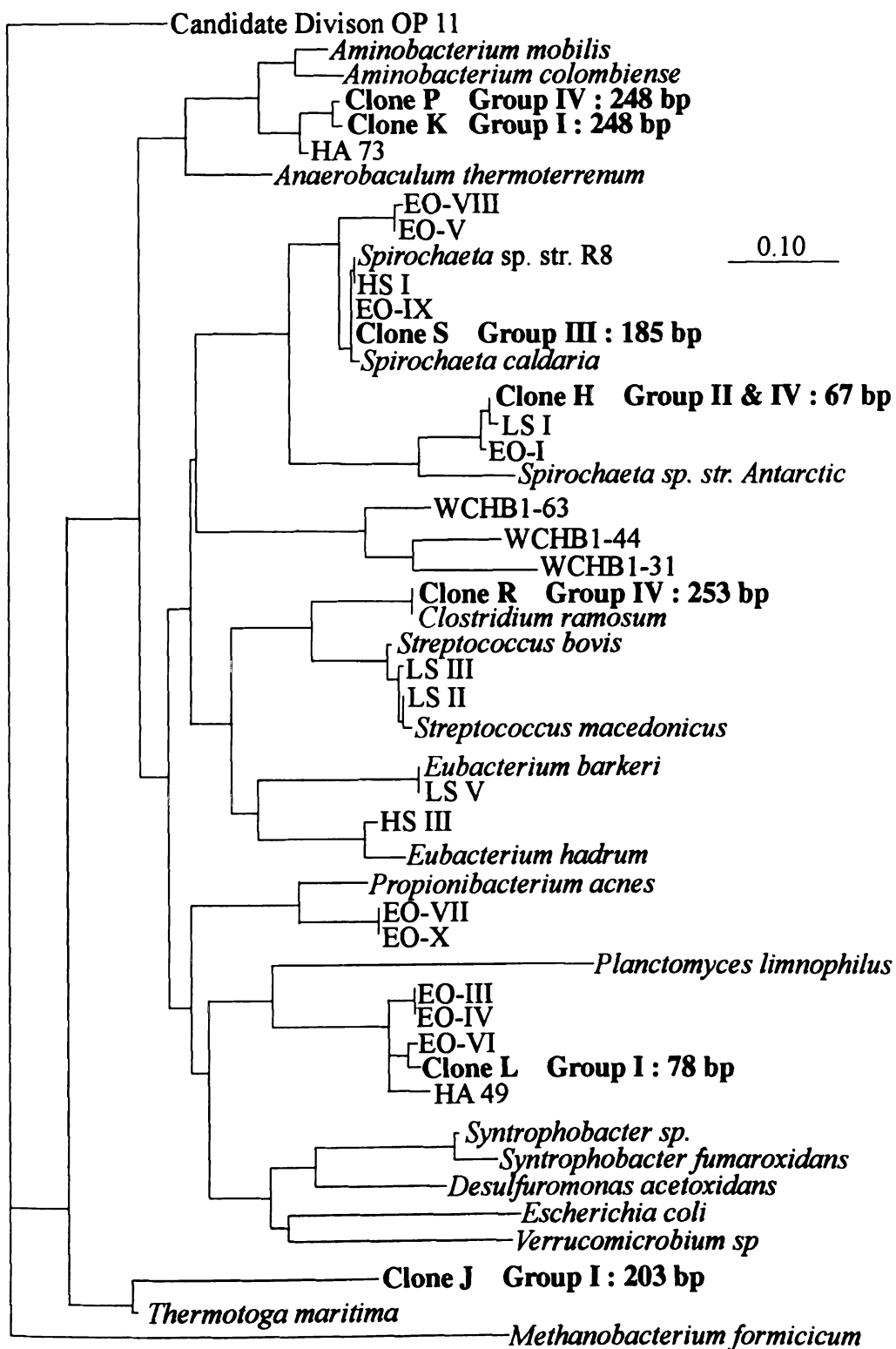
Group III fragments persisted the longest in both reactors, and were most abundant from the end of phase A to the beginning of the four-day HRT, thus they persisted in the reactors for over 300 days. Most of the group III fragments did not disappear after the four-day HRT started, but decreased in abundance while the group IV fragments increased. Group IV contained fragments that increased after the HRT of the reactors was decreased to four days or less. In reactor S2, the pattern was slightly different than in reactor M3. Group IV fragments in reactor S2 increased transiently 12 volume changes after start-up and then increased again after the HRT was decreased to four days. The transient increase in group IV fragments in reactor S2 corresponds with the brief decrease in the fragments of group II in the same reactor (Figure 4.3).

Those fragments located in the center of the output were present at constant levels throughout both experimental phases. In reactor M3, fragments that appeared at fairly constant levels included the archaea derived fragments A221, A215, and A217.

Terminal restriction fragment identification. (i) Bacteria. Six clones were sequenced that matched terminal restriction fragments found in both communities. Four of these six clones matched fragments that were among the eight terminal restriction fragments (out of 48 bacterial fragments identified) that had a maximum normalized peak height greater than 25 % of the total peak height in a given profile. Of these four fragments, two of them (fragments 185 and 253) accounted for over 50 % of the total peak height of a profile in at least one sample. The other two clones sequenced matched fragments that had a maximum normalized peak height of over 10 % of the total peak height in a given profile.

From the phase A bacteria clone library from reactor S2 (sample 3), four 16S rDNA clones were retrieved that matched predominant T-RFLP fragments (Figure 4.4). Clones L and J matched terminal restriction fragments 78 and 203, respectively, and were classified to SOM group I in both S2 and M3 reactors. T-RFLP analysis of S2 and M3 communities with three restriction enzymes confirmed the presence of matching fragments for these clones in all three digests, suggesting that the shared T-RFLP fragments indicate the presence of similar organisms in reactors S2 and M3. Clone L was 95.8 % similar to a sequence found previously in a glucose digesting reactor, and was also closely related to sequences cloned from an anaerobic vinasses waste digester (12,15). However, Clone L had only 77 % sequence similarity to any cultivated organism

Figure 4.4. Maximum likelihood tree of cloned *Bacteria* 16S rRNA genes from reactors M3 and S2 and other methanogenic environments. Clones retrieved in this study are in bold. The SOM group and terminal restriction fragment length (Group x : y bp) is shown to the left of each clone. The backbone of this tree was cast in ARB using 969 unambiguously aligned nucleotides between *E. coli* positions 95 and 1295. Partial sequences were appended to the tree in ARB using the maximum likelihood algorithm with 261 unambiguously aligned nucleotides between *E. coli* positions 154 and 474. The origin of cloned genes from other methanogenic environments is indicated as follows: EO, LS, HS = glucose-fed methanogenic reactors (11,12); HA = anaerobic vinasses reactor (15); RFS = termite hindgut (21); WCHB1 = hydrocarbon contaminated aquifer (9).



represented in the RDP database. Clone J grouped with *Thermotoga*-related sequences, but was 20 % divergent from any isolated organism (Figure 4.4).

Clone H matched the 67 bp terminal restriction fragment found in group II in reactor S2 and group IV in reactor M3. This sequence was most similar to spirochete-related sequences cloned from glucose digesting reactors on two separate occasions (11,12). These sequences group with unusual spirochetes that are reported to lack cell walls and the typical spiral morphology (14). Clone K matched the 248 base pair restriction fragment and was 96.2 % similar to a cloned sequence from an anaerobic vinasses waste digester (15). This sequence clustered with the *Anaerobaculum thermoterrenum* group that is separate from all other bacteria divisions (23) and includes many sequences cloned from anaerobic habitats, such as *Aminobacterium mobilis*, an organism isolated from anaerobic sludge that degrades amino acids (3), and *Synergistes jonessi*, a rumen organism that degrades amino acids and pyridinediols (1).

In the phase B bacteria library from reactor S2 (sample 56), three clones were found that matched predominant terminal restriction fragments found in both reactors. Clone S matched the 185 base pair terminal restriction fragment classified to SOM group III in both reactors (Figure 4.4). Restriction digests of S2 and M3 communities during this period with *HhaI* and *MspI* revealed predominant fragments that also matched with those of clone S. Clone S was 99.5 % similar to *S. caldaria*, and other sequences closely related to this group have been observed in seven different glucose-fed methanogenic reactors in four different studies (10-12,34). Clone R matched the 253 base pair terminal restriction fragment classified to SOM group IV in both reactors. Again, additional restriction digests confirmed the presence of matching fragments in both communities.

Clone R was 100 % similar to *Clostridium ramosum* and to a cloned sequence from a perturbed glucose anaerobic digester (11). The third clone, Clone P, was 99 % similar to Clone K from the phase A bacteria library and matched terminal restriction fragment 248.

(ii) **Archaea.** The archaea clone library from reactor M3 yielded four different 16S rDNA sequences after screening of 30 clones. Clones AA and AB were 98.5 % and 99 % similar to *Methanosarcina sicilae* and had a terminal restriction fragment of 220 bp (Figure 4.5). *In silico* digestion of the RDP database with the TAP T-RFLP program (<http://www.cme.msu.edu/RDP/html/analyses.html>) (24) revealed that a 220 bp fragment was indicative of sequences related to *Methanosarcina barkeri* and *Methanosarcina siciliae*, while a 217 bp fragment was indicative of sequences related to *Methanosarcina mazei*. No 16S rDNA clones were obtained that had a 217 bp terminal restriction fragment, but a clone found previously in a similar bioreactor matches this restriction fragment (12). The *in silico* digest also indicated that the only archaea sequence that yields a 215 bp fragment after digestion with *Hae*III was *Methanosaeta concilii* (Figure 4.5). Digestion with *Hha*I confirmed the presence of matching fragments in both communities for the different *Methanosarcina* and *Methanosaeta* species. Two other clones, AC and AD, composed 17 % of the archaea clone library and grouped with *Methanobacterium* species. Clones AC and AD had a *Hae*III terminal restriction fragment of only 22 base pairs, which is indistinguishable from the primer fragments in T-RFLP analysis. Fragments matching this clone were found in *Hha*I digests. No other clone types were detected.

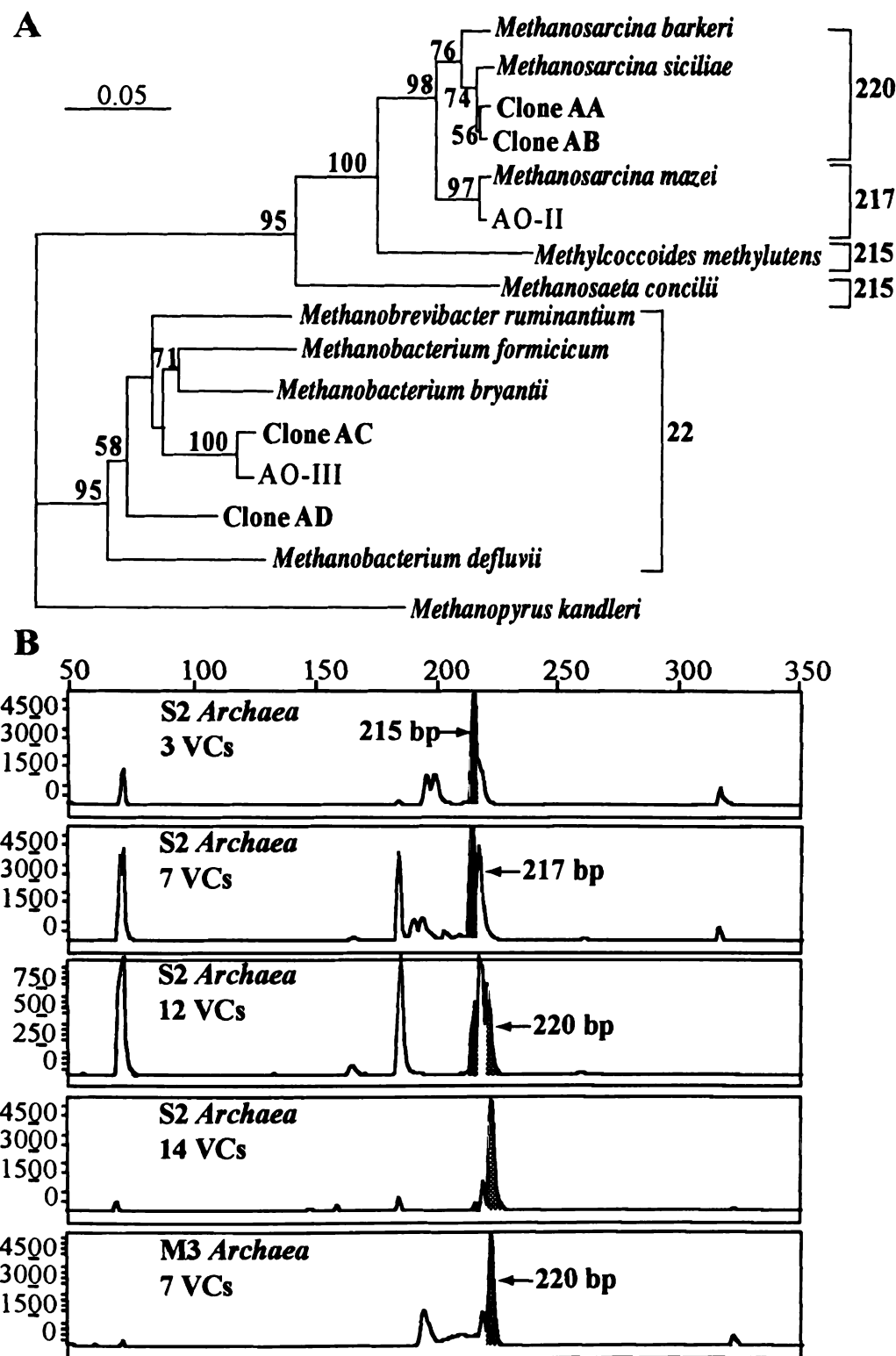


Figure 4.5. Succession of methanogenic phylotypes in reactor S2. (A) Neighbor-joining tree of cloned Archaea 16S rDNA genes. The number next to each node indicates bootstrap values from 100 parsimony bootstraps. Numbers to the right of each bracket indicate the length of the 16S rDNA terminal restriction fragment for each phylogenetic group. (B) Archaea community T-RFLP profiles of reactors S2 and M3 after different volume changes (VCs) in phase A.

Discussion

Principal components analysis is a very useful tool in ecological studies. PCA is a method that is applicable to single treatments and descriptive studies, thus allowing statistical analysis of pseudo- or un-replicated ecosystems, a problem faced in many ecosystem studies (6). However, PCA is based on the analysis of variance in normally distributed variables, thus requiring that all variables have a normal distribution. In addition, it is assumed that the variables are related in a linear fashion. These assumptions may not be met by the data. One or both of these problems may be corrected by a transformation of the raw data (*i.e.* a log transformation); however adherence to these assumptions is difficult to test, especially in time-series experiments, and they are often violated by biological data (16,26). There is evidence that PCA is robust even if the data is not normally distributed; however, to make strong conclusions from a statistical analysis, the assumptions of the analysis method should be met (28,29).

In contrast, Kohonen self-organizing maps do not make any assumptions about the distribution of the input variables or their relationships to one another, making SOM ordination an attractive alternative to traditional ordination methods for biological systems. In addition, SOMs may be capable of analyzing data sets with more variability than principal components or correspondence analysis because the dimensionality of the output space is determined by the investigator. This allows the exploration of different output dimensions (size and number of axes) to compromise between finding the best fit and the best visual representation of the data in a smaller n -dimensional space. For example, to create PCA ordination plots that were interpretable the data set for each reactor in this study had to be divided into separate analyses for phase A and phase B

because more than three principal factors, and thus more than three dimensions, were required to describe the variability in the data. This was not necessary for the analysis of the same T-RFLP profiles using the Kohonen self-organizing map algorithm. Unfortunately, it is harder to ascertain the importance of each axis and the meaning of distance and directionality in an SOM output, although a correlation between distance within a SOM output, geometric similarity of the input, and PCA have been demonstrated (4,13). In addition, the only way to assess the quality of a SOM output is to perform multiple independent analyses and compare the results. Because of these pitfalls, SOM analysis is most amendable to low-level data exploration of particularly large and variable data sets, while PCA and other traditional ordination techniques are more useful for smaller data sets and rigorous testing of hypotheses.

Despite the differences between the two methods, they yielded complementary results that demonstrate important aspects of community structure dynamics. The tight clustering of samples taken between 9 and 14 volume changes in the PCA ordination plots demonstrated that approximately 9 volume changes were required for the bioreactor bacteria communities to stabilize. Although the ordination of the phase A S2 and M3 community T-RFLP profiles resulted in strikingly similar patterns, it should be noted that the factors extracted from the S2 community are different than those extracted from the M3 community. Thus, the similarity of the ordination patterns for the two communities does not indicate complete convergence of the M3 and S2 communities. However, both PCA and SOM analysis identified fragments 78 and 203 as important during the early start-up phase in both reactors (Table 4.2 and Figure 4.3). Reactor operation was very stable (above 90 % COD removal) in both the S2 and M3 reactors despite the dynamic

nature of the community structure during this period. This finding is in agreement with a previous study of methanogenic bioreactors, which found that a dynamic community could sustain a functionally stable system (12).

The clustering of samples seen in the PCA ordination plots of phase B samples clearly shows which HRTs affected the bacteria community structure. Both communities were affected by the 2 day HRT, while only the S2 community was significantly affected by the 4 day HRT (Figure 2B and D). The fragments indicated as important during the 4 and 2 day HRTs by both PCA and SOM analysis overlapped, and all of the fragments with high loadings for the second factor were found in SOM group IV.

Thirteen of the 66 terminal restriction fragments analyzed (both bacterial and archaeal) were associated with the same SOM group in both reactors. The PCA indicated that five fragments that accounted for a significant amount of variability between samples behaved similarly in both reactors. Both of these results indicate that the two bacterial communities shared numerically abundant community members during each stage of reactor operation. The SOM identified more fragments that behaved similarly in both reactors because all fragments were represented in the output, regardless of their contribution to the overall variability. Fragments 78, 81, 203, and A192 were found in group I in both reactors. Three of these fragments had relatively large peak heights, suggesting that they were not just minor components of the community. In group III, four fragments were common between the two reactors. Of these, fragment 185 was the most dominant member of the community as judged by its relative peak height. In group IV, four fragments were in common between the two reactors, with 253 and 258 being the most abundant.

The similarity of community change and response in reactors M3 and S2, as illustrated by the appearance of the same terminal restriction fragments at the same time, presumably indicating similar phylotypes and organisms, is intriguing. Although PCR bias likely renders community sampling incomplete, it should be somewhat representative and, when kept constant, allows the comparison of communities under different conditions, as is done here. It appears that a type of successional change occurred in both reactors as comparable phylotypes appeared transiently at the same time prior to the establishment of similar stable communities. This observation indicates that two relatively different communities converged through analogous stages of community development and responded similarly to changes in environmental conditions. These observations indicate that microbial community change is not a stochastic process, but may occur in successional stages, even when the starting communities are very different. In plant communities, the repeatability and similarity of successional change in many different communities has long been noted. However, in microbial communities extensive data showing that succession is repeatable and similar in different communities is limited. This study indicates that theories such as the resource-ratio hypothesis may be applicable to microbial community succession as well (30).

Not only are there similarities between the reactors in this study, but the bacterial sequences retrieved from these reactors are also closely related to those found in other anaerobic bioreactors (Figure 4.4). Sequences corresponding to two of the most abundant fragments, 185 and 253, have been found repeatedly in glucose-fed anaerobic reactors (10, 11, 33). Fragments 78 and 203 corresponded to phylotypes related to sequences previously found in methanogenic environments that are divergent from cultured

organisms (Figure 4.4). The number of sequences repeatedly observed in simple environments that are not related to cultivated organisms emphasizes our lack of cultured representatives of microbial diversity even in common mesophilic environments.

Another interesting convergence occurred in the archaea communities of reactors S2 and M3. The archaea community in the S2 reactor changed steadily during phase A, while the M3 archaea community remained relatively unchanged. This was probably a result of the different inoculum source for the two reactors. The change that occurred in the S2 archaea community was easily tracked by T-RFLP and led to convergence of the two archaea communities (Figure 4.5). There was a progression of acetoclastic methanogen species in the S2 community after start-up that is demonstrated by the decrease of fragment A215 (*Methanosaeta concilii*) and the concomitant increase of fragments A217 and A220 (*Methanosarcina* species). The dominance of *Methanosarcina* over *Methanosaeta* is unexpected because *Methanosaeta* species have a higher affinity for acetate than *Methanosarcina* species. The observations made possible by T-RFLP can now be used to form new hypotheses about interactions between these two genera.

In conclusion, describing these types of community shifts over time in many complex microbial communities is difficult with labor intensive techniques, such as 16S rDNA cloning and fluorescent *in situ* hybridization, thus the first step of rapid community fingerprinting (by T-RFLP or similar techniques such as denaturing gradient gel electrophoresis) and robust data analysis is invaluable to microbial ecology. In addition, similarities between complex communities are not always apparent by manual inspection of T-RFLP profiles or similar data, especially when the communities are diverse and/or dynamic. PCA provided insight into overall community dynamics and continues to be of

great importance in analysis of ecological data, but the analysis was complicated by the large number of terminal restriction fragments and the amount of change observed between samples. This problem would be compounded in natural microbial communities that are subject to more variability than lab-scale, single-substrate, stirred bioreactors. SOM analysis efficiently reduced the dimensionality of the data, providing a meaningful ordination of all the input variables, and should be of great help in the analysis of natural microbial communities in the future.

Acknowledgements. This research was supported by NSF Grant DEB 9120006 to the Center for Microbial Ecology. SLD was partially supported by the Michigan State University Distinguished Fellowship Program. We are also grateful to T.L. Marsh, A.P. Topchy and B. Punch for their helpful discussions concerning this research.

References

1. Allison MJ, Mayberry WR, McSweeney CS, Stahl DA (1992) *Synergistes jonesii*, gen. nov., sp. nov.: A rumen bacterium that degrades toxic pyridinediols. Syst Appl Microbiol 15:522-529
2. Amann RI, Ludwig W, Schleifer K (1995) Phylogenetic identification and in situ detection of individual microbial cells without cultivation. Microbiol Rev 59:143-169
3. Baena S, Fardeau ML, Labat M, Ollivier B, Garcia JL, Patel BK (2000) *Aminobacterium mobile* sp. nov., a new anaerobic amino-acid-degrading bacterium. Int J Syst Evol Microbiol 50:259-264
4. Blayo F, Demartines P (1991) Data analysis: How to compare Kohonen neural networks to other techniques? In: Prieto A (ed) Artificial Neural Networks. Springer-Verlag, Germany, pp 469-475
5. Brower JE, Zar JH, von Ende CN (1990) Field and Laboratory Methods for General Ecology. Wm.C.Brown, Dubuque, IA

6. Carpenter SR (1989) Replication and treatment strength in whole-lake experiments. *Ecology* 70:453-463
7. Chon T-S, Park YS, Moon KH, Cha EY (1996) Patternizing communities by using an artificial neural network. *Ecological Modeling* 90:69-78
8. DeLong EF (1992) Archaea in coastal marine environments. *Proc Natl Acad Sci USA* 89:5685-5689
9. Dojka MA, Hugenholtz P, Haack SK, Pace NR (1998) Microbial diversity in a hydrocarbon- and chlorinated-solvent-contaminated aquifer undergoing intrinsic bioremediation. *Appl Environ Microbiol* 64:3869-3877
10. Dollhopf SL, Hashsham SA, Dazzo FB, Hickey RF, Criddle CS, Tiedje JM (2001) The impact of fermentative organisms on carbon flow in methanogenic systems under constant low substrate conditions. *Appl Microbiol Biotech* In Press
11. Fernandez A, Hashsham S, Dollhopf SL, Raskin L, Glagoleva O, Dazzo FB, Hickey RF, Criddle C, Tiedje JM (2000) Flexible community structure correlates with stable community function in methanogenic bioreactor communities perturbed by glucose. *Appl Environ Microbiol* 66:4058-4067
12. Fernandez A, Huang S, Seston S, Xing J, Hickey RF, Criddle C, Tiedje JM (1999) How stable is stable? Function vs community stability. *Appl Environ Microbiol* 65:3697-3704
13. Foody GM (1999) Applications of the self-organising feature map neural network in community data analysis. *Ecological Modelling* 120:97-107
14. Franzman PD, Dobson SJ (1992) Cell wall-less, free-living spirochetes in Antarctica. *FEMS Microb Let* 97:289-292
15. Godon J, Zumstein E, Dabert P, Habouzit F, Moletta R (1997) Molecular microbial diversity of an anaerobic digester as determined by small-subunit rDNA sequence analysis. *Appl Environ Microbiol* 63:2802-2813
16. Greig-Smith (1980) The development of numerical classification and ordination. *Vegetatio* 42:1-9
17. Hashsham S, Fernandez A, Dollhopf SL, Dazzo FB, Hickey RF, Tiedje JM, Criddle C (2000) Parallel processing of substrate correlates with greater functional stability in methanogenic bioreactor communities perturbed by glucose. *Appl Environ Microbiol* 66:4050-4057
18. Hirst JD, Stenberg MJE (1992) Prediction of structural and functional features of protein and nucleic acid sequences by artificial neural networks. *Biochemistry* 32:7211-7218

19. Kohonen T (1998) The self-organizing map. *Neurocomputing* 21:1-6
20. Lek S, Guegan JF (1999) Artificial neural networks as a tool in ecological modelling, an introduction. *Ecological Modelling* 120:65-73
21. Lilburn T, Schmidt TM, Breznak JA (1999) Phylogenetic diversity of termite gut spirochaetes. *Environ Microbiol* 1:331-345
22. Loeffler FE, Ritalahti KM, Tiedje JM (1997) Dechlorination of chloroethenes is inhibited by 2-bromoethansulfonate in the absence of methanogens. *Appl Environ Microbiol* 63:4982-4985
23. Maidak BL, Cole JR, Lilburn TG, Parker CTJ, Saxman PR, Stredwick JM, Garrity GM, Li B, Olsen GJ, Pramanik S, Schmidt TM, Tiedje JM (2000) The RDP (Ribosomal Database Project) continues. *Nucleic Acids Res* 28:173-174
24. Marsh TL, Saxman P, Cole J, Tiedje JM (2000) Terminal restriction fragment length polymorphism analysis program, a web-based research tool for microbial community analysis. *Appl Environ Microbiol* 66:3616-3620
25. Noble PA, Almeida JS, Lovell CR (2000) Application of neural computing methods for interpreting phospholipid fatty acid profiles of natural microbial communities. *Appl Environ Microbiol* 66:694-699
26. Potvin C, Roff DA (1993) Distribution-free and robust statistical methods: Viable alternatives to parametric statistics. *Ecology* 74:1617-1628
27. Strunk O, Ludwig W (1997) ARB: Software for Phylogenetic Analysis. Technical University of Munich, Munich, Germany
28. Tabachnick BG, Fidell LS (1983) *Using Multivariate Statistics*. Harper & Row, New York
29. Thorndike RM (1978) *Correlational Procedures for Research*. Gardner Press, Inc., New York
30. Tilman D (1985) The resource-ratio hypothesis of plant succession. *American Naturalist* 125:827-852
31. Toronen P, Kolehmainen M, Wong G, Castren E (1999) Analysis of gene expression data using self-organizing maps. *FEBS Letters* 451:142-146
32. Towner H (1998) *EcoStat for Windows*. Trinity Software, Plymouth, NH
33. Wu C (1993) Classification neural networks for rapid sequence annotation and automated database organization. *Comput Chem* 17:219-227

34. Xing J, Criddle C, Hickey R (1997) Long-term adaptive shifts in anaerobic community structure in response to a sustained cyclic substrate perturbation. *Microb Ecol* 33:50-58

CHAPTER 5

INTERSPECIES INTERACTIONS AFFECTING A *SPIROCHAETA* SPECIES IN METHANOGENIC CHEMOSTATS

Introduction

Interspecies interactions are an integral part of microbial community structure and function in all ecosystems. It is very rare to observe a pure culture of a microorganism in a natural setting. Even symbiotic and parasitic organisms are interacting with their hosts and are therefore interacting with another species. Although the study of microorganisms in pure culture is a convenient and powerful technique that has vastly increased our knowledge of genetics, biochemistry, and microbial diversity, it is very artificial. Batch culture methods are also unnatural systems for studying many microorganisms. Continuous culture systems, such as bioreactors and chemostats, provide a better simulation of the nutrient limitation that prevails in most environments (9,14,26). The chemostat provides a means of enriching for organisms that have a low saturation constant (K_s) and maximum specific growth rate (μ_{max}), which are difficult to select for in typical batch enrichment cultures, but may be more prevalent in the environment. In addition, the growth rate of organisms in a chemostat are easily manipulated, making it possible to study the growth and interactions of species at doubling times closer to those found in natural environments.

Spiral-shaped microorganisms have intrigued microbiologists since they were first described over one hundred years ago because of their distinctive shape and fascinating motility (1). Many spiral-shaped organisms, including the members of the order

Spirochaetales (referred to as spirochetes), are slow-growing microorganisms hypothesized to be adapted to growing at low substrate concentrations. The spirochetes are a phylogenetic group that is united by common morphological traits, but is very diverse physiologically, and includes aerobic, anaerobic (facultative and obligate), fermentative, and homoacetogenic microorganisms (1,15). Spirochetes can be free-living, host-associated, or pathogenic and are known to cause a variety of human and animal diseases such as syphilis, Lyme disease, and digital dermatitis. Because of the slow-growth rates exhibited by many spirochetes they should be amenable to enrichment and study in continuous culture systems, yet only a few studies have examined the growth of spirochetes in continuous culture (18,19,25).

In this study we investigated the competitive ability and interspecies interactions of an obligately anaerobic fermentative spirochete, *Spirochaeta* sp. str. R8, in glucose-fed continuously stirred methanogenic bioreactors operated with long generation times (weeks to days) and low substrate concentrations. We present evidence that fermentative spirochetes are excellent competitors for glucose, but that their population can be limited by the supply of required vitamins, such as pantothenate, making their abundance dependent upon the excretion of these vitamins by other community members.

Materials & Methods

Bioreactor operation. Two 16-liter glucose-fed continuously stirred tank bioreactors were operated anaerobically at 34°C with a loading rate of 0.5 g glucose/liter-day and a dilution rate of 0.06 days⁻¹ for 20 volume changes before this study commenced (5). The dilution rate was achieved by continuous delivery of a buffered

glucose solution (8.0 g/L glucose + 7.0 g/L NaHCO₃) and a separate concentrated nutrient solution using separate peristaltic and syringe pumps, respectively (27). Bioreactors S2 (Sediment 2) and M3 (Municipal 3) were inoculated with sediment from the Red Cedar River and fluid from a 250 mL variable volume reactor initially seeded with municipal sewage sludge, respectively. The dilution rate of the bioreactors was manipulated by increasing the flow rate through the bioreactors without modifying the glucose or nutrient concentrations of the influent. Each dilution rate was applied for at least eight volume changes to allow the community to adapt and stabilize. A third bioreactor, bioreactor R1 (Rumen 1), served as a reference and was operated at identical conditions at a dilution rate of 0.06 days⁻¹ throughout the entire experiment. This reactor was inoculated with rumen fluid and operated for over 650 days (approximately 40 volume changes) prior to this study. Chemical oxygen demand (COD), volatile fatty acids (VFAs), and pH were monitored biweekly as previously described (10).

T-RFLP analysis. Community DNA was extracted from 1 mL samples using a beadbeaterTM and phenol-chloroform extraction method (4,16). Amplification of bacterial 16S rRNA genes from community DNA with the bacterial specific forward primer 8F-HEX and the universal reverse primer 1392R was performed as previously described (4). Amplification products were digested with HaeIII and run on a Perkin Elmer Applied Biosystems 373A automated sequencer. The resulting chromatograms were normalized to 10,000 fluorescence units for comparisons of fragment abundance in different samples.

FISH. Slides and samples were prepared as described previously (23). Briefly, samples (0.5 mL) were fixed in 3 % paraformaldehyde and stored in 50 % ethanol at -20°C. Fixed cell suspensions (1-5 µl) were spread onto 5 mm wells of black-coated 10

well slides, dehydrated in 50, 80, and 98 % alcohol and air dried. Hybridization and washing steps were carried out in 50 ml screw top tubes in a water bath of the desired temperature. The hybridization buffer consisted of 0.5 M NaCl, 0.02 % SDS, and 0.1 M TrisHCl (pH 8.0). The wash buffer was identical except for an increase in SDS to 0.05%. Hybridization stringency was varied by changing the hybridization and washing temperatures. After washing, all slides were counterstained with 0.1 µg/ml DAPI for 10 min at 4°C. A Zeiss Axioskop model 50 microscope (Zeiss Inc., Thornwood, NY) equipped with a mercury lamp and a SPOT digital camera (Diagnostic Instruments Inc., Sterling Heights, MI) was used to capture all epifluorescent images. Zeiss filter sets 488015, 488026, and 488002 were used for CY3, CY5, and DAPI imaging, respectively.

Two new oligonucleotide probes, SpiroR8-177 and ClostS9-182, were designed to target 16S rRNA gene sequences closely related to *Spirochaeta* sp. str. R8 and *Clostridium ramosum* str. S9 using the PROBE-DESIGN and PROBE-MATCH tools included in the ARB software package (24) (Figure 5.1). Probes SpiroR8-177 (5'-CACAGCCCCGGTAACCACATT-3') and ClostS9-182 (5'-TCACCATGCAGTGTCCGTACC-3') were synthesized and labeled with the CY3 or CY5 fluorochrome, respectively, by Molecular Probes (Portland, OR). Unlabeled helper probes that hybridized to either side of SpiroR8-177 were designed to increase accessibility of the rRNA in this region (8). The 5' (5'-GGTATT ACCCACTATTTCTAGUG-3') and 3' (5'-CATAGCTCCTTTCTTTACCAGG-3') helper probes were added to the hybridization buffer at the same time as the labeled probe with a final concentration of 1 ng/ml. The conditions for the new probes were optimized using positive and negative controls. The

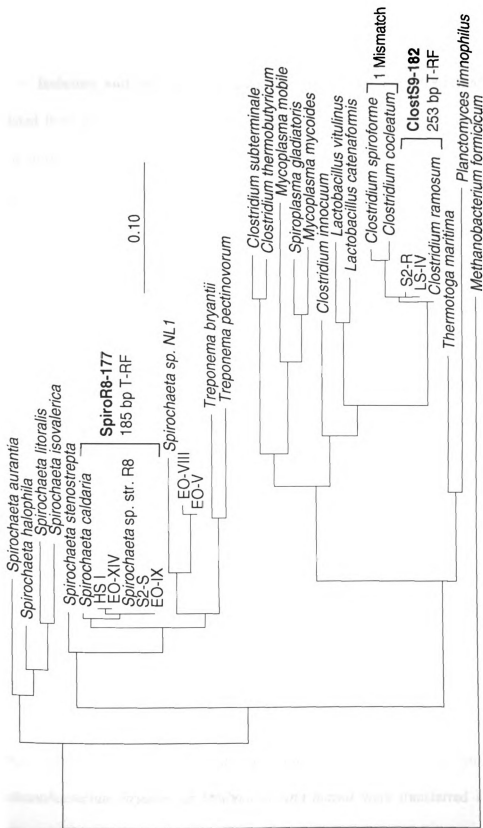


Figure 5.1. 16S rRNA gene terminal restriction fragments generated with restriction enzyme *Hae*III and specificity of oligonucleotide probes used for *in situ* hybridization. Except for the two organisms noted, all sequences in the database had more than 2 mismatches with the oligonucleotide probes designed in this study.

optimum hybridization and washing temperatures were determined to be 37°C for SpiroR8-177 and 43°C for ClostS9-182.

Isolation and culture techniques. *Spirocheata* sp. strain R8 (DSM 13955) was isolated from R1 bioreactor fluid as previously described (4). Strain S9 was isolated by serial dilution of S3 bioreactor fluid in anaerobically prepared tryptic soy broth plus 0.2 % glucose and 50 ug/mL rifampin with a headspace of N₂:CO₂ (80:20). The highest positive dilution tube was then serially diluted in the same medium plus 0.7 % agar. Routine cultivation was performed at 37°C in mineral medium (22) plus 5 % (v/v) rumen fluid, 5 mM glucose, 10mM MOPS buffer, 0.4 g/L sodium sulfide nonahydrate, 0.6 g/L cysteine, 0.13 g/L bacto peptone and 0.13 g/L yeast extract adjusted to a pH of 7.2 with headspace of N₂:CO₂ (80:20). A 100X cofactor solution (pH 7.2) containing (per 100 ml): pyridoxal HCl, 10 mg; pyridoxal phosphate, 10 mg; calcium folinic acid, 2 mg; β-NAD, 2 mg; coenzyme A, 2 mg; FAD, 2 mg; nicotinamide, 1 mg; folic acid, 0.1 mg; riboflavin, 0.02 mg; thiamine pyrophosphate, 100 mg, was added to enhance growth (15). For determination of growth requirements, yeast extract, bacto peptone, and rumen fluid were omitted from the media. Cell yields were determined after logarithmic growth had ceased by DAPI staining and filtration of paraformaldehyde-fixed cell suspensions.

All methanogen cultures were obtained from the Oregon Collection of Methanogens in Portland, Oregon. *Methanobacterium bryantii* M.o.H. (OCM 110) and *Methanosarcina mazei* S-6 (OCM 26) were grown in the medium described above, minus glucose and over-pressurized with H₂. Cocultures of strain R8 and *Methanobacterium bryantii* or *Methanosarcina mazei* were transferred in the glucose medium described above without added yeast extract or cofactors.

16S rRNA gene sequencing. PCR amplification of the 16S rRNA gene from strain S9 was performed on whole cells after one freeze-thaw cycle. The bacterial primer 8F and the universal primer 1392R were used for amplification as previously described (4). The resulting amplicons were cloned into pCR2.1 per the manufacturers instructions (Invitrogen, San Diego, CA), screened for homogeneity by restriction analysis, and approximately 1400 bp were sequenced via the automated dye dideoxy terminator method by the MSU sequencing facility. Sequence similarity was determined using the GenBank BLAST function (www.ncbi.gov).

Continuous culture. Competition experiments were carried out at 37°C in an anaerobic 500 mL chemostat. A mineral medium (22) plus 5 % (v/v) rumen fluid, 0.13 g/L yeast extract, 0.13 g/L bacto-peptone, 5 mM glucose, 10 mM MOPS buffer, 0.4 g/L sodium sulfide nonahydrate, and 0.6 g/L cysteine adjusted to a pH of 7.2 with a headspace of N₂:CO₂ (80:20) was used in all competition experiments. A vitamin solution was also added to give the following final concentrations (per liter): biotin, 2.0 µg; folic acid, 2.0 µg; pyrodoxin, 10.0 µg; thiamine HCl, 5.0 µg; riboflavin, 5.0 µg; nicotinic acid, 5.0 µg; cobalamin, 0.1 µg; paraminobenzoate, 5.0 µg; lipoic acid, 5.0 µg; b-nicotinamide adenine dinucleotide, 2.0 µg; folinic acid, 2.0 µg; flavin adenine dinucleotide, 2.0 µg; pyridoxal 5-phosphate, 10.0 µg; thiamine pyrophosphate, 30.0 mg. Calcium D-pantothenate (500 µg/ml) was added separately in specific experiments. An Ismatec IPC multichannel peristaltic pump controlled the flow rate of the sterile medium into the culture vessel. The pH was monitored daily and maintained at 7.1±0.1.

Organisms were pre-grown in batch culture and anoxically inoculated into the chemostat. Each competition experiment was initiated by inoculating the chemostat

vessel with strain S9 and allowing the optical density to reach equilibrium before inoculating with strain R8. At equilibrium, the medium supported approximately 10^9 cfu/mL (based on serial dilution in agar shakes). Samples (1 mL) were withdrawn every 12 or 24 hours and immediately diluted to 10^7 cells/ml and mounted on an agarose-coated slide. The number of rod- and spiral-shaped cells in 25 fields of view were manually counted, resulting in the enumeration of over 500 cells for each sample.

Results

T-RFLP. The effect of different dilution rates on bioreactor communities S2 and M3 was assessed with 16S rDNA based-T-RFLP analysis. Dilution rates of 0.25 and 0.50 days⁻¹ had the most noticeable effect on the community structure in both reactors, while little to no change occurred in the R1 reference community (5). In particular, two specific fragments of 185 bp and 253 bp appeared to be the most affected (Figure 5.2a). These fragments matched the predicted terminal restriction fragment (T-RF) lengths for specific groups of *Spirochaeta*- (185 bp) and *Clostridium*- (253 bp) related 16S rDNA sequences previously cloned from similar bioreactors (4,6,7,10) (Figure 5.1). The 185 bp fragment also matched the predicted T-RF for *Spirochaeta* sp. str. R8, which was previously isolated from bioreactor R1. This data suggested that in both the S2 and M3 communities *Spirochaeta*-related organisms decreased due to the increase in dilution rate, while *Clostridium*-related organisms increased (Figure 5.2b).

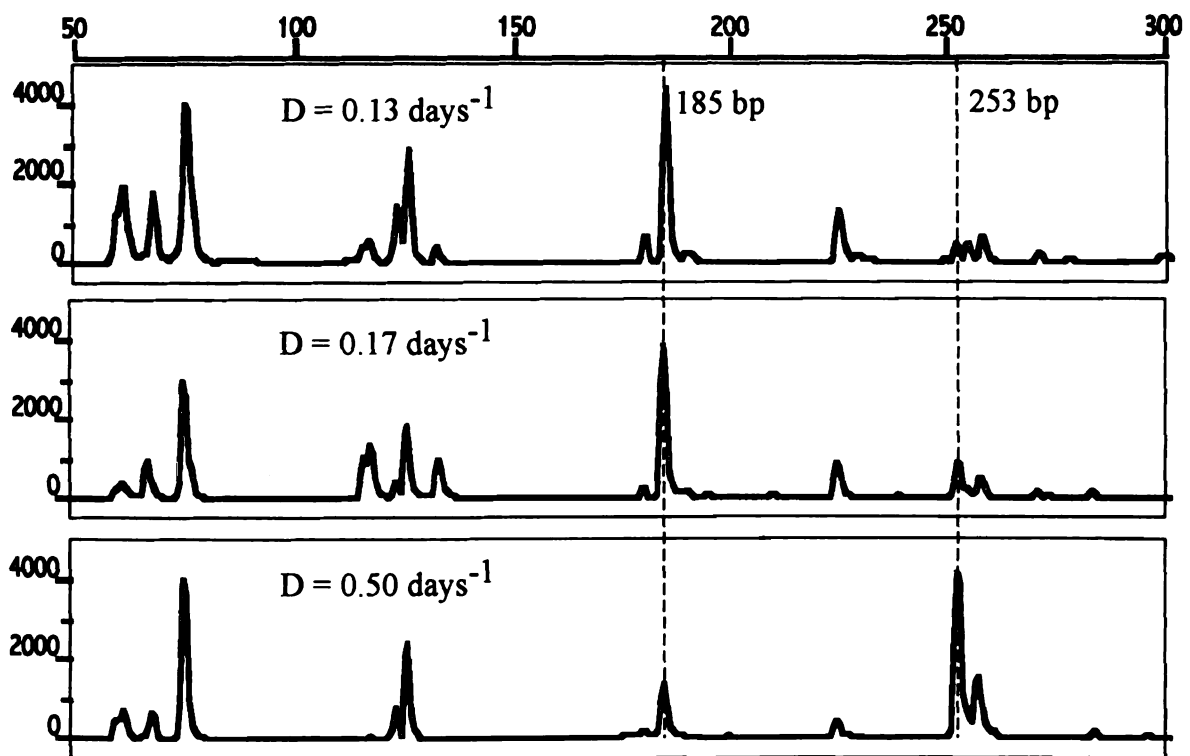


Figure 5.2a. T-RFLP electropherograms of M3 communities at different dilution rates. The electropherograms were generated by restriction of amplified bacterial 16S rRNA genes with the restriction enzyme *Hae*III. The 185 bp and 253 bp fragments were indicative of *Spirochaeta* and *Clostridium* species, respectively.

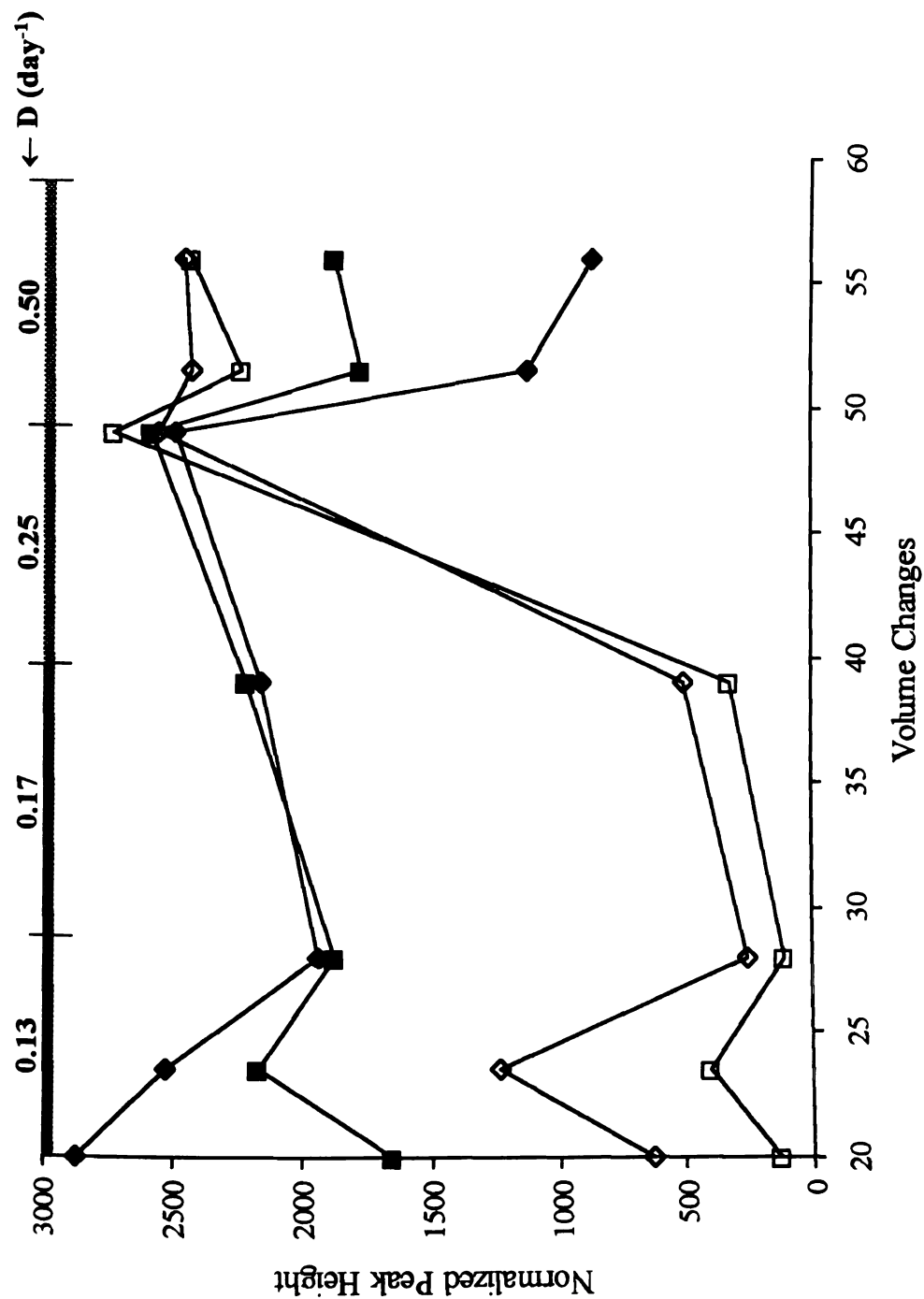


Figure 5.2b. Change in normalized peak height of terminal restriction fragments unique for *Spirochaeta* species (closed symbols) and *Clostridium ramosum* (open symbols) generated by restriction of amplified bacterial 16S rRNA genes with enzyme *HaeIII* from bioreactor communities S2 (\blacksquare , \square) and M3 (\blacklozenge , \diamond). The shading corresponds to the dilution rate applied during that time period, as noted along the top axis.

FISH. To confirm results obtained with the PCR-based T-RFLP method, oligonucleotide probes were designed for specific groups of *Spirochaeta*- and *Clostridium*-related sequences (Figure 5.1). Probe ClostS9-182 was specific for *C. ramosum* when hybridized at 43°C and gave strong signals with little background after hybridization with the bioreactor samples. Probe SpiroR8-177 was specific when hybridized at 37°C, but initially gave very weak signals that were difficult to detect. The use of helper probes boosted the signal noticeably (8).

Between 45 and 55 % of DAPI stained cells hybridized with SpiroR8-177 in all samples of the reference reactor R1 (data not shown). Probe SpiroR8-177 hybridized with 22 to 44 % of DAPI stained cells in the S2 and M3 bioreactor samples taken when the dilution rate was below 0.25 days⁻¹ (Figures 5.3 and 5.4). After ten volume changes at a dilution rate of 0.25 days⁻¹, the number of cells detected with SpiroR8-177 decreased slightly in both bioreactor communities, and dropped significantly after four and seven volume changes at a dilution rate of 0.50 days⁻¹.

Cells detected with probe ClostS9-182 in samples taken when the dilution rate was less than 0.25 days⁻¹ gave relatively weak signals (Figure 5.3c and d). In some cells the DAPI stain showed condensation of the genomic DNA, indicating that at dilution rates less than 0.25 days⁻¹ some members of the population were in a quiescent or dormant state, although they were not completely washed out of the bioreactor. Less than 1 % of DAPI stained cells hybridized with ClostS9-182 in all samples of reference reactor R1. After ten volume changes at a dilution rate of 0.25 days⁻¹ in reactors M2 and S3, the number of cells detected with ClostS9-182 increased from approximately 5 % to between 15 and 25 % in both bioreactor communities (Figure 5.4). After four volume

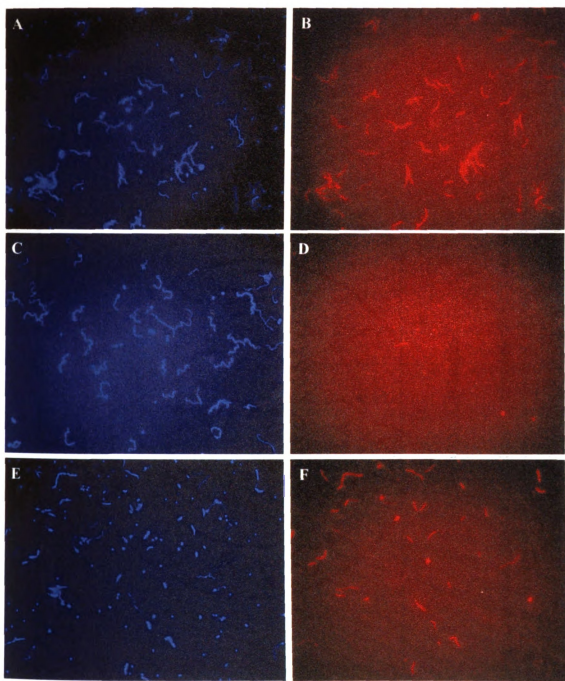


Figure 5.3. Micrographs of bioreactor fluid after hybridization with fluorescently labeled oligonucleotide probes. DAPI (left) and FISH (right) micrographs are shown for identical fields. Bioreactor community M3 after 10 volume changes at $D = 0.17 \text{ days}^{-1}$ hybridized with probe SpiroR8-177 (A and B). Bioreactor community S2 after 8 volume changes at $D = 0.13 \text{ days}^{-1}$ (C and D) and after 7 volume changes at $D = 0.50 \text{ days}^{-1}$ (E and F) hybridized with probe ClostS9-182. Images are presented in color.

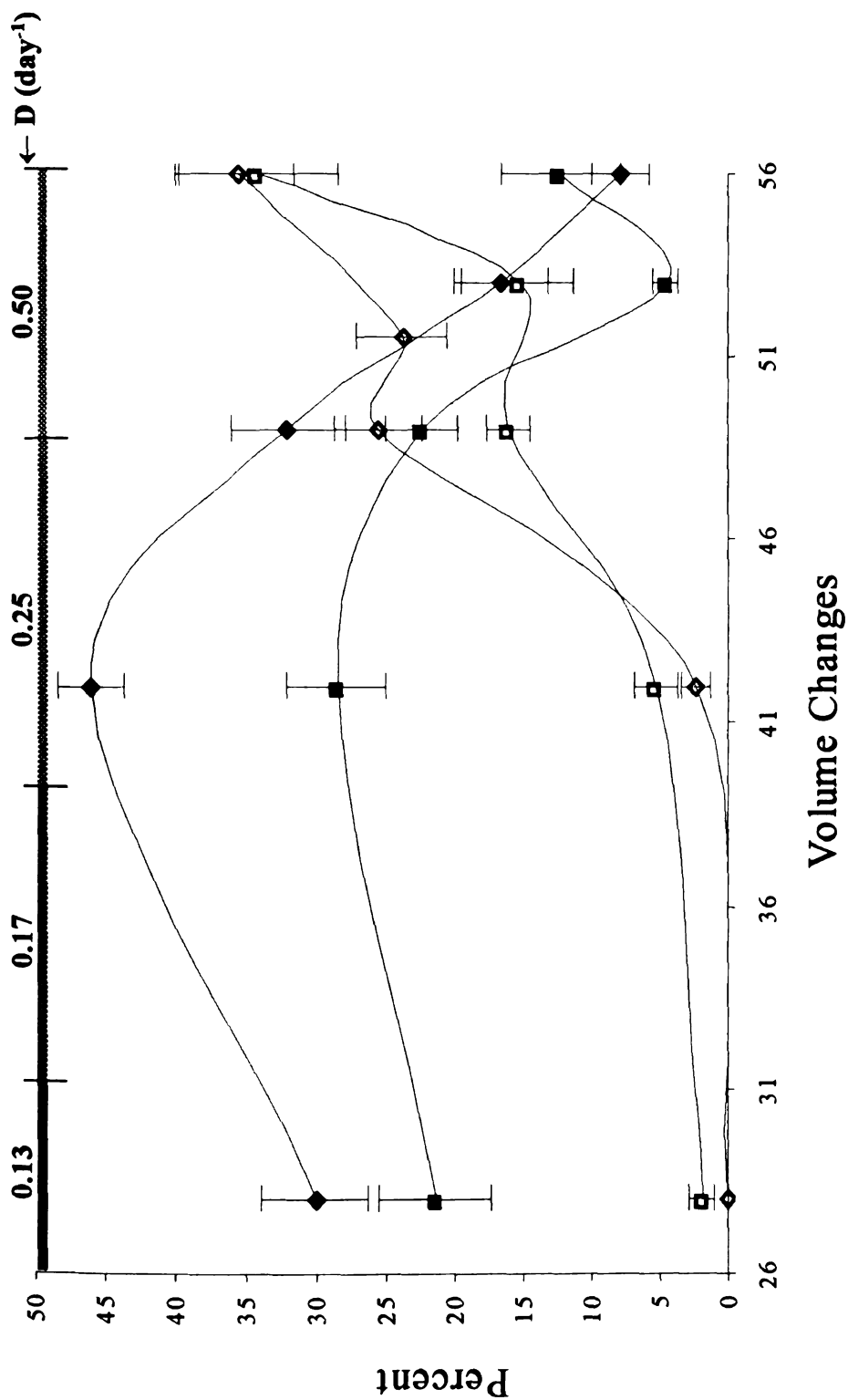


Figure 5.4. Percent of DAPI stained cells that hybridized with probes SpiroR8-177 (closed symbols) and ClostS9-182 (open symbols) in the S2 (■) and M3 (◆) bioreactor communities. The shading corresponds to the dilution rate applied during that period, as noted along the top axis.

changes at D of 0.50 days⁻¹, little change in the percentage of ClostS9-182 positive cells was detected, but after seven volume changes they increased to 35 % of DAPI stained cells in both the S2 and M3 bioreactor communities.

Strain R8 and S9 characteristics. *Spirochaeta* sp. str. R8 (DSM 13955) was previously isolated from the control bioreactor R1. The 16S rRNA gene sequence was only 0.5 % divergent from *S. caldaria*. Strain R8 ferments glucose to acetate, ethanol, lactate and hydrogen, a common fermentative pattern among free-living anaerobic spirochetes (4). No growth occurred in minimal media without pantothenate, and growth yield increased as the supply of pantothenate was increased. If coenzyme A (CoA) was added instead of pantothenate, greater growth yields resulted (Table 5.1). Yeast extract also stimulated growth more than predicted from the assayed amount of pantothenate present per gram of extract. Thiamine pyrophosphate and a mixture of volatile fatty acids were also stimulatory for growth in mineral medium lacking rumen fluid and decreased the number of spheroid bodies present in 4 day old cultures. Rumen fluid (5 % v/v) provided more robust growth than the volatile fatty acids and thiamine pyrophosphate combined (data not shown). In minimal glucose medium plus 5 % rumen fluid and 0.13 g/L of yeast extract strain R8 grew at a maximum specific growth rate of 0.14 hr⁻¹ (doubling time of 5 hours).

Strain S9 was isolated from a 10⁹ dilution of fluid from bioreactor S2. The 16S rRNA gene sequence of this strain was 100 % identical to that of *Clostridium ramosum*. Strain S9 required B vitamins or yeast extract for growth and had a maximum specific growth rate of 1.4 hr⁻¹.

Table 5.1. Growth yields in glucose minimal medium.

Additions	Yield (cells/ml) ^a
None	No Growth
100 µg/ml Ca pantothenate	0.2 X 10 ⁷
5% Rumen Fluid, 0.13 g/l YE	0.4 X 10 ⁷
200 µg/ml Ca pantothenate, 5% Rumen Fluid, 0.13 g/l YE	7.4 X 10 ⁷
50 µg/ml Coenzyme A, 5% Rumen Fluid, 0.13 g/l YE	9.0 X10 ⁷

^aOriginal inoculum size of 3.0 X 10⁵ cells/ml

Competition in continuous culture. Strain R8 increased rapidly after inoculation into a stable continuous culture of S9 cells, regardless of whether or not excess pantothenate was supplied in the medium (Figure 5.5). The washout of S9 cells (and thus the increase in the relative frequency of R8 cells) was more rapid when excess pantothenate was supplied. Under these conditions the washout rate of S9 was only slightly slower than that expected of a non-growing population, indicating that as a substantial population of R8 established, glucose concentrations were so low that S9 could no longer maintain growth (Figure 5.5a). R8 outcompeted S9 at all dilution rates employed when excess pantothenate was supplied, even those dilution rates at which R8 was not competitive within the bioreactor community, eventually leading to a population of 96 % R8 cells and 4 % S9 cells after only four volume changes. The overall increase in dilution rate over the course of the experiment from 0.17 to 1.0 days⁻¹ corresponds to a reduction in doubling time of nearly four days (from 4.2 days at $D = 0.17 \text{ days}^{-1}$ to 0.7 days at $D = 1.0 \text{ days}^{-1}$).

With only yeast extract and rumen fluid supplying a small amount of pantothenate, strain R8 increased to approximately 40 % of the total cells in the chemostat, after which a stable coexistence of approximately 40 % R8 and 60 % S9 cells was established (Figure 5.5b). This ratio of R8 to S9 cells was maintained even when the dilution rate was increased from 0.17 to 0.25 days⁻¹ and from 0.25 to 0.50 days⁻¹.

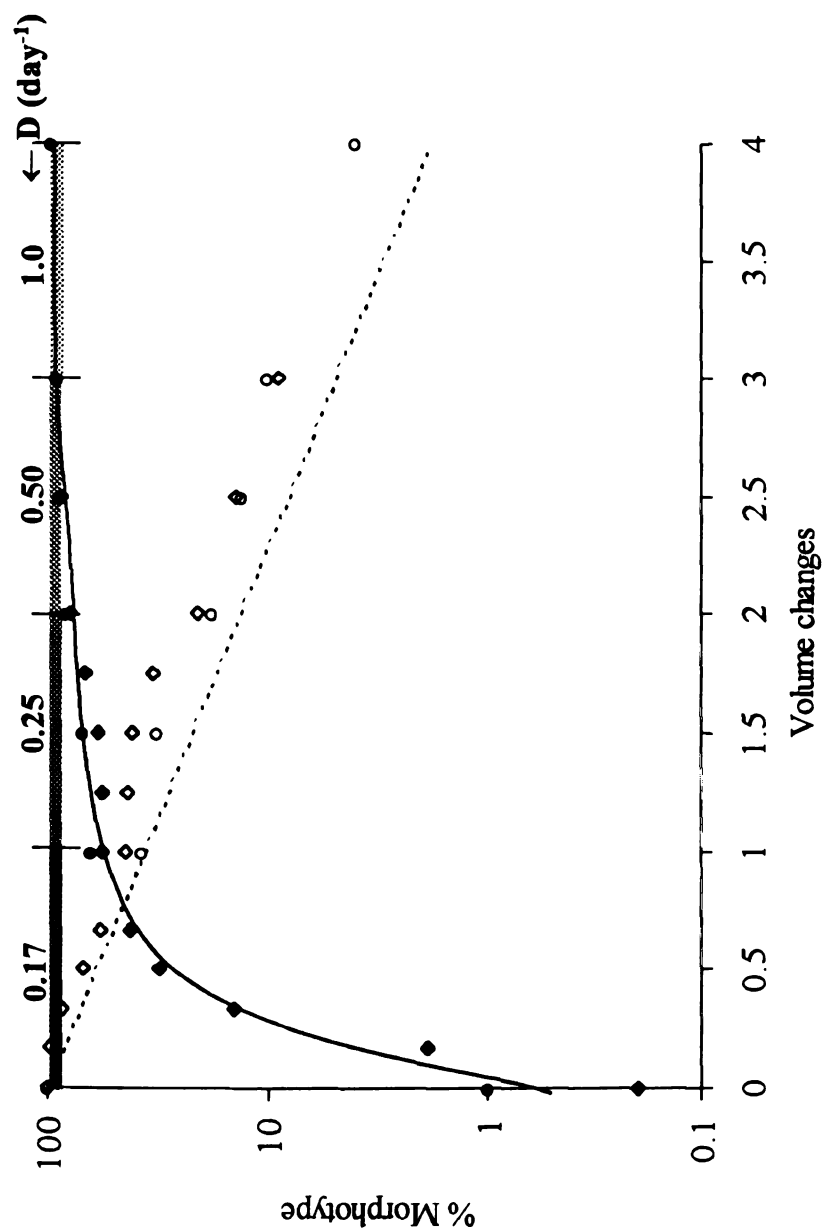


Figure 5.5a. Population size of *Spirochaeta* sp. str. R8 (◆, ●) and *Clostridium ramosum* str. S9 (◇, ○) during competition in continuous mixed culture with 500 µg/mL of pantothenate supplied. Data is shown from two separate competition experiments performed under identical conditions. The dashed line indicates the washout rate of a non-growing population.

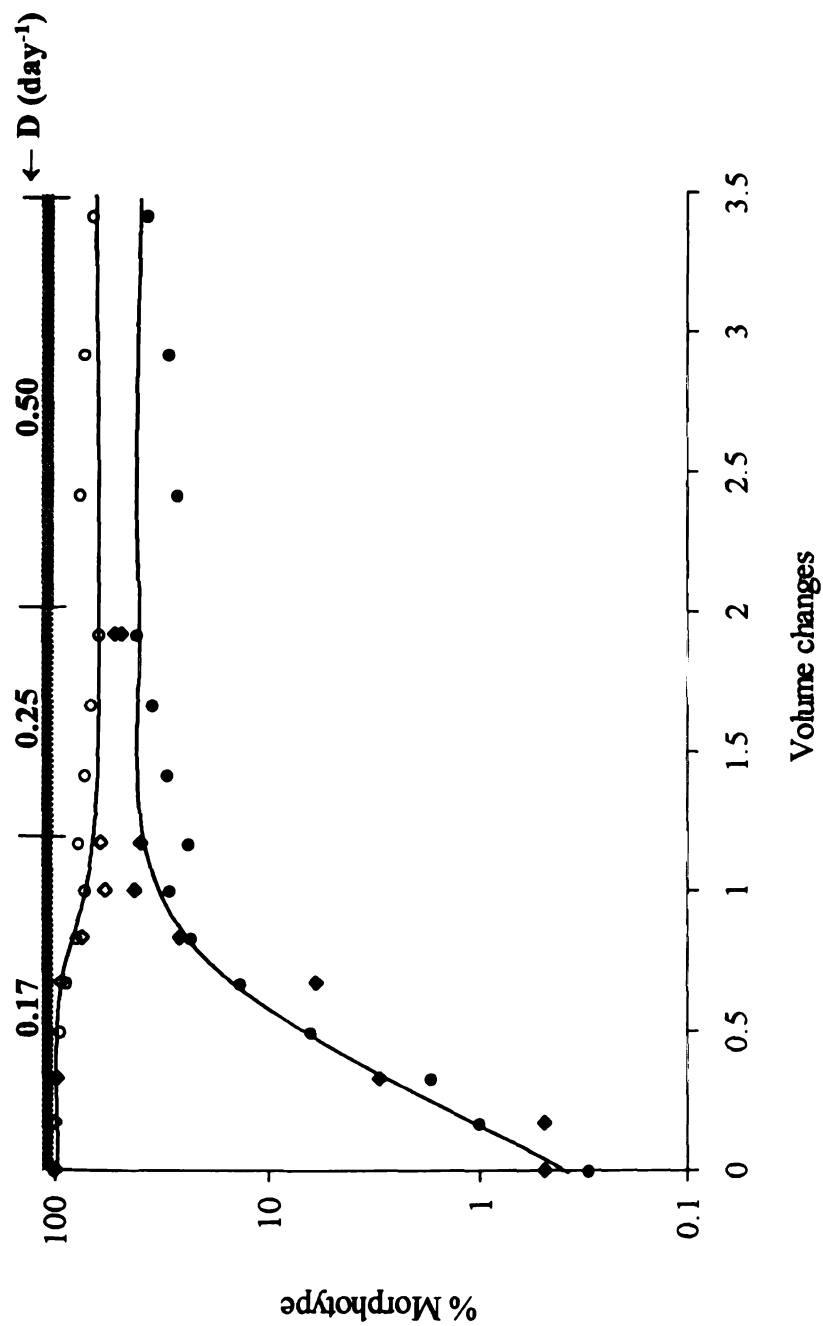


Figure 5.5b. Population size of *Spirochaeta* sp. str. R8 (\blacklozenge, \bullet) and *Clostridium ramosum* str. S9 (\circ) during competition in continuous mixed culture. Data is shown from two separate competition experiments performed under identical conditions.

Me

the

Ad

and

inc

Me

and

old

sta

mu

the

was

resp

wet

to

Methanogenic coculture. Coculture of *Spirochaeta* sp. str. R8 with *Methanobacterium bryantii* lead to significant increases in cell yield, without increasing the amount of acetate (i.e. ATP) produced per mole of glucose utilized (Table 5.2). Addition of excess hydrogen to the coculture increased the amount of methane produced and the yield of R8 cells. Addition of hydrogen to a pure culture of strain R8 did not increase cell yield. Stable cocultures of strain R8 and *Methanosarcina mazei* or *Methanobacterium bryantii* without added pantothenate were transferred over 10 times and repeatedly gave similar cell yields as pure cultures of R8 with added pantothenate (data not shown). The addition of *M. bryantii* to a competition experiment between strains S9 and R8 in medium without excess pantothenate allowed strain R8 to attain a much higher percent of the total cells than when the two strain were competed alone in the same medium (Figure 5.6). A stable coexistence of 92 % strain R8 and 8 % strain S9 was maintained for two volume changes after the initial increase in the R8 population in response to the addition of *M. bryantii*. One percent of the total cells in this triculture were F₄₂₀ autofluorescent, indicating that *M. bryantii* composed approximately 1 % of the total population ($\sim 10^8$ cells/mL).

Table 5.2. Growth yields of *Spirochaeta* strain R8 in batch coculture with *Methanobacterium bryantii*^a.

Additions	Yield (R8 cells/ml) ^b	Acetate produced ^d (mmoles)	Lactate produced ^d (mmoles)	Ethanol produced ^d (mmoles)
None	0.4 X 10 ⁷ (±0.07 X 10 ⁷) ^c	0.48 (±0.08)	0.28 (±0.01)	1.25 (±0.06)
<i>Methanobacterium bryantii</i>	3.0 X 10 ⁷ (±0.4 X 10 ⁷)	0.55 (±0.11)	0.30 (±0.12)	1.10 (±0.23)
<i>Methanobacterium bryantii</i> + 1 atm H ₂	114 X 10 ⁷ (no duplicate)	ND ^e	ND	ND
1 atm H ₂	0.3 X 10 ⁷ (no duplicate)	ND	ND	ND

^aPerformed in glucose minimal media plus 5 % rumen fluid, 0.13 g/L yeast extract, and 0.13 g/L bacto-peptone.

^bOriginal inoculum size of 5.0 X 10⁵ cells/ml. Values are the average of duplicate cultures.

^cStandard deviation of duplicate cultures.

^dPer 1 mmole glucose. Values are the average of duplicate cultures.

^eNot determined

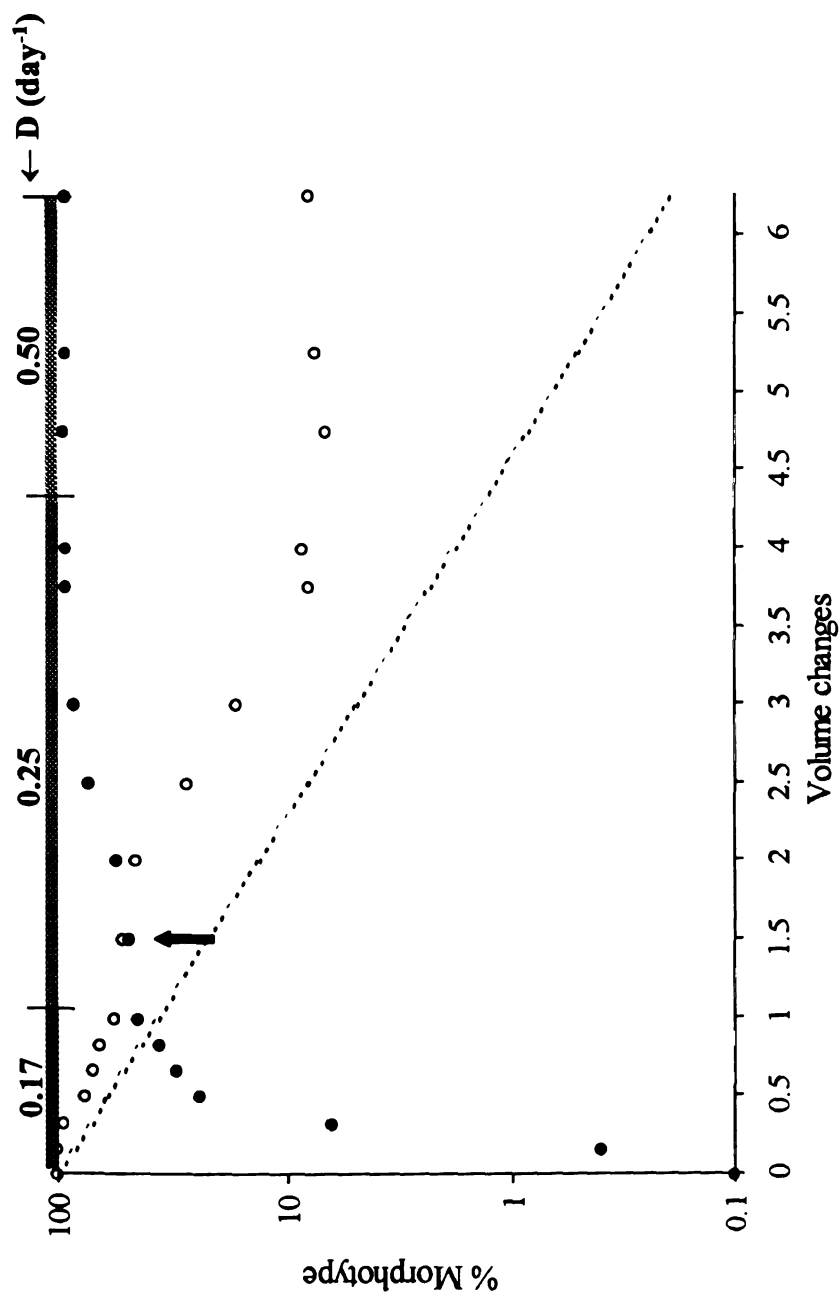


Figure 5.6. Population size of *Spirochaeta* sp. str. R8 (●) and *Clostridium ramosum* str. S9 (○) during competition in continuous mixed culture. The arrow indicates the addition of 1.8×10^8 *Methanobacterium bryantii* cells to the chemostat. The dashed line indicates the washout rate of a non-growing population.

Disc

limi

pop

bio

(3)

en

fer

co

pr

fe

Sp

al

o

(

(

(

.

.

Discussion

The observation of a high proportion of fermentative spirochetes in a glucose-limited bioreactor community suggests that the spirochetes were outcompeting other populations for glucose. The abundance of spirochetes in numerous glucose-fed bioreactors in our studies and others demonstrates that this is not an isolated observation (3,5-7). In the mineralization of one mole of glucose to methane and carbon dioxide, enough free energy is released to form approximately 5.5 moles of ATP (21). Glucose-fermenting organisms perform the most energetically favorable reactions in this conversion and can capture from 37 to 74 % of the energy released, depending upon the products formed and the fermentation pathways employed. Most *Spirochaeta* species ferment glucose to acetate, ethanol, and lactate via the Embden-Meyerhof pathway. *Spirochaeta* species also contain the low potential electron carrier ferredoxin and may be able to vary the amount of acetate produced depending upon hydrogen concentration in order to produce more ATP, potentially producing up to 4 moles of ATP per glucose (1,21).

Strain R8 produced approximately 0.5 moles acetate per mole of glucose utilized (Table 5.1), which provides an extra 0.5 moles of ATP per glucose in addition to the two ATP formed during glycolysis. Fermentation patterns of other acetate and ethanol producing spirochetes demonstrate variable acetate to glucose ratios, resulting in a range of 2.3 to 3.0 moles of ATP produced per mole glucose (1). In a bioreactor dominated by spirochetes approximately 1.3 moles of acetate were produced for every 1.0 mole of ethanol produced (4). Based on this ratio, up to three moles of ATP could have been produced per mole of glucose utilized *in situ*. These data indicate that the spirochetes in

the bioreactor community were probably producing between 2.5 and 3 moles of ATP glucose, which would result in 45 to 54 % of the total energy available from the conversion of glucose to carbon dioxide and methane.

Based on these calculations, *Spirochaeta* sp. str. R8 should have constituted approximately 50 % of the community if it was the dominant glucose-utilizing population. The highest frequency of strain R8 cells detected by FISH in a bioreactor community was 45 % of the total DAPI stained cells. In bioreactor S2, strain R8 only accounted for 25 % of the community, indicating that perhaps other populations were utilizing glucose in addition to strain R8. An additional consideration is that when biomass is calculated from cell volume, the contribution of spirochetes can decrease significantly because of their slender morphology (6). Previous studies found that the specific products produced by strain R8 (acetate and ethanol) were rapidly utilized by bioreactor fluid containing a high proportion of spirochetes (4). The data presented here suggest that strain R8 was a dominant, although likely not the sole, population utilizing glucose in these bioreactor communities.

The decrease in the abundance of spirochete R8 in bioreactor communities S2 and M3 when the dilution rate was increased to 0.25 and 0.50 days⁻¹ indicated that conditions were more favorable for strain R8 at low dilution rates (Figure 5.4). The concomitant increase in the *Clostridium ramosum* population suggested that the two strains were in direct competition for glucose. At the higher dilution rates, glucose concentrations increased to a point where *Clostridium ramosum* was the better competitor. However, when the two strains competed directly in continuous culture, spirochete R8 remained dominant over clostridium S9 at dilution rates of 0.25, 0.50, and 1.0 days⁻¹ (Figure 5.5a).

Only when pantothenate was limiting the growth of spirochete R8 was clostridium S9 able to maintain a large population, and the two strains coexisted in relatively equal numbers (Figure 5.5b). This suggests that the reason for the decrease in the abundance of spirochetes at high dilution rates was not directly related to glucose competition, but was the result of some other inhibition of spirochete growth, such as pantothenate limitation.

Spirochaeta sp. str. R8. required CoA for optimum growth. Although pantothenate could replace this requirement, growth yields were significantly lower even when higher concentrations of pantothenate were added. Similar results were obtained in nutritional studies of *S. litoralis* (11), however most other organisms requiring pantothenate do not respond to externally supplied CoA. The cell membrane may be impermeable to CoA, therefore a specific transport mechanism or external degradation of CoA may be required for uptake. An insufficient intracellular supply of CoA severely limits protein and phospholipid production in *E. coli*, and the cessation of amino acid and protein synthesis eventually causes growth stasis (13). In the heterofermentative lactic acid bacterium *Oenococcus oeni*, CoA deficiency causes a shift in glucose fermentation products away from products that are formed by enzymes utilizing CoA as a cofactor. In *Spirochaeta* sp. str. R8, this type of shift would decrease the amount of acetate and ethanol produced because the phosphoroclastic reactions involved in their formation require CoA. This would likely reduce the amount of ATP formed per mole of glucose, resulting in much less efficient growth.

In these glucose-fed bioreactors, the only source of vitamins and cofactors would be the excretion of vitamins by community members or the scavenging of vitamins from dead microbial cells. To support a large population of cells (approximately 5.0×10^9

cells/ml (4)) a significant continuous supply of CoA precursors must have been available to strain R8, therefore the scavenging of vitamins from dead cells would not have been sufficient. *Escherichia coli* secretes up to 3 µg/ml of pantothenate during logarithmic growth (12). The secretion of pantothenate in *E. coli* is a mechanism for regulating levels of CoA inside the cell. However, other fermentative organisms screened for pantothenate excretion excrete two to three orders of magnitude less pantothenate than *E. coli* (20). No measurable amount of pantothenate was excreted by *Clostridium ramosum* str. S9 when culture fluid was bioassayed with *Lactobacillus plantarum* (data not shown).

A potential source of CoA precursors for spirochete R8 in the bioreactor community would be excretion by microorganisms in other trophic groups. Two methanogens (*Methanobacterium bryantii* M.o.H. and *Methanosarcina mazei*) screened in this study relieved the pantothenate requirement of R8 when grown in coculture. The increase in strain R8 cell yield in coculture was not due to an increase in acetate or ATP production from glucose (Table 5.2). Very low numbers of methanogens enhanced the growth of R8, further supporting the view that the methanogens were supplying a vitamin or cofactor that enhanced the growth of spirochete R8. Methanogens likely supply pantothenate or another similar molecule that allows strain R8 to synthesize CoA. However, it is possible that the methanogens supplied amino acids and/or fatty acids whose synthesis requires CoA, allowing strain R8 to grow well with small amounts of CoA. Alternatively, the presence of methanogens may have altered culture conditions or induced expression of genes such that strain R8 could synthesize CoA *de novo*.

This study demonstrates that *Spirochaeta* sp. str. R8 is well adapted to compete for low concentrations of glucose within a tightly linked anaerobic food web were

sufficient vitamins and cofactors are supplied. In general, spirochetes have a high surface area to volume ratio, which may confer a competitive advantage for substrate and nutrient uptake (17). They are also able to detect and chemotax towards very low sugar concentrations (25). However, spirochetes are limited by their requirement for cofactors and vitamins such as CoA, folate, and thiamine. In fact, spirochetes are usually found in carbon-limited environments that are not considered oligotrophic, such as the termite hind-gut, rumen fluid, hydrothermal and marine mats, and sediments (2). All of these environments are either host-associated and/or involve a tightly linked anaerobic food web. The newly-discovered homoacetogenic spirochetes also require exogenous vitamins and cofactors and are limited to the termite gut (15).

Our results demonstrate that vitamin requirements can impact the competitive fitness of an organism, and may affect the total abundance of a population in a community. The localization of spirochetes to host-associated and non-oligotrophic anaerobic environments supports this hypothesis. The supply of vitamins may come from the host, organisms in other trophic levels, or the breakdown of detritus in these environments. Spirochetes appear to specialize in metabolic interactions with a host or other co-occurring organisms for the supply of vital cofactors that are central to the spirochetes' energy-producing metabolism. The advantage of these interactions for a spirochete may be the lowering of maintenance energy, thus allowing for a lower growth rate and better scavenging of growth substrates. The organisms furnishing the cofactors required by spirochetes may in turn benefit from the sequestering of all fermentable substrates entering the system, preventing any potential carbon sources from leaving the community unprocessed.

Free-living fermentative spirochetes may be the common ancestors of all extant spirochete species. Portions of the Embden-Meyerhof energy-yielding pathway exist in all spirochete species that have been assayed for them, even in obligately aerobic strains (1). Studying the primitive free-living spirochete species may therefore increase our understanding of the fastidious disease-causing *Treponema* and *Borellia* species. In addition, understanding the positive and negative interactions occurring within microbial communities that prevent competitive exclusion may unlock answers to our questions about the maintenance of astounding microbial diversity in seemingly simple, unstructured environments.

References

1. Canale-Parola E (1977) Physiology and evolution of spirochetes. *Bacteriol Rev* 41:181-204
2. Canale-Parola E (1992) Free-living sacchrolytic spirochetes: The genus *Spirochaeta*. In: Balows A, Truper HG, Dworkin M, Schleifer K (eds) *The Prokaryotes, A Handbook on the Biology of Bacteria: Ecophysiology, Isolation, Identification, Applications*, vol 2. Springer-Verlag, New York, NY, pp 3524-3536
3. Delbes C, Moletta R, Godon J (2001) Bacterial and archaeal 16S rDNA and 16S rRNA dynamics during an acetate crisis in an anaerobic digester ecosystem. *FEMS Microbiol Ecol* 35:19-26
4. Dollhopf SL, Hashsham SA, Dazzo FB, Hickey RF, Criddle CS, Tiedje JM (2001) The impact of fermentative organisms on carbon flow in methanogenic systems under constant low substrate conditions. *Appl Microbiol Biotech* In Press
5. Dollhopf SL, Hashsham SA, Tiedje JM (2001) Interpreting 16S rDNA T-RFLP data: Application of self-organizing maps and principle component analysis to describe community dynamics and convergence. *Microb Ecol* In Press
6. Fernandez A, Hashsham S, Dollhopf SL, Raskin L, Glagoleva O, Dazzo FB, Hickey RF, Criddle C, Tiedje JM (2000) Flexible community structure correlates with stable community function in methanogenic bioreactor communities perturbed by glucose. *Appl Environ Microbiol* 66:4058-4067

7. Fernandez A, Huang S, Seston S, Xing J, Hickey RF, Criddle C, Tiedje JM (1999) How stable is stable? Function vs community stability. *Appl Environ Microbiol* 65:3697-3704
8. Fuchs BM, Glockner FO, Wulf J, Amann R (2000) Unlabeled helper oligonucleotides increase the in situ accessibility to 16S rRNA of fluorescently labeled oligonucleotide probes. *Appl Environ Microbiol* 66:2603-3607
9. Harder W, Dijkhuizen L (1983) Physiological response to nutrient limitation. *Ann Rev Microbiol* 37:1-23
10. Hashsham S, Fernandez A, Dollhopf SL, Dazzo FB, Hickey RF, Tiedje JM, Criddle C (2000) Parallel processing of substrate correlates with greater functional stability in methanogenic bioreactor communities perturbed by glucose. *Appl Environ Microbiol* 66:4050-4057
11. Hespell RB, Canale-Parola E (1998) Glucose and pyruvate metabolism of *Spirochaeta litoralis*, an anaerobic marine spirochete. *J Bact* 116:931-937
12. Jackowski S, Rock CO (1981) Regulation of coenzyme A biosynthesis. *J Bacteriol* 148:926-932
13. Jackowski S, Rock CO (1986) Consequences of reduced intracellular coenzyme A content in *Escherichia coli*. *J Bacteriol* 166:866-871
14. Jannasch HW (1967) Enrichments of aquatic bacteria in continuous culture. *Arch Microbiol* 59:165-173
15. Leadbetter JR, Schmidt TM, Graber JR, Breznak JA (1999) Acetogenesis from H₂ plus CO₂ by spirochetes from termite guts. *Science* 283:686-689
16. Loeffler FE, Ritalahti KM, Tiedje JM (1997) Dechlorination of chloroethenes is inhibited by 2-bromoethansulfonate in the absence of methanogens. *Appl Environ Microbiol* 63:4982-4985
17. Matin A, Veldkamp H (1978) Physiological basis of the selective advantage of a *Spirillum* sp. in a carbon-limited environment. *J Gen Microbiol* 105:187-197
18. Mikx FH (1997) Environmental effects on the growth and proteolysis of *Treponema denticola* ATCC 33520. *Oral Microbiol Immunol* 12:249-253
19. Mikx FH, Jacobs F, Satumalay C (1992) Cell-bound peptidase activities of *Treponema denticola* ATCC 33520 in continuous culture. *J Gen Microbiol* 138:1837-1842
20. Sahm H, Eggeling L (1999) D-Pantothenate synthesis in *Corynebacterium glutamicum* and use of *panBC* and genes encoding L-valine synthesis for D-pantothenate overproduction. *Appl Environ Microbiol* 65:1973-1979

21. Schink B (1997) Energetics of syntrophic cooperation in methanogenic degradation. *Microbiol Mol Biol Rev* 61:262-280
22. Shelton DR, Tiedje JM (1984) Isolation and partial characterization of bacteria in an anaerobic consortium that mineralizes 3-chlorobenzoic acid. *Appl Environ Microbiol* 48:840-848
23. Snaidr J, Amann R, Huber I, Ludwig W, Schleifer KH (1997) Phylogenetic analysis and in situ identification of bacteria in activated sludge. *Appl Environ Microbiol* 63:2884-2896
24. Strunk O, Ludwig W (1997) ARB: Software for phylogenetic analysis. Technical University of Munich, Munich, Germany
25. Terracciano JS, Canale Parola E (1984) Enhancement of chemotaxis in *Spirochaeta aurantia* grown under conditions of nutrient limitation. *J Bacteriol* 159:173-178
26. Veldkamp H (1977) Ecological studies with the chemostat. *Adv Microb Ecol* 1:59-94
27. Xing J, Criddle C, Hickey R (1997) Long-term adaptive shifts in anaerobic community structure in response to a sustained cyclic substrate perturbation. *Microb Ecol* 33:50-58

CHAPTER 6

SUMMARY

The activity of glucose-utilizing organisms is important in aquatic environments. Total monosaccharide concentrations range from 2.0 μM to 0.02 μM , with glucose consistently accounting for 40 to 50 % of total monosaccharides (1). Dissolved sugars constitute up to 80 % of the biomass of aquatic primary producers and 15 to 90 % of photo-assimilated carbon is released by prokaryotic or eukaryotic algae during growth. In mammalian gastrointestinal tracts, ruminant mammals, and wood-digesting insects, sugar fermentation is also important to the nutrition of the animal. Recently the microorganisms that carry out fatty acid oxidation and terminal electron accepting processes have received the most attention in microbial ecology studies. The impact of fermentative microorganisms on community structure and function has received relatively little attention in the current revolution of molecular microbial ecology. This thesis has emphasized the impact of competition and cooperation on the composition of the fermentative guild in anaerobic microbial communities. In summary:

- In methanogenic environments species richness, species evenness, and community change is greater in bacterial communities than in archaeal communities. In addition, microbial communities in a mass action environment can be dynamic while ecosystem function is stable.
- Even the highly selective environment of a mesothermic glucose-fed methanogenic reactor can maintain a large number of functional redundant

species over long periods of time. Organisms with no cultivated relatives were also repeatedly detected in this presumably well-studied environment.

- The presence of different fermentative organisms can establish different routes of carbon flow in methanogenic communities. These differences in community structure and carbon flow influence the ability of a system to recover from perturbation events.
- Although microbial communities are dynamic, community change is not a stochastic process, and may occur in successional stages, even when the starting communities are very different. In microbial communities, extensive data showing that succession is repeatable and similar in different communities is limited.
- Certain *Spirochaeta* species are successful in glucose-fed methanogenic bioreactors operated at low dilution rates. Spirochete species in general are amenable to enrichment and study in continuous culture systems.
- *Spirocheata* sp. str. R8 has a low half saturation constant and maximum specific growth rate, making it a superior competitor at low glucose concentrations. In addition, strain R8 benefits from cooperative interactions with co-occurring species that supply cofactors and vitamins, lowering the maintenance energy required for growth and allowing growth at lower substrate concentrations.

- The competitive ability of a particular species may be affected by a cofactor or vitamin requirement, and thus the abundance of one species may be linked to other species in the community that fulfill their nutritional requirements. For example, methanogens may be important in supplying vitamins to fermentative organisms in anaerobic environments.

References

1. Mopper K, Dawson R, Liebezeit G, Ittekkot V (1980) The monosaccharide spectra of natural waters. *Marine Chemistry* 10:55-66

MICHIGAN STATE LIBRARIES



3 1293 02177 0718